
Catalytic upgrade of ethanol to n-butanol by Guerbet chemistry

Thesis submitted in accordance with the requirements of
Cardiff University for the degree of Doctor of Philosophy by

Guillermo Nicolau Palou

School of Chemistry

Cardiff University

2019



Supervisor

Dr. Ceri Hammond

Abstract

Moving towards a more sustainable society requires the discovery and development of alternative catalytic routes to replace the current dependence of fossil fuels and petrochemical industry. In this respect, the valorisation of biomass into commodity compounds, such as alcohols, represents a great opportunity. The most prominent bioalcohol to date is ethanol; however, several drawbacks prevent this compound from its full implementation as biofuel. This thesis provides a detailed investigation of a catalytic route to upgrade renewable ethanol to a more efficient biofuel as is n-butanol, through the so-called Guerbet reaction.

This work begins in Chapter 3, with a first approach to the Guerbet reaction using Ru-based homogeneous catalyst is presented, the elucidation of the mechanistic aspects of the Guerbet chemistry and the problems related to the use of homogeneous catalysts in basic conditions. Taking the knowledge gained from the study of this system, a different approach is adopted, tackling the different steps of the Guerbet upgrade of ethanol through model reactions, in order to find the most appropriated catalyst for every step to finally combine them in one optimised process. With this aim, in Chapter 4, the first step of the Guerbet reaction, the acceptorless dehydrogenation of alcohols, is investigated using a Pd based catalyst, where various kinetic, steric, electronic, and thermodynamic elements of this transformation are evaluated in great detail. Following this, Chapter 5 is focused on the next steps of the Guerbet reaction, the Aldol condensation and the Meerwein–Ponndorf–Verley reduction, using Lewis acidic heterogeneous catalysts, paying special attention to the selectivity and durability of the catalysts selected. Subsequently, the combination of the selected catalysts in previous chapters is discussed in Chapter 6, showing how the choice of metal, support, operational conditions and relative amount of each catalyst determines the product distribution and catalytic activity obtained. In closing, Chapter 7 evaluates the consequences of the findings of this research, and the pertaining challenges from this work.

List of abbreviations

IEA	International Energy Agency
EIA	Energy Information Administration
EEA	European Environment Agency
USD	United States Dollar
EU	European Union
°C	Degree Celsius
L	Litre
g	Gram
h	Hour
min	Minute
m	Meter
SBR	Styrene-butadiene rubber
ABS	Acrylonitrile-butadiene-styrene rubber
RON	Research octane number
VOC	Volatile organic compound
ABE	Acetone-butanol-ethanol fermentation
K	Kelvin
MPV	Meerwein-Ponndorf-Verley transfer hydrogenation
X	Conversion
Y	Yield
S	Selectivity
C.B.	Carbon balance
TON	Turnover number
TOF	Turnover frequency
CT	Contact time
STY	Space time yield
β	Beta zeolite
Al-β	Aluminium containing Beta zeolite
deAl-β	Dealuminated Beta zeolite

H-β	Proton form Beta zeolite
Sn-β	Sn Beta zeolite
Hf-β	Hf Beta zeolite
Zr-β	Zr Beta zeolite
SSI	Solid state incorporation method
HDT	Hydrothermal synthesis
TEOS	Tetraethyl orthosilicate
TEAOH	Tetraethylammonium hydroxide
HT	Hydrotalcite
wt.%	Weight percentage of total mass
GC	Gas chromatography
FID	Flame ionisation detector
HPLC	High-performance liquid chromatography
PTFE	Polytetrafluoroethylene
<i>P</i>	Pressure
<i>V</i>	Volume
<i>n</i>	Mols
<i>R</i>	Ideal gas constant
<i>T</i>	Temperature
<i>M</i>	Molar
PE	1-Phenylethanol
PFR	Plug flow reactor
ID	Internal diameter
TPED	Phase separator cylinder
MS	Mass spectroscopy
SGE	Gas tight syringe
QGA	Quadruple gas analyser
RT	Retention time
EtOH	Ethanol
Bp	Biphenyl
CF	Calibration factor

XRD	Powder X-ray diffraction
λ	Wavelength
θ	Angle
d	Spacing between planes
V	Volts
A	Ampere
v	Gas absorbed
BET	Brunauer-Emmett-Teller method
C	Brunauer-Emmett-Teller constant
N	Avogadro number
BJH	Barret-Joyner-Halenda model
TEM	Transmission electron microscopy
XPS	X-Ray photoelectron spectroscopy
rpm	Revolutions per minute
E_{act}	Activation energy
k	Kinetic constant
T.V. Gas	Theoretical volume of gas
C.V. Gas	Collected volume
σ	Hammett constant
ρ	Reaction constant
KIE	Kinetic isotope effect
SDA	Structure direct agent
ρ	Substrate turnover
Fur	Furfural
ICP-AES	Inductively coupled plasma atomic emission spectroscopy
LA	Lewis acid

Table of contents

1. Introduction	1
1.1. Towards a more sustainable future	1
1.2. Biomass	4
1.3. Ethanol	5
1.3.1. Ethanol production	6
1.3.2. Ethanol as renewable bulk chemical	8
1.3.2.1. Ethylene	9
1.3.2.2. Diethyl ether	10
1.3.2.3. Acetaldehyde	10
1.3.2.4. Hydrogen (H ₂)	11
1.3.2.5. Ethyl acetate	12
1.3.2.6. 1,3-Butadiene	12
1.3.3. Other uses of ethanol	13
1.3.4. Ethanol as fuel	14
1.3.4.1. Drawbacks of ethanol as a fuel	15
1.4. n-Butanol	17
1.4.1. Current use of n-butanol	17
1.4.2. n-Butanol as fuel	18
1.4.3. n-Butanol production	19
1.4.3.1. ABE process	19
1.4.3.2. Oxo process	20
1.5. Guerbet reaction	22
1.6. Objectives of the thesis	26
2. Experimental and methods	30
2.1. Formula and expressions	30
2.2. Catalysts employed	31

2.2.1. Catalyst preparation	31
2.2.1.1. Solid state incorporation	31
2.2.1.2. Hydrothermal synthesis	32
2.2.1.3. Ag/HT synthesis	33
2.2.1.4. Commercial catalysts used throughout the thesis	34
2.3. Kinetic evaluation	34
2.3.1. Batch Guerbet reaction of ethanol	34
2.3.2. Batch acceptorless dehydrogenation of 1-phenylethanol on glass reactor.....	35
2.3.3. Batch acceptorless dehydrogenation of 1-phenylethanol in stainless steel reactor body with a pressurised connection vessel ..	36
2.3.4. Batch acceptorless dehydrogenation of benzyl alcohol, and deuterated and <i>p</i> -substituted analogues, in stainless steel reactor body with a pressurised connection vessel.....	37
2.3.5. Hot filtration experiment.....	38
2.3.6. Batch hydrogenation of acetophenone and styrene.....	38
2.3.7. Continuous flow: acceptorless dehydrogenation of 1-phenylethanol.....	39
2.3.8. Continuous flow: Aldol condensation of benzaldehyde with acetone	40
2.3.9. Continuous flow: Meerwein–Ponndorf–Verley transfer hydrogenation of furfural	41
2.3.10. Continuous flow: Acceptorless dehydrogenation of 2-butanol and ethanol	41
2.3.11. Continuous flow: Guerbet reaction of ethanol	42
2.4. Analytical methods	43
2.4.1. Mass spectroscopy.....	43
2.4.1.1. Experimental details	43
2.4.2. Chromatography.....	44
2.4.2.1. Gas Chromatography (GC).....	44
2.4.2.1.1. Quantification of Guerbet products.....	45
2.4.2.1.2. Quantification of acceptorless dehydrogenation products.....	48
2.4.2.1.3. Quantification of Aldol condensation and MPV reaction products.....	49
2.2.4.1.4. Identification of unknown products	49

2.5. Catalyst characterisation techniques	49
2.5.1. Powder X-Ray Diffraction (XRD)	50
2.5.1.1 Experimental details	51
2.5.2. Surface area and porosimetry analysis.....	51
2.5.2.1. Experimental details	52
2.5.3. Electron Microscopy	52
2.5.3.1. Transmission electron microscopy (TEM).....	52
2.5.3.1.1. Experimental details	53
2.5.4. X-Ray Photoelectron Spectroscopy (XPS)	53
2.5.4.1. Experimental details	54
3. Upgrade of ethanol by Guerbet reaction	56
3.1. Introduction.....	56
3.2. Results and discussion.....	59
3.2.1. The catalyst.....	59
3.2.2. Investigation on the catalytic runs.....	59
3.2.3. General considerations.....	62
3.3. Conclusions	64
4. Acceptorless alcohol dehydrogenation.....	66
4.1. Introduction.....	66
4.2. Results and Discussion	69
4.2.1. The catalyst, preliminary kinetic measurements	69
4.2.2. Impact of temperature	70
4.2.3. Impact of catalyst/substrate ratio and stirring rates.....	72
4.2.4. Optimisation of the reactor	74
4.2.5. Analysis of gas products.....	76
4.2.6. Side reactions and impact of H ₂ accumulation.....	76
4.2.7. Side reactions and 1-phenylethanol stability.....	78
4.2.8. Hot filtration test	80
4.2.9. Optimised kinetic studies.....	81

4.2.10. Mechanistic studies	83
4.2.11. Optimisation of the catalyst.....	86
4.2.12. Characterisation of Pd/C	88
4.2.12.1. X-Ray diffraction	88
4.2.12.2. X-ray Photoelectron Spectroscopy	90
4.2.12.3. Impact of structural change	91
4.2.13. Stability of the catalyst over time	94
4.3. Conclusions	96
5. Aldol condensation & Meerwein-Ponndorf-Verley reduction	99
5.1. Introduction.....	99
5.1.1. Next steps of the Guerbet reaction	99
5.1.2. Model reactions	102
5.2. Results and Discussion	104
5.2.1. Meerwein–Ponndorf–Verley reduction.....	104
5.2.1.1 Characterisation of hydrothermal β zeolites	104
5.2.1.2. Catalytic activity.....	107
5.2.1.3. Characterisation of post synthetical β zeolites.....	112
5.2.1.4. SSI versus HDT	114
5.2.2. Aldol condensation	120
5.3. Conclusions	124
6. Multistep upgrade of ethanol by Guerbet reaction	127
6.1. Introduction.....	127
6.2. Results and Discussion	128
6.2.1. Dehydrogenation of ethanol	128
6.2.2. Condensation of ethanol.....	131
6.2.3. Alternatives to Pd/C.....	134
6.2.4. Guerbet reaction over Pd/Al ₂ O ₃ and effect of Hf- β HDT.....	136

6.2.5. Gaseous products	143
6.2.6. Adaptability of the system and optimisation to n-butanol	146
6.3. Conclusions	148
7. Conclusions and pertaining challenges ...	150
7.1. Final conclusions	150
7.2. Pertaining challenges and final remarks.....	153
7.2.1. Optimisation of analytical methods	154
7.2.2. Improving n-butanol selectivity and other products	155
Acknowledgements	158

1. Introduction

1.1. Towards a more sustainable future

The technological, medical and civil developments achieved since the industrial revolution, among other factors, have led to an exponential growth of the human population, which is predicted to reach around 11 billion people by the end of this century. This increase of population, alongside new lifestyle and consumption patterns, has prompted a surge in energy demand and chemical consumption, which has created consequently an expansion of the chemical industry, as reported by institutions such as the International Energy Agency (IEA), the U.S. Energy Information Administration (EIA), and the European Environment Agency (EEA) (Figure 1.1).

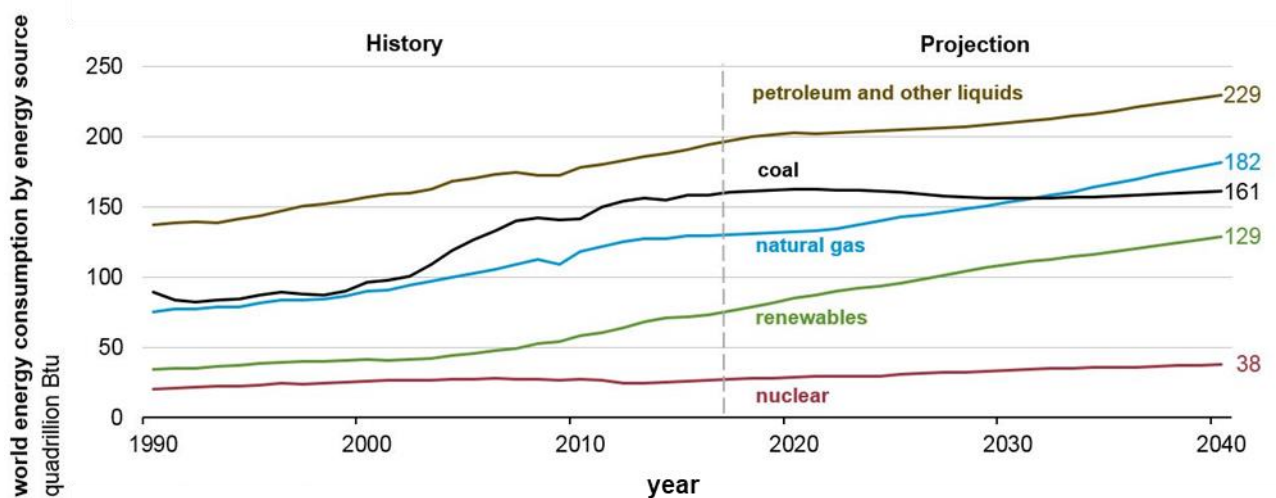


Figure 1.1: World energy consumption in British thermal units (Btu) projection. Retrieved from "International Energy Outlook" 2018.¹

Chapter 1

As reported in Figure 1.1, 80 % of the world's energy supply is currently based on fossil fuel feedstock, with approximate levels of: 37 % crude oil, 25 % coal and 23 % natural gas. In addition to being the primary source of the world's energy production, crude oil is also one of the main building blocks of the chemical industry. Global crude oil consumption can be divided into: 56 % transportation, 28 % industry, 11 % other uses and 5 % power.² Currently, crude oil consumption keeps increasing by approximately 1.5 million barrels every year, and its global demand is predicted to reach 100 million barrels per day in the near future.²

In parallel with the crude oil consumption, world coal consumption has also been increasing over the past 30 years; going from 3,600 to 8,700 million tonnes per annum.³ Nowadays, in addition to playing a key role in both iron and steel industries, coal is mainly used as source for electricity production.⁴ However, coal consumption has been predicted to slightly decrease or at least stabilise for 2022, in favour of renewable sources.⁵

Finally, the global natural gas consumption has also been predicted to grow by 1.6 % per year for the next five years.⁶ Natural gas is mainly used as fuel to generate electricity, accounting for approximately a quarter of the electricity generated globally, as well as a fuel for heating processes in industry, and heating buildings and water in the residential sector. Despite the use of natural gas in the residential sector, the industrial sector represents the main reason of its growing consumption, since natural gas burns cleaner than coal or petroleum.

Over the last years, growing concerns have led to the necessity to find alternative resources for energy and chemical production. Firstly, crude oil, coal and natural gas are finite. Estimations based on the known reserves predict that the crude oil and gas reserves will be drained by 2066 and 2068, respectively, leaving coal as the only remaining cost-effective fossil fuel past that date, although that, too, will run out by 2129.⁷ Secondly, these energy sources also lead to environmental problems, such as increasing CO_x and NO_x concentrations in the atmosphere, which contribute to the greenhouse effect responsible for global warming. In fact, CO₂ emissions increased by 3.4 % in 2013 due to the combustion of coal alone.⁸ To face these issues, governments around the globe are currently developing greener policies, with stricter control of emissions and environmental regulations, in order to reduce the pollution and move towards a more sustainable chemical society.⁹ For these reasons, including the foreseen energy deficit, many studies have been focussed on the development of alternative and sustainable energy sources in order to reduce humanity's dependence on the non-renewable fossil sources.

The possible alternatives cover a wide range of renewable energy sources, from solar to geothermal, wind or water-based technologies and even nuclear; however, none of these alternative energy sources are a suitable alternative for chemical production. Chemical

industry is based on C-containing materials and therefore it requires more sustainable C-based raw materials. Regarding alternative C-based raw materials for the petrochemical industry, the options are limited to either atmospheric carbon or biomass; the only two largescale sources of renewable carbon on the planet.

The use of atmospheric carbon (CO_2) may contribute to reduce their climate impact while replacing the fossil fuel feedstock to generate valuable fuels and chemicals. The most promising technologies explored to convert CO_2 are based on its catalytic hydrogenation and electro- and photo-catalytic processes.

From the catalytic hydrogenation of CO_2 , highly important industrial compounds can potentially be produced including methane, higher hydrocarbons and other oxygenated compounds such as alcohols (methanol) and carboxylic acids (formic and acetic acid). However, an efficient catalytic hydrogenation of CO_2 is still under investigation.¹⁰

From electrocatalytic reduction of CO_2 , especially over metal electrodes, also methane and higher hydrocarbons, small carboxylic acids, CO and H_2 can be generated. Nevertheless, despite many advances in this field, electrocatalytic CO_2 reduction generally suffers from high overpotentials and low current densities, requiring the development of quite complex systems and the maturity of this technology is still insufficient for practical implementation.¹¹

Photocatalytic conversion of CO_2 can also give rise to methane and other higher hydrocarbons, formaldehyde and other oxygenated small products, and H_2 . Photocatalytic transformation of CO_2 using solar energy is potentially more sustainable and favourable than other technologies because of zero addition of supplementary energy consumption and environmental deterioration. The development of selective catalysts is under continuous investigation to make this technology applicable for the industry.^{12,13}

Herein, although existing routes are currently being explored to convert atmospheric CO_2 to liquid products, they present low efficiency and productivity, and they are more complicated and expensive than those used for exploitation of plant-based resources. Overall, biomass is generally considered the only renewable resource with the potential to replace the fossil feedstock in the energy sector and for the production of chemicals.

1.2. Biomass

The term biomass has different definitions but encompasses all the matter that is biologically-produced and based on C, H and O. The estimated biomass production in the world is approximately 100 billion metric tons of C per year.^{14,15} It can derive from waste of human activity or can have vegetable bases.

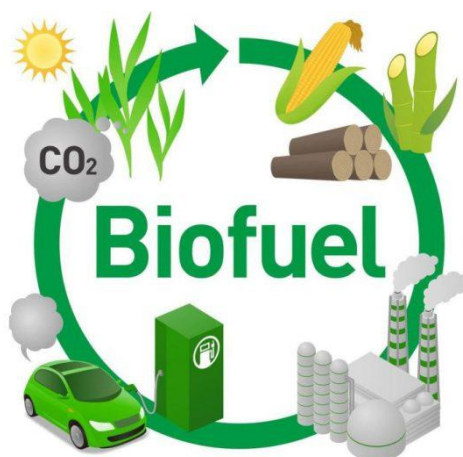


Figure 1.2: C cycle for biofuels. Retrieved from <https://newvitruvian.com/>¹⁶

Biomass is an attractive alternative to fossil fuels due to its large variety of sources and its potential abundance. The chemical treatment of biomass allows a wide array of different products to be obtained, which may be exploited into established industrial processes. One of the promising applications of biomass is for energy production, where fuels derived from biomass (biofuels) are generally considered C neutral. On combustion, the C from biomass is released into the atmosphere as CO₂, which, after a period of time ranging from a few months to decades, is absorbed by plants and transformed again into biomass through photosynthesis. Thus, biomass represents an abundant and renewable source of energy. In the same way, bulk chemicals produced from biomass can, in principle, be CO₂ neutral and thus may represent a solution to the highlighted important environmental issues.

From a general point of view, biomass can be converted through:

- 1- Thermal conversion: This process uses heat to upgrade biomass into more manageable and practical gases and compounds. The basic routes are torrefaction, pyrolysis, and gasification, differentiated by the time and temperature of the process, and consequently the extent of the occurring reaction.¹⁷

- 2- Biological conversion: This method creates desirable products using enzymes, which are biological catalysts able to catalyse natural processes with high selectivity. Since enzymes are involved in biological reactions, their use with biomass-derived substrates can lead to very efficient and successful processes. A good example is the obtainment of alcohols derived from biomass, such as sugar fermentation to produce bioethanol, which is an interesting substitute to fossil feedstock for energy production and chemical industry.
- 3- Chemical conversion: This method results in the formation of a range of products, which can be used for several purposes, from fuels to the synthesis of new classes of chemicals or monomers for the polymer industry. Amongst these methods, chemical methods have several advantages, such as improved scalability, productivity, process economics and ability to target more varied compounds than can be achieved by fermentation alone.

All these processes require a high input of energy, but the demand could be covered by the use of the same biofuels derived from biomass or from different renewable energy sources already mentioned like solar or wind energy.

1.3. Ethanol

Ethanol is considered to be one of the most promising chemicals to reduce human dependence on the fossil feedstock, due to its potential as a renewable and versatile platform molecule. Ethanol also has an established large volume production, with a market size of 78 billion US dollars (USD) in 2018.¹⁸

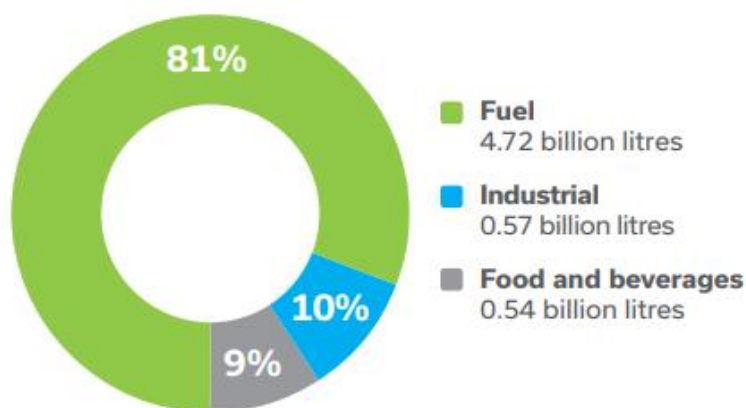


Figure 1.3: Bioethanol production in Europe by its end-use in 2018. Retrieved from “Renewable ethanol production by end use” 2019.¹⁹

Despite being mainly used as fuel, ethanol has a great potential to become a key compound in the chemical industry as direct replacement of the current fossil feedstock. Moreover, the prospect of creating biorefineries, which combine the production of biofuels with renewable chemicals, not only limits non-renewable fuel consumption, but also provides a financial incentive for the establishment of a robust and competitive biobased economy.

1.3.1. Ethanol production

Ethanol can be obtained by two different ways, those being a petrochemical route and a fermentation route. Petrochemical ethanol is obtained from ethylene hydration and is becoming less attractive as the price of oil continues to increase. Conversely, the production of ethanol from biomass fermentation has become increasingly efficient and competitive, thus leading to a less expensive end product. Nowadays, mainly all the ethanol on the market derives from biomass.²⁰

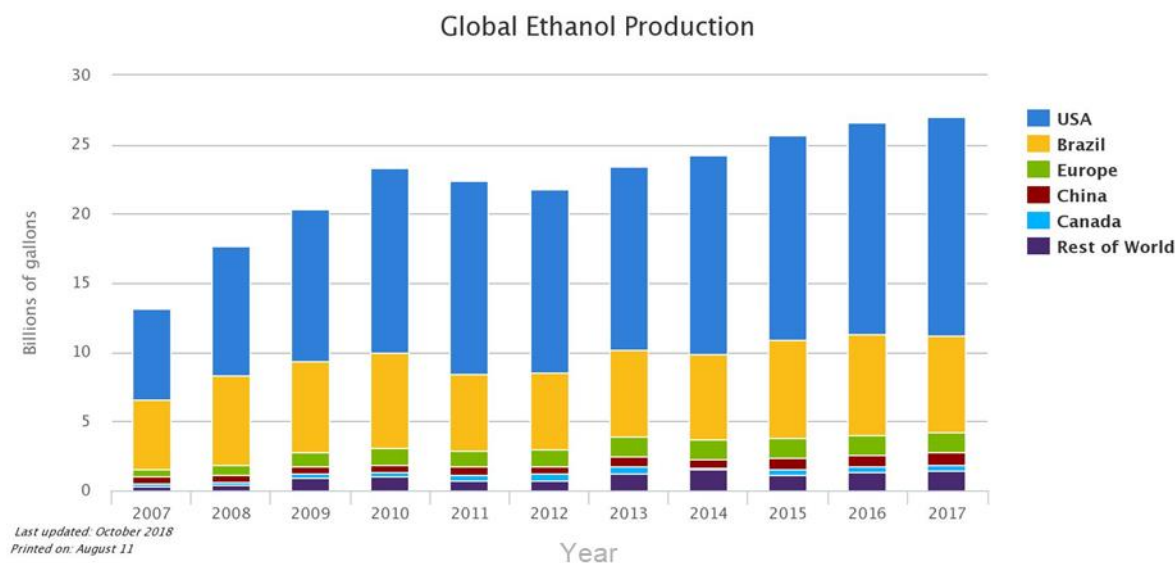


Figure 1.4: Global ethanol production. Retrieved from “Global ethanol production” 2017.²¹

The process for the production of bioethanol has been studied extensively in countries such as the USA and Brazil. Together, these two countries contribute more than 80 % of the world’s production of bioethanol. Currently, conventional processes for bioethanol production use easily fermentable sugars as feedstock, such as sugarcane in Brazil, corn in the US, and wheat and sugar beet in the European Union (EU). The ethanol obtained from these sources is known as 1st generation ethanol. The main disadvantage of 1st generation bioethanol is the fact it competes with arable land for the cultivation of food crops, thus resulting in the increase of food prices and directly competing with the production of food.^{22,23} For this reason, it is necessary to focus on different biomass derivatives for ethanol production. Unlike 1st generation sources, 2nd generation bioethanol is produced from residual biomass, such as forest, industrial, or municipal wastes. These feedstocks do not affect food sustainability, have a low and stable price, and practically do not demand extra land use.²⁴ However, this new methodology has its own disadvantages. The feedstock used for 2nd generation ethanol (lignocellulosic biomass) cannot be directly fermented and a preliminary step of preparation is needed. This process involves cleaning and size reduction by milling, grinding, or chopping, followed by a hydrolysis process to obtain fermentable sugars. These pre-treatments result in a large amount of energy being consumed.^{25,26} Furthermore, 3rd generation processes are studied for the conversion of non-terrestrial plants, such as algae and seaweeds, as they do not need to be grown on land.

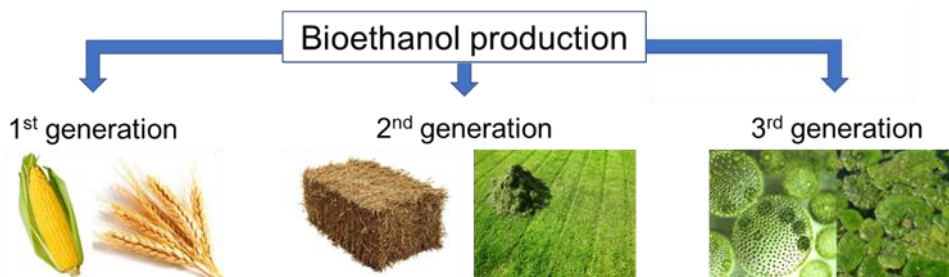
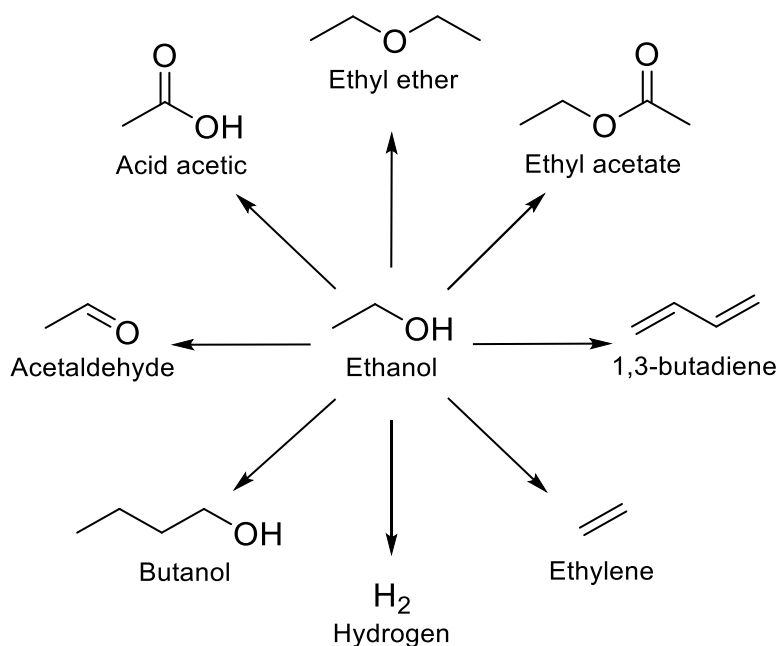


Figure 1.5: Bioethanol classification from source.

Regardless of which process will eventually prove to be the most efficient, all efforts are leading to a sustainable and low-cost supply of ethanol. As previously mentioned, all the developments related to ethanol are currently focused in the use of this alcohol as biofuel; however, ethanol can also be a very profitable precursor for other chemicals.

1.3.2. Ethanol as renewable bulk chemical

As has been detailed previously, ethanol is a very interesting substrate with an increasing level of production. Currently, the only chemical synthesised through ethanol fermentation is acetic acid.²⁷ This chemical is typically used as building block for the production of other compounds; primarily vinyl acetate monomer followed by acetic anhydride and ester production. The growing availability of ethanol and any decrease in its price will make the use of bioethanol as a bulk chemical more attractive from an economical point of view, since ethanol can be used to obtain high value chemicals, such as ethylene, acetaldehyde, n-butanol, hydrogen and various other compounds typically produced from fossil fuel feedstock, as shown in Scheme 1.1.



Scheme 1.1: Different products that can be obtained from ethanol.

1.3.2.1. Ethylene

Ethylene is one of the most important products in the world. The global production of this chemical exceeded 150 million tons in 2016,²⁸ more than any other organic compound, and the demand keeps increasing.^{29,30} The principal use of ethylene is its polymerisation to form polyethylene (Figure 1.6), which is the most common form of plastic.

Typically, ethylene is obtained from crude oil by thermal cracking,³¹ involving complex radical reactions that require high temperatures (700-1000 °C). Other routes like ethane dehydrogenation³² amongst others, are gaining increasing attention; however, in a more sustainable focus, the production of ethylene from biomass is establishing its own market. Dehydration of ethanol to produce this valuable product is a known reaction³¹⁻³³ and with the already mentioned increasing production of bioethanol, ethanol conversion to ethylene is becoming economically very attractive. Nevertheless, the total substitution of crude oil with ethanol for the production of ethylene is unlikely in the near future, unless the production of bioethanol increases substantially, as the demand of ethylene currently exceeds by three times the global production of bioethanol.

Global Ethylene Demand by Application

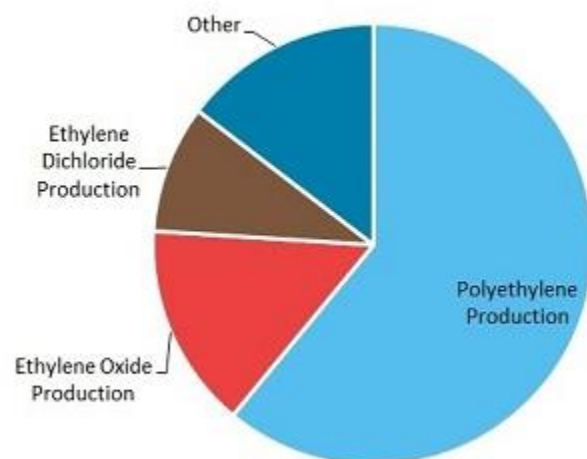


Figure 1.6: Global ethylene demand by application. Retrieved from “Ethylene: World Market Outlook and Forecast up to 2028” 2019.³³

1.3.2.2. Diethyl ether

Diethyl ether is a colourless volatile liquid with interesting applications as solvent and as a fuel additive. It is used to aid the starting of internal combustion engines, especially during cold weather, or in engines that are difficult to start using conventional starting procedures. In this last case, diethyl ether is used in combination with other petroleum distillates taking advantage of its high volatility and low flash point. This product is closely related to ethylene, as the main way to obtain diethyl ether is as by-product in the hydration of ethylene.³⁴ Diethyl ether is also a side product of bioethanol dehydration to obtain ethylene.¹⁷⁻¹⁹ This process is exothermic and competes with the production of ethylene described in 1.3.2.1, and is favoured at lower temperatures.³⁵

1.3.2.3. Acetaldehyde

This chemical is part of the enzymatic degradation of ethanol to CO_2 and can be found naturally in coffee, bread or produced by plants.³⁶ Acetaldehyde is an important bulk chemical with a production higher than 1 million tonnes per year.³⁷ It is used for the production of acetic anhydride, ethyl acetate, crotonaldehyde and especially pyridines, pentaerythritol and acetic acid. Until the 1960s, acetaldehyde was produced commercially from acetylene treated with sulfuric acid over mercuric sulphate.³⁸ Nowadays, acetaldehyde is mainly produced from

ethylene by the so-called Wacker process.^{39,40} This reaction involves the direct oxidation of ethylene to acetaldehyde with a $\text{PdCl}_2/\text{CuCl}_2$ catalyst in water, at the presence of air or other oxidants. Nevertheless, with the increasing production of bioethanol, the dehydrogenation of ethanol to acetaldehyde in presence of oxidants is becoming an interesting route for synthesis. However, ethanol oxidation still shows several drawbacks associated with this approach, such as high catalyst cost and high reaction temperatures.⁴¹

1.3.2.4. Hydrogen (H_2)

H_2 is recognised as being one of the most promising sources of energy in the near future. This element is a high efficiency, low polluting fuel, with water being the only by-product of its combustion, which can be used for transportation, heating and power generation. Although H_2 presents a growing market, there are still some drawbacks associated with the use of H_2 as a fuel, mainly related to its difficult and dangerous storage.

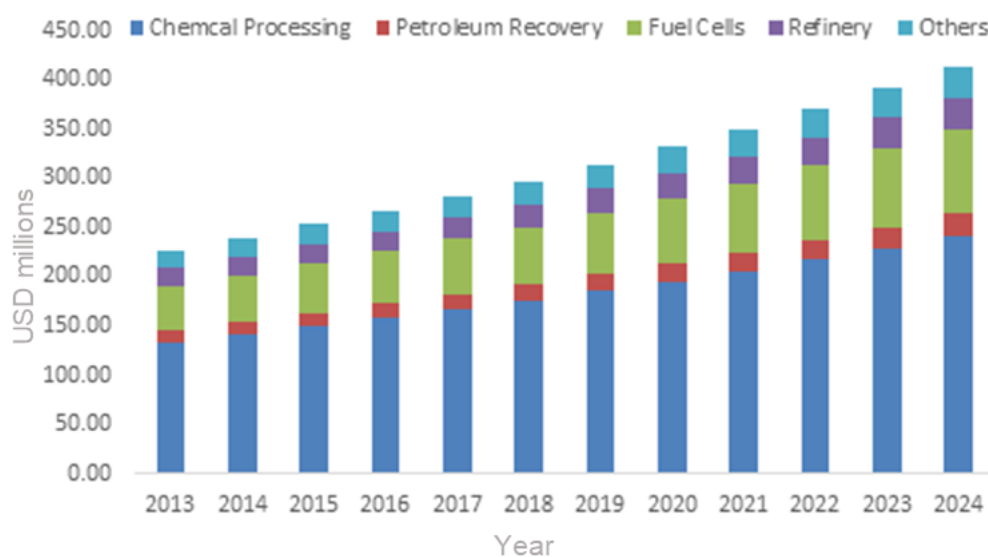


Figure 1.7: U.S H_2 generator market size, by application, 2013-2024 (USD million). Retrieved from “Global markets Insights, Hydrogen Generator Market Size by Product” 2016.⁴²

Until the technology to use H_2 reaches more efficient levels, H_2 is mainly used in petroleum and chemical industries. The two main applications of H_2 are for processing of fossil fuels and for producing ammonia. Specifically, bulk H_2 is currently produced by steam reforming of methane, which is the cheapest method at present.⁴³ This process consists of heating the gas between 700-1100 °C in the presence of steam and nickel and iron oxide catalysts. Steam reforming of renewable chemicals would be more desirable from an environmental point of view if efficient catalysts can be developed to ensure the process to be competitive. For this

reason, production of H₂ from ethanol is regarded as a promising and viable way to move towards renewable energy sources.^{43,44}

1.3.2.5. Ethyl acetate

Ethyl acetate is commonly used as a solvent for extraction processes, for glues production and in cigarettes manufacture due to its characteristic sweet smell. With a production of more than 6 million tonnes per year,⁴⁵ it is mainly synthesised by the esterification of acetic acid with ethanol. Another possible method to synthesise ethyl acetate is the so-called Tishchenko reaction.⁴⁶ Alternatively, a direct one-step conversion of two molecules of ethanol is also feasible.

1.3.2.6. 1,3-Butadiene

1,3-Butadiene is one of the most important chemicals in the petrochemical industry and its production reached 12 million tonnes in 2018.⁴⁷ Butadiene is widely used in the production of polymers and polymer intermediates. For instance, close to 50 % of the overall butadiene produced is employed for the synthesis of styrene–butadiene rubber (SBR). This synthetic rubber is an extensively used material, employed in the production of car tires. Other important applications are the synthesis of acrylonitrile–butadiene–styrene (ABS) copolymer, chloroprene and adiponitrile, amongst others. Butadiene could also potentially be used for the synthesis of aromatic building blocks, such as styrene, by consecutive dimerisation/aromatisation.

1,3-Butadiene is currently almost entirely produced as a by-product of steam cracking of naphtha or gas oil feedstocks.¹⁵ The steam cracker product mixture consists mainly of H₂, ethylene, propylene, and butadiene. However, the mixture contains other C₄ products such as butane. To recover butadiene from the mixture, various distillation steps are needed. After separation of the C₁, C₂, and C₃ fractions, one or more extractive distillation steps are used to isolate butadiene from the other C₄ compounds. This last step is the most complicated and energy consuming, as the different C₄ products have similar boiling points. An alternative to the steam cracking is the oxidative dehydrogenation of butane and butene.⁴⁸

Prior to the dominant steam cracking process, butadiene was produced from acetylene or from ethanol. The process to produce butadiene from ethanol was first developed in Russia at the start of the twentieth century during the search for a method to produce synthetic rubber from

low-cost alcohols. This reaction is known as the Lebedev process, named after the Russian chemist Sergei Lebedev. For a long period of time, the Lebedev process was generally not economically viable because butadiene was very efficiently produced from petrochemical sources.⁴⁹

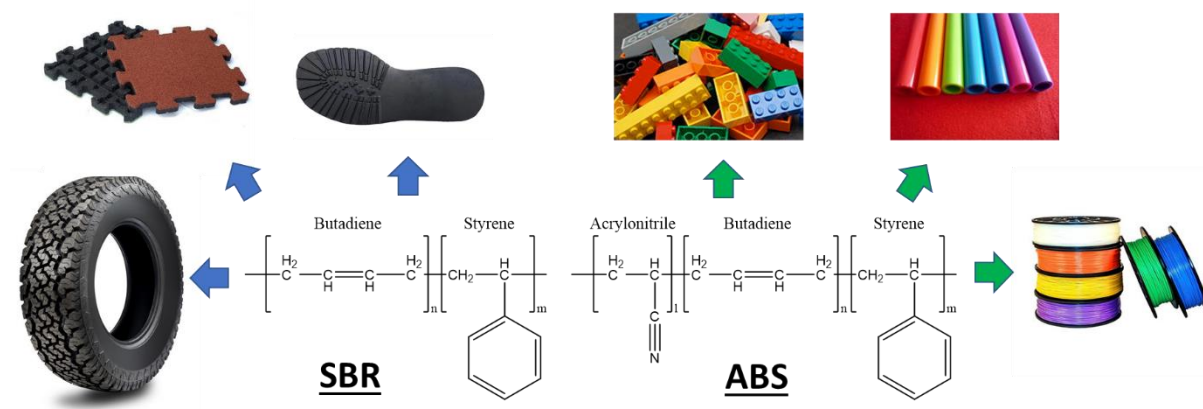


Figure 1.8: General representation of Styrene-Butadiene Rubber (SBR) and Acrylonitrile-Butadiene-Styrene (ABS) copolymer, for material synthesis applications.

1.3.3. Other uses of ethanol

In addition to the mentioned applications of ethanol as bulk chemical, this product is a profitable chemical with an existing market, especially in the alimentary industry,⁵⁰ being a valuable ingredient in the production of alcoholic beverages.

Asides from its recreational use, ethanol is also used as a solvent. In fact, ethanol is an effective solvent for polar, nonpolar, hydrophilic and hydrophobic compounds. Broadly used to extract and concentrate flavours and aromas, can be found in paints, tinctures and selfcare products as mouth washers, perfumes and deodorants. Ethanol has also medical applications. Its use as antiseptic has been known for centuries⁵¹ and is still used for disinfection for its antibacterial and antifungal effects.⁵² Ethanol is also used in medicine as an effective antidote for methanol or ethylene glycol intoxication.⁵³

1.3.4. Ethanol as fuel

Besides the use of ethanol in industry and its possible introduction as renewable bulk chemical, nowadays the main application of ethanol is as a biofuel.¹² Ethanol has been known as an effective energy source since the 17th century. However, it was not until 1826 that ethanol was used to power an internal combustion engine. Nevertheless, during the American civil war, the taxes over alcohol and the discovery of kerosene as a cheaper alternative relegated the use of ethanol for petroleum derivatives.⁵⁴ The long history of competition between gasoline and ethanol is out of the scope of this work, indeed the actual engines evolved to be more compatible with fossil fuels.

Nowadays, ethanol is mainly used as an additive to conventional fuels (blended gasoline) but its market is increasing day by day. Different studies prove how fuels with higher contents of ethanol produce fewer emissions of contaminating gases, such as CO and NO_x.⁵⁵ Thus, new legislations around the world are aiding the addition of different amounts of biobased ethanol to the traditional fuels, especially in the transport sector, to reduce the emission of gases that contribute to the greenhouse effect.⁵⁶ In 2009, the Europe Union adopted its climate and energy package for 2020. The package sought to tackle the dominance on oil use in transport by setting a sectoral target for a minimum 10 % share of renewable energy use in all energy consumed in transport. In their National Renewable Energy Action Plans, sent to the European Commission in 2010, Member States collectively forecast that the majority (8 %) of this 10 % target would be met through bioethanol.

The general categories of ethanol-gasoline blends are E5, E10, E15, E30 and E85. This nomenclature indicates the ethanol content in the mixture. For instance, E10 is gasoline with 10 % ethanol content. Gasoline dispensing pumps generally indicate the ethanol content of the fuel.

The importance of ethanol is evident, and its immediate use is increasing day by day. Nevertheless, as a fuel, ethanol presents different limitations that prevent its complete integration as energy source especially in the transport sector.

1.3.4.1. Drawbacks of ethanol as a fuel

As previously described, the production of bioethanol from biomass is an attractive and renewable option to move away from fossil feedstocks; however, its complete application as a fuel faces several problems.

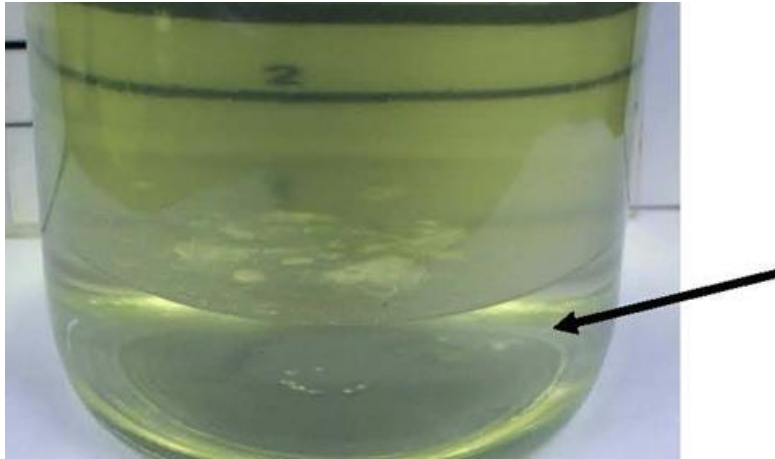


Figure 1.9: Phase separation in ethanol-gasoline blends.⁵⁷

One of the most immediate problems that ethanol presents is related to water. Ethanol is highly hygroscopic, meaning that it can absorb large quantities of water, even from the atmosphere. The absorbed water dilutes the fuel value of the ethanol and may cause phase separation of ethanol-gasoline blends, which causes engine stall. This means that containers of ethanol fuels must be kept tightly sealed. Another side effect derived from this high miscibility is that ethanol cannot be efficiently shipped through existing pipelines like liquid hydrocarbons, over long distances.⁵⁸

Ethanol possesses a higher octane rating than conventional gasoline (RON, the higher the octane number, the more compression the fuel can withstand before igniting), which means the engine can be made more efficient by raising its compression ratio.^{59,60} However, another significant drawback of ethanol is that it contains close to 30 % less energy per unit volume than gasoline (Table 1.1). In theory, this would reduce the distance that a vehicle using ethanol can cover by 30 %, requiring more frequent re-fuelling.

Table 1.1: Comparison of energy density and research octane number (RON) for different kinds of fuel.^{54,61}

<u>Type of fuel</u>	<u>Energy density (MJ/L)</u>	<u>RON</u>
Ethanol	24	108
E85 ^[a]	25	105
E10 ^[c]	31	93
Gasoline	34	91

[a] Blended gasoline with 85 % content of ethanol. **[b]** Blended gasoline with 10 % of ethanol.

Moreover, ethanol as fuel presents other problems in cold weather; at low temperatures, ethanol and blended fuels fail to reach the necessary vapour pressure (below 45 kPa) for the fuel to evaporate and spark the ignition. Thus, starting a cold ethanol engine becomes difficult.

The last inconvenience related to the use ethanol is that it can be corrosive for the engine. Ethanol seems to be especially corrosive in old vehicles and boats, harming rubber and plastic parts.^{62,63}



Figure 1.10: Effects of ethanol in engines.

For all these reasons, ethanol may not be the most appropriate candidate to be used as fuel. Therefore, a desirable substitute would be an agent that shares the benefits of ethanol but lack of its obstacles. This search leads to higher alcohols, such as n-butanol, which can be more efficient as fuel.

1.4. n-Butanol

As has been described, ethanol is an important platform molecule with a large market as biofuel and interesting opportunities as bulk chemical. To date, bioethanol has dominated the biofuel market, especially used blend with conventional fuels. However, ethanol has a number of significant drawbacks compared to gasoline. By contrast, higher alcohols possess fuel properties closer to gasoline and can do not demonstrate the problems associated with ethanol.⁶⁴ In this context, n-butanol is an attractive alternative to ethanol.

1.4.1. Current use of n-butanol

The n-butanol market was estimated at 4.18 billion USD in 2017 and is projected to reach 5.58 billion USD by 2022.⁶⁵ n-Butanol is mainly used as solvent and as feedstock for syntheses but is also widely used as a diluent in lacquers to improve the resistance to humidity. When added to paints and resins, even in small amounts, n-butanol reduces their viscosity and thus improves their use and application. n-Butanol is also used as a component of hydraulic and brake fluids.

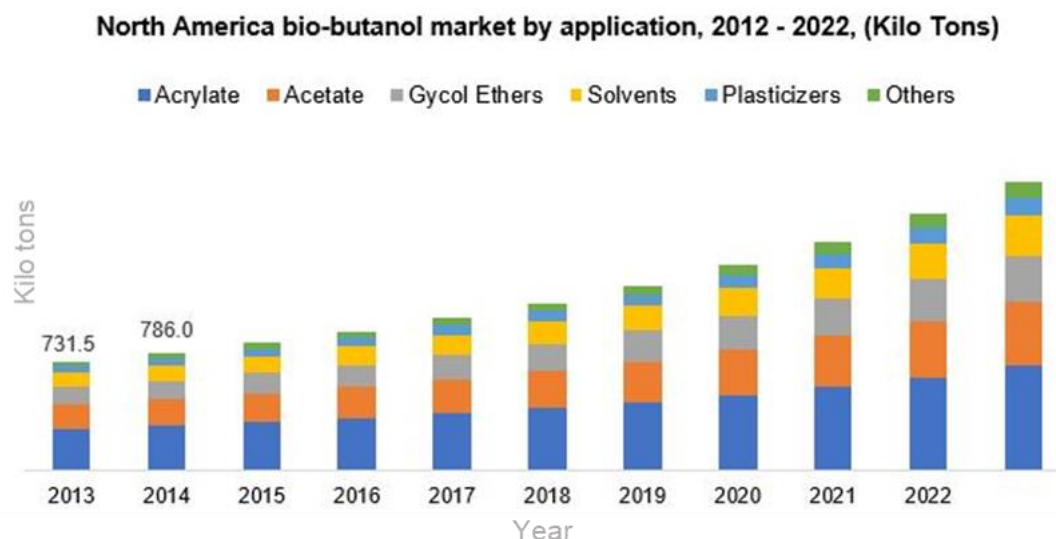


Figure 1.11: n-Butanol market by application. Retrieved from "The energy and fuel data sheet" 2011.⁶⁶

The current major application of n-butanol (more than half of its production)⁶⁷ is the synthesis of butyl acrylate and butyl acetate. These two important industrial products have applications in the production of polymers, paints, cleaning products, antioxidant agents, enamels,

adhesives, textiles, caulks, paper finishes, lacquers and hardened coatings. Butyl acetate is also used in the pharmaceutical industry as a solvent or an extraction agent.

1.4.2. n-Butanol as fuel

n-Butanol has been shown to be an effective substitute for the traditional fuels, both as a standalone fuel and when blended with gasoline. In direct comparison with ethanol:

- 1- n-Butanol does not present the same problems of absorption and solubility with water previously observed with ethanol. Because of the length of n-butanol's C chain, it is also easier to mix with higher hydrocarbons, including gasoline.
- 2- n-Butanol possesses a higher energy density than ethanol, exhibiting 90 % of the energy density of traditional gasoline (Table 1.2).
- 3- n-Butanol is also a cleaner burning fuel, generating fewer volatile organic compound (VOC) emissions compared to gasoline, which helps prevent damage to the environment.^{67,68}
- 4- n-Butanol is safer to handle with a Reid Value of 0.33 psi, which is a measure of a fluid's rate of evaporation, when compared to gasoline at 4.5 and ethanol at 2.0 psi.⁶⁹
- 5- n-Butanol is far less corrosive for rubbers and metallic parts than ethanol^{70,71} and can be shipped and distributed through existing pipelines and filling stations and can be used in unmodified petrol engines.

For these reasons n-butanol is a promising biofuel. The main reason why n-butanol has not been considered as an alternative fuel is that its production has never been cost effective at large scale when renewable are used as feedstock.

Table 1.2: Comparison of energy density and research octane number (RON) for different kinds of fuel.^{54,72}

<u>Type of fuel</u>	<u>Energy density (MJ/L)</u>	<u>RON</u>
Ethanol	24	108
E85 ^[a]	25	105
n-Butanol	30	96
Gasoline	34	91

[a] Blend gasoline with 85 % content of ethanol.

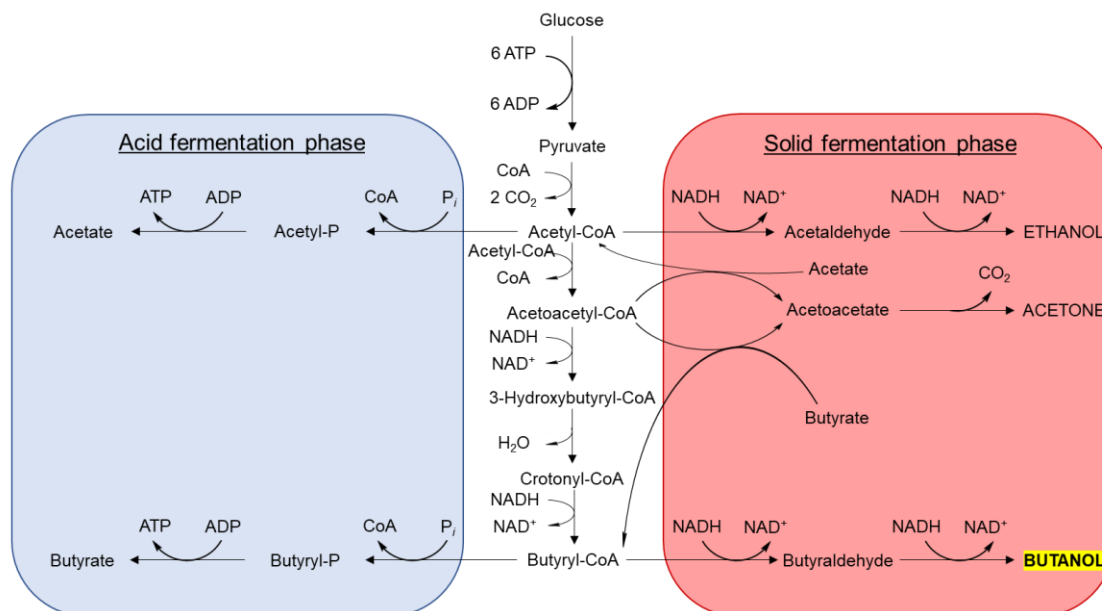
1.4.3. n-Butanol production

As has been described in previous sections, n-butanol is an excellent alternative to conventional fossil fuels. However, for its full implementation an effective and economically attractive method of production is essential. Typically, n-butanol can be obtained from two different processes: from fermentation of sugars during the ABE (acetone, butanol, ethanol) process or *via* the hydroformylation of propylene.

1.4.3.1. ABE process

Before the rise of the petroleum industry, n-butanol was manufactured by a complicated and difficult fermentation of sugar or starch. The fermentation method is known as the ABE (acetone, butanol, ethanol) fermentation, receiving the name from the three products that are obtained. Initially, ABE fermentation was performed with the bacteria *Clostridia acetobutylicum*, which secrete numerous enzymes that facilitate the breakdown of polymeric carbohydrates into monomers.⁷³ The first reports of production of n-butanol from fermentation are attributed to L. Pasteur in 1862,⁷⁴ but the industrial production of n-butanol was not launched until 1916.⁷⁵ This method was used during World War to obtain acetone for the production of ammunitions. It was not until 1920 that n-butanol produced during the ABE process started to be used. By 1927, n-butanol became the key product of the ABE process whilst acetone was considered as a by-product; however, there is relatively little product in the final mixture after a fermentation run, with also containing H₂, isopropanol, acetic, lactic, propionic and butyric acids, CO₂, and lipids. Recovery and purification of n-butanol from the fermented mixture is difficult, causing an increase of the production cost. Furthermore, n-butanol is toxic for the bacteria when the concentration reaches a certain level (>20 g/L), it

inhibits the bacterial cells from producing more n-butanol.⁷⁶ Therefore, despite a growing demand for n-butanol, its global fermentation-based production began to decline during the second part of the last century.



Scheme 1.2: General scheme of acetone-butanol-ethanol (ABE) fermentation process.

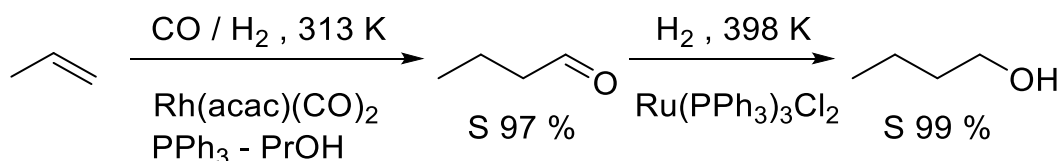
1.4.3.2. Oxo process

Currently, the most efficient method for making n-butanol is from hydroformylation, followed by a consecutive hydrogenation, known collectively as the oxo process. Hydroformylation, or oxo process is one of the largest volume homogeneous catalytic process in the world.⁷⁷ In this reaction, CO and H₂ are added to the C-C double bond of alkenes in liquid phase in the presence of an adequate catalyst, which leads to the formation of aldehydes that can be consecutively hydrogenated to form the corresponding alcohols.

This reaction was discovered in 1938 by the German chemist Otto Roelen using ethylene. Roelen's initial work identified aldehydes and ketones in the product, and the reaction was named the 'oxo' reaction.⁷⁸ Sometime later, working with other olefins such as propylene, Roelen discovered that the reaction shows preference for the aldehyde product, with little formation of ketones. Therefore, the reaction was renamed "hydroformylation". Both names are in common use, but oxo process or oxo synthesis is the most conventional and recognisable name. The classic oxo process, performed with a cobalt catalyst (HCo(CO)₄), uses very high pressure (between 200 and 450 bar depending upon the substrate) and a

range of temperatures from 140 to 180 °C. However, high CO pressure is needed to ensure catalyst stability during hydroformylation. Another major problem of the process is that involves a costly and difficult catalyst recovery cycle. A modification of the classic cobalt process was commercialised in the 1960s, using the cobalt complex $\text{HCo}(\text{CO})_3\text{PR}_3$ as a catalyst. The updated process operates at a lower pressure (around 50 bar) than the 'classic' process, although higher temperature is required (150-200 °C).⁷⁹ In 1976, a more stable and selective homogeneous Rh based catalyst started to be used, in combination with a triphenylphosphine ligand, and around 95 % of the n-butanol produced nowadays uses a Rh catalyst over the Co option (Scheme 1.3).⁸⁰

After hydroformylation, the butyraldehyde product is immediately reduced, usually with the Ru complex with the triphenylphosphine ligand as catalyst ($\text{Ru}(\text{PPh}_3)_3$). Under proper conditions (ratios of PPh_3 with Rh or Ru of $10^3/1$), propylene is almost completely converted into n-butanol with only traces of isobutanol.⁷⁸ The oxo process has been optimised during one hundred years of petrochemistry and is still the most efficient way to produce n-butanol, though the actual industrial method is still very complicated.⁸¹ The Rh catalyst has a tendency to deactivate over time due to the formation of Rh clusters,⁸² which is termed 'intrinsic' deactivation, to distinguish it from deactivation caused by an external source such as catalyst poisons present in the feedstocks. A second problem is the poisoning of the Ru hydrogenating catalyst by CO. For that reason, the addition of CO has to be almost stoichiometric. Alternatively, excess of CO can be purged from the reactor with multiple rinsing with helium before starting the hydrogenation.⁷⁹ Finally, the hydrogenation step benefits from a higher temperature compared to the previous hydroformylation step, making it necessary to have strict control of the timing and conditions.



Scheme 1.3: Basic scheme for oxo process of propene to butyraldehyde followed by hydrogenation to n-butanol,⁷⁰ with conditions, catalysts used and selectivity (S) for the obtained products.

Given the increasing production of bioethanol, and rising price of crude oil, the condensation of two molecules of ethanol to form n-butanol is a commercially and environmentally very attractive alternative to the oxo process and the current fossil fuel feedstock. Condensation of ethanol to n-butanol is possible through the Guerbet reaction.

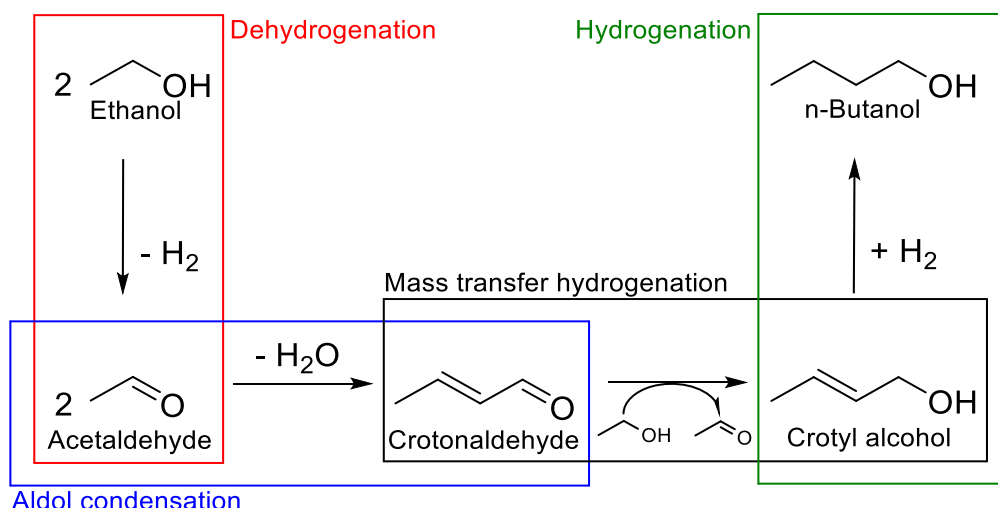
1.5. Guerbet reaction

The Guerbet reaction is long-established method to synthesise higher alcohols from the condensation of two shorter chain alcohols. The coupling can be achieved from two molecules of the same alcohol (self-condensation), leading to linear alcohol or two different alcohols (cross-condensation), leading to a branched alcohol.⁸³ The Guerbet reaction is industrially used to produce long chain alcohols as 2-ethyl-1-hexanol, octanol, 2-pentyl-1-nonanol, n-decanol and heptyl-1-undecanol, all from shorter chain alcohols;⁸⁴ however, this reaction is especially difficult to accomplish in the case of ethanol.

Although different reaction mechanisms have been proposed, it is commonly accepted that the Guerbet reaction includes four different reaction steps: the initial alcohol is first dehydrogenated; the resulting carbonyl compounds are coupled by aldol addition and subsequent dehydration; and finally they are hydrogenated to yield the desired saturated alcohols. Applied to the production of n-butanol, ethanol is first dehydrogenated to form acetaldehyde, which undergoes a self-aldol condensation yielding crotonaldehyde, and then the crotonaldehyde is subsequently reduced to crotyl alcohol, before being finally hydrogenated to the desired n-butanol product (Scheme 1.4). This mechanism is supported by several arguments:

- 1- Intermediate products of the pathway are often observed^{85,86} and can be reduced to the product alcohol under the same conditions.^{87,88}
- 2- The conditions applied in the Guerbet reaction are suitable for the Aldol condensation.⁸⁹
- 3- Addition of C¹³-labelled acetaldehyde to the reaction mixture of ethanol results in a high amount of C¹³-containing Guerbet products⁹⁰ and the rate of product formation is proportional to the concentration of the aldehyde.^{91,92}
- 4- At least one of both reacting alcohols requires an α -methylene group in order to undergo Guerbet condensation, a requisite for the formation of the Aldol condensation product, which cannot occur if both alcohols do not possess an α -hydrogen atom.⁹³

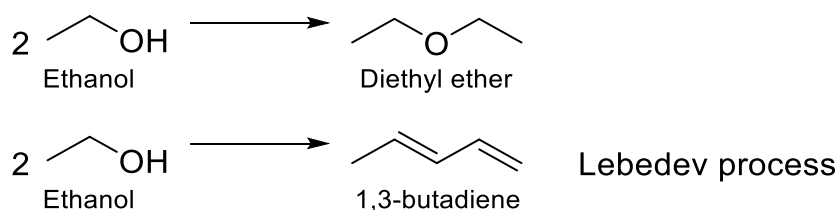
All this evidence supports the aldol-type mechanism for the Guerbet reaction.



Scheme 1.4: General reaction scheme for the Guerbet reaction of ethanol.

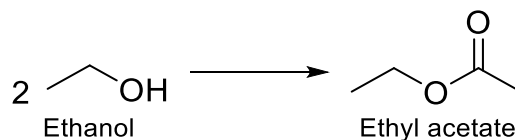
Typically, the Guerbet reaction generates several by-products, many of them generated by further reaction of intermediates.⁹⁴ The most common side reactions include dehydration to olefins or ethers, esterification, oxidation to carboxylic acids and further Aldol condensation to higher alcohols.

Dehydration: Typically, direct dehydration of the initial alcohols results in ethers; for ethanol, the product is diethyl ether. The dehydration of the α,β -unsaturated alcohol intermediates is also possible leading to olefins, which is the case of ethanol for the formation of 1,3-butadiene through the mentioned Lebedev process.⁹⁵



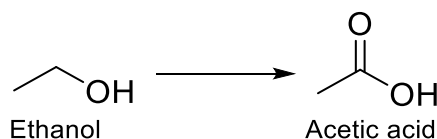
Scheme 1.5: Overall reaction scheme for the dehydrogenation of ethanol.

The Tishchenko reaction: Another frequently reported side reaction is ester formation, which can occur by Tishchenko reaction. In this process, alkoxide species react with aldehydes to form esters *via* a hydride shift.⁹⁶ In the case of ethanol, the product is ethyl acetate.



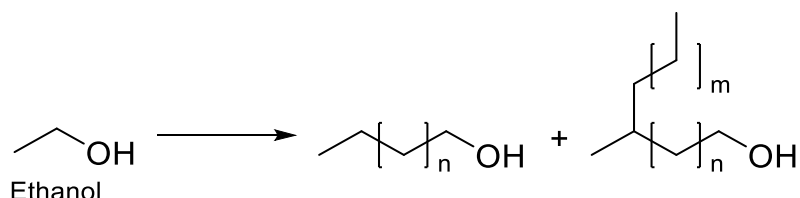
Scheme 1.6: Overall reaction scheme for Tishchenko reaction of ethanol.

The Cannizzaro reaction:^{97,98} During this reaction the reduction of an aldehyde to the corresponding alcohol occurs simultaneously with the oxidation of an aldehyde to the corresponding carboxylic acid. In the case of ethanol, the product is acetic acid.



Scheme 1.7: Overall reaction scheme for Cannizzaro reaction of ethanol.

Further condensation and “cascade of reactions”: Heavier by-products can be formed with undesired consecutive condensation reactions. The described ketones and aldehydes can undergo Aldol condensation to form longer chain carboxylic groups, which can perform the Guerbet hydrogenation to form higher alcohols. In a similar way the produced alcohols can undergo Guerbet reactions to form even higher products in a cycle described as a cascade reaction.^{99,100}



Scheme 1.8: Example scheme for the “cascade of reactions” with formation of linear and branched products.

All the side reactions detailed above make the Guerbet reaction a very complex system (Scheme 1.9), especially in the case of ethanol due to the high reactivity of the acetaldehyde.

A different approach is to carry out the reaction in basic conditions or over basic materials, using different dehydrogenating agents to start the reaction. This second strategy may seem more appealing as the dehydration of the initial alcohol is less probable; however, strong basic conditions leads to the major challenge presented by the Guerbet reaction of ethanol, the uncontrollable “cascade of reactions” at high conversions/reaction times, the Aldol condensation has proven to be uncontrollable. As has been highlighted above, the different products of the Guerbet reaction can suffer consecutive condensation reactions, leading to longer chain and ramified products. Some breakthroughs have been made in the last years using homogeneous catalysts based on metals like Ir or Ru,^{107,108} where different ligands prevent the “cascade of reactions”, improving the selectivity towards n-butanol. Although previous studies of the Guerbet upgrade of ethanol using homogeneous catalysts present better performance for the production of n-butanol at milder conditions, heterogeneous catalysts are more attractive for multiple reasons, including: variety of facile preparation methods; low production costs; high resistance to common reaction conditions; durable lifetime and easy recovery from the reaction mixture, which may allow reusability; and generally lead to great industrial advantages.¹⁰⁹ Herein, the identification of a heterogeneous catalyst that can achieve high selectivity towards n-butanol and high conversion of ethanol remains a challenge.

1.6. Objectives of the thesis

The main focus of this thesis is to investigate the catalytic upgrade of ethanol to n-butanol through Guerbet chemistry using heterogeneous catalysts. The present work divides the Guerbet reaction into its different steps in order to try to find the most adequate combination of different catalysts.

Chapter 3 aims to familiarise with the Guerbet reaction, testing the upgrading of ethanol using a homogeneous Ru based catalyst identified from the literature. The initial focus is to elucidate the reaction network and explore the viability of the Guerbet reaction to obtain n-butanol from ethanol, and to provide a benchmark against which heterogeneous catalysts can be compared. The first step of the Guerbet reaction, acceptorless dehydrogenation of alcohols is then investigated in Chapter 4; using heterogeneous catalysts, extensive optimisation along with kinetic studies for the transformation of different alcohols into their respective aldehydes with release of H₂ are presented. The following steps of the Guerbet reaction, the Aldol condensation and the Meerwein–Ponndorf–Verley (MPV) transfer hydrogenation, are

evaluated in Chapter 5, with a comparison of different heterogeneous catalysts and their activity, selectivity and stability. To finalise the research, in Chapter 6 the selected catalysts for the different steps of the Guerbet reaction are combined in an attempt to perform the full reaction with heterogeneous catalysts.

References

- ¹U.S. Energy Information Administration, "International Energy Outlook 2018"
- ²S. Dale, T. D. Smith, "Back to the future: electric vehicles and oil demand", BP, 2016
- ³IndexMundi, "World Coal Consumption by Year" 2013
- ⁴International Energy Agency, "Share of electricity production from fossil fuels", The World Bank, 2016
- ⁵International Energy Agency, "Global coal consumption forecast to slow", The Guardian, 2017
- ⁶International Energy Agency, "IEA sees global gas demand rising to 2022 as US drives market transformation", 2017
- ⁷Our World in Data, "Years of fossil fuel reserves left", based on BP Statistical Review of World Energy 2016
- ⁸M. S. Roni, S. Chowdhury, S. Mamun, M. Marufuzzaman, W. Lein, S. Johnson, *Renew. Sustain. Energy Rev.*, 2017, **78**, 1089–1101
- ⁹P. Gallezot, "Catalysis for Renewables: From Feedstock to Energy Production", Wiley, Weinheim, 2007
- ¹⁰E. V. Kondratenko, G. Mul, J. Baltrusaitis, G. O. Larrazábal, J. Pérez-Ramírez, *Energy Environ. Sci.*, 2013, **6**, 3112 - 3135
- ¹¹G. Centi, S. Perathoner, *Catal. Today*, 2009, **148**, 191 - 205
- ¹²S. C. Roy, O. K. Varghese, M. Paulose, C. A. Grimes, *ACS Nano*, 2010, **4**, 1259 - 1278
- ¹³S. Das, W. M. A. Wan Daud, *RSC Adv.*, 2014, **4**, 20856 - 20893
- ¹⁴C. O. Tuck, E. Perez, I. T. Horvath, R. A. Sheldon, M. Poliakoff, *Science*, 2012, **337**, 695
- ¹⁵R. A. Sheldon, *Green Chem.*, 2014, **16**, 950
- ¹⁶Retrieved from <https://newvitruvian.com/> 2019
- ¹⁷A. Akhtar, V. Krepl, T. Ivanova, *Energy Fuels*, 2018, **32**, 7, 7294-7318
- ¹⁸"2019 Ethanol Industry Outlook". Renewable Fuels Association. 2019
- ¹⁹European renewable ethanol association ePURE, Resources & Statics, "Renewable ethanol production by end use", 2019
- ²⁰Japanese Ministry of economy, trade & industry, "World Fuel Ethanol Analysis and Outlook" 2016
- ²¹U. S. Department of energy, "Global ethanol production 2017"
- ²²K. Dutta, A. Daverey, J. Lin, *Renew. Energy*, 2014, **69**, 114–122
- ²³C. Manochio, B. R. Andrade, R. P. Rodriguez, B. S. Moraes, *Renew. Sustain. Energy Rev.*, 2017, **80**, 743–755
- ²⁴H. Zabed, J. N. Sahu, A. N. Boyce, G. Faruq, *Renew. Sustain. Energy Rev.* 2016, **66**, 751–774
- ²⁵A. H., Sebayang, H. H. Masjuki, H. C. Ong, S. Dharma, A. S. Silitonga, T. M. Mahlia, H. B. Aditiya, *RSC Adv.*, 2016, **6**, 14964–14992.
- ²⁶L. Rocha, M. Raud, K. Orupöld, T. Kikas, *Agron. Res.*, 2017, **15**, 830–847
- ²⁷O. Hromatka, H. Ebner, *Ind. Eng. Chem. Res.*, 1959, **51**, 10, 1279–1280
- ²⁸"The Ethylene Technology Report", Research and Markets, 2016
- ²⁹S. Gong, C. Shao, L. Zhu, *Energy.*, 2019, **182**, 280-295
- ³⁰Chemical economics handbook, HIS Markit, 2019
- ³¹D. Y. Ngan, P. Jeffrey, A. J. Baumgartner (2003), US Patent No. US 6,632,351 B1
- ³²E. Heracleous, A. F. Lee, K. Wilson, A. A. Lemonidou, *J. Catal.*, 2005, **231**, 1, 159-171
- ³³"Ethylene (ET): World Market Outlook and Forecast up to 2028", Merchant research and consulting, 2019
- ³⁴"Ethers, by Lawrence Karas and W. J. Piel". Kirk-Othmer Encyclopedia of Chemical Technology. 2004

- ³⁵ D. Varisli, T. Dogu, G. Dogu, *Chem. Eng. Sci.*, 2007, **62**, 5349-5352
- ³⁶ M. Uebelacker, D. W. Lachenmeier, *J. Anal. Methods. Chem.*, 2011, **2011**, 1-13
- ³⁷ Acetaldehyde, *Chemical economics handbook, HIS Markit*, 2016
- ³⁸ A. S. Hester, K. Himmler, *Ind. Eng. Chem.*, 1959, **51**, 12, 1424-1430
- ³⁹ K. Muniz "Catalytic Oxidation in Organic Synthesis", *Science of Synthesis*, 20188
- ⁴⁰ R. A. Fernandes, D. A. Chaudhari, *J. Org. Chem.*, 2014, **79**, 12, 5787-5793
- ⁴¹ D. Lai, J. Li, P. Huang, D. Wang, *J. Nat. Gas Chem.*, 1994, **3**, 2, 211-218
- ⁴² *Global markets Insights, Hydrogen Generator Market Size by Product*, 2016
- ⁴³ G. Manzolini, S. Tosti, *Int. J. Hydrog. Energy*, 2008, **33**, 20, 5571-5582
- ⁴⁴ F. Díaz Alvarado, F. Gracia, *Chem. Eng. J.*, 2010, **165**, 2, 649-657
- ⁴⁵ PR Newswire, Apr. 4, 2018, Retrieved from <https://markets.businessinsider.com/news/stocks/>
- ⁴⁶ T. Seki, T. Nakajo, M. Onaka, *Chem. Lett.*, 2006, **35**, 8, 824-829
- ⁴⁷ Butadiene, *Chemical economics handbook, HIS Markit*, 2018
- ⁴⁸ J. Grub, E. Löser, "Butadiene". *Ullmann's Encyclopedia of Industrial Chemistry*, 2012
- ⁴⁹ S. Shylesh, A. A. Gokhale, C. D. Scown, D. Kim, C. R. Ho, A. T. Bell, *ChemSusChem*, 2016, **9**, 1462–1472
- ⁵⁰ "Alcohol use and safe drinking", *US National Institutes of Health*, 2014
- ⁵¹ S. S. Block, "Disinfection, Sterilization, and Preservation" *Lippincott Williams & Wilkins*, 2001
- ⁵² L. A. Pohorecky, J. Brick, *Clin. Pharmacol. Ther.*, 1988, **36**, 2–3, 335-427
- ⁵³ R. Scalley, "Treatment of Ethylene Glycol Poisoning". *American Family Physician*, 2002
- ⁵⁴ H. O. Hardenberg, "Samuel Morey and his atmospheric engine", 1992
- ⁵⁵ V. E. Geoa, D. J. Godwina, S. Thiyagarajana, C.G. Saravananb, F. Alouic, *Fuel*, 2019, **256**, 115806
- ⁵⁶ *US Energy information Administration, "Renewable fuel standard program" 2017*
- ⁵⁷ Retrieved from <https://www.mycleanfuel.com/category-s/191.htm>, 2019
- ⁵⁸ W. Horn, F. Krupp, "Earth: The Sequel: The Race to Reinvent Energy and Stop Global Warming", 2006
- ⁵⁹ "Transportation Energy Data Book". *Centre for Transportation Analysis of the Oak Ridge National Laboratory*. 2018
- ⁶⁰ M. Eyidogan, A. N. Ozsezen, M. Canakci, A. Turkcan, *Fuel*, 2010, **89**, 10, 2713-2720
- ⁶¹ I. Staffell, "The energy and fuel data sheet", *University of Birmingham*, 2011
- ⁶² W. Hsieh, R. Chen, T. Wu, T. Lin, *Atmos. Environ*, 2002, **36**, 3, 403-410
- ⁶³ B. Bahri, A. A. Aziz, M. Shahbakhti, M. Farid, M. Said, *Appl. Energy*, 2013, **108**, 24,33
- ⁶⁴ S. Atsumi, A. F. Cann, M.R. Connor, C. R. Shen, K. M. Smith, M. P. Brynildsen, K. J. Y. Chou, T. Hanai, J. C. Liao, *Metab. Eng.*, 2008, **10**, 305–311
- ⁶⁵ "n-Butanol Report 2018-2022: Global \$5.58 Bn Market Driven by Growing Construction Industry in Emerging Economies", *Research & Markets*, 2018
- ⁶⁶ "Bio-butanol Market Analysis by Application (Acrylates, Acetates, Glycol Ethers, Solvents, Plasticizers), And Segment Forecasts To 2022", *Grand view Research*, 2015
- ⁶⁷ D. C. Rakopoulos, C. D. Rakopoulos, E. G. Giakoumis, A. M. Dimaratos, D. E. Kyritsis, *Energ. Convers. Manage.* 2010, **51**, 10, 1989-1997
- ⁶⁸ N. Qureshi, B. C. Saha, B. Dien, R. E. Hector, M. A. Cotta, *Biomass Bioenerg.*, 2010, **34**, 559-565
- ⁶⁹ K. Brekke, "Butanol an energy alternative?" *Ethanol Today*, 2007
- ⁷⁰ T. V. Rasskazchikova, V. M. Kapustin, S. A. Karpov, *Chem. Tech. Fuels Oil*, 2004, **40**, 203-210
- ⁷¹ B. Rajesh Kumar, S. Saravanan, *Renew. Sust. Energ. Rev.*, 2016, **60**, 84–115
- ⁷² I. Staffell, "The energy and fuel data sheet", *University of Birmingham*, 2011
- ⁷³ A. Poehlein, J. D. Montoya, S. K. Flitsch, P. Krabben, K. Winzer, S. J. Reid, D. T. Jones, E. Green, N. P. Minton, R. Daniel, P. Dürre, *Biotechnol Biofuels*, 2017, **10**, 58
- ⁷⁴ L. Pasteur, *Bull. Soc. Chim. Fr.*, 1862, **52**, 1862
- ⁷⁵ P. Duerre, "Handbook of Clostridia", *CRC Press*, 2005
- ⁷⁶ T. C. Ezeji, N. Qureshi, H. P. Blaschek, *Appl. Microbiol. Biotechnol.*, 2004, **63**, 6, 653–658
- ⁷⁷ M. Beller, B. Cornils, C. D. Frohning, C. W. Kohlpaintner, *J. Mol. Catal A: Chemical*, 1995, **104**, 17
- ⁷⁸ H. Hahn, G. Dämbkes, N. Rupprich, H. Bahl, G. D. Frey, "Ullmann's Encyclopedia of Industrial Chemistry", 2013
- ⁷⁹ "Hydroformylation. In: *Aqueous Organometallic Catalysis. Catalysis by Metal Complexes*", Springer, Dordrecht, 2002
- ⁸⁰ J. Zakzeski, H. R. Lee, Y. L. Leung and A. T. Bell, *Appl. Catal. A: General*, 2010, **374**, 201
- ⁸¹ Jerry D. Unruh; Debra A. Ryan, 1999, US Patent No 5,922,921
- ⁸² W. P. Griffith, *Platinum Metals Rev.*, 2007, **51**, 3, 150
- ⁸³ C. Carlini, M. Di Girolamo, M. Macinai, M. Marchionna, M. Noviello, A. M. R. Galletti, G. Sbrana, *J. Molec. Catal. A: Chem.*, 2003, **204**, 5, 721-728

- ⁸⁴ G. Knothe, *Lipid Technol.*, 2002, **14**, 101-104
- ⁸⁵ P. L. Burk, R. L. Pruett and K. S. Campo, *J. Mol. Catal.*, 1985, **33**, 1-14
- ⁸⁶ J. I. Di Cosimo, C. R. Apesteguía, M. J. L. Ginés and E. Iglesia, *J. Catal.*, 2000, **190**, 261-275
- ⁸⁷ V. Nagarajan and N. R. Kuloor, *Indian J. Technol.*, 1966, **4**, 46-54
- ⁸⁸ S. Ogo, A. Onda and K. Yanagisawa, *Appl. Catal., A*, 2011, **402**, 188-195
- ⁸⁹ A. S. Ndou and N. J. Coville, *Appl. Catal., A*, 2004, **275**, 103-110
- ⁹⁰ M. J. L. Gines and E. Iglesia, *J. Catal.*, 1998, **176**, 155-172
- ⁹¹ V. Nagarajan, *Indian J. Technol.*, 1971, **9**, 380-386
- ⁹² S. Veibel and J. I. Nielsen, *Tetrahedron*, 1967, **23**, 1723-1733
- ⁹³ C. H. Weizmann, E. Bergmann and M. A. X. Sulzbacher, *J. Org. Chem.*, 1950, **15**, 54-57
- ⁹⁴ H. Tsuji, F. Yagi, H. Hattori and H. Kita, *J. Catal.*, 1994, **148**, 759-770
- ⁹⁵ A. Chiericato, J. Velasquez Ochoa, C. Bandinelli, G. Fornasari, F. Cavani, M. Mella, *ChemSusChem*, 2015, **8**, 377-388.
- ⁹⁶ H. Hattori, *Chem. Rev.*, 1995, **95**, 537-558
- ⁹⁷ J. J. Bravo-Suárez, B. Subramaniam, R. V. Chaudhari, *Appl. Catal., A*, 2013, **455**, 234-246
- ⁹⁸ A. Gangadharan, M. Shen, T. Sooknoi, D. E. Resasco, R. G. Mallinson, *Appl. Catal., A*, 2010, **385**, 80-91
- ⁹⁹ T. Moteki, A. T. Rowley, D. W. Flaherty, *ACS Catalysis* 2016, **6**, 11, 7278-7282
- ¹⁰⁰ T. Moteki, D. W. Flaherty, *ACS Catal.*, 2016, **6**, 7, 4170-4183
- ¹⁰¹ D. Gabriëls, W. Y. Hernández, B. Sels, P. Van Der Voort, A. Verberckmoes, *Catal. Sci. Technol.*, 2015, **5**, 3876-3902
- ¹⁰² M. Guerebet, C. R. Hebd, *Séances Acad. Sci.*, 1899, **128**, 511-513
- ¹⁰³ J. I. Di Cosimo, V. K. Díez, M. Xu, E. Iglesia and C. R. Apesteguía, *J. Catal.*, 1998, **178**, 499-510
- ¹⁰⁴ D. L. Carvalho, R. R. de Avillez, M. T. Rodrigues, L. E. P. Borges, L. G. Appel, *Appl. Catal., A*, 2012, **415-416**, 96-100
- ¹⁰⁵ T. W. Birky, J. T. Kozlowski and R. J. Davis, *J. Catal.*, 2013, **298**, 130-137
- ¹⁰⁶ T. Tsuchida, J. Kubo, T. Yoshioka, S. Sakuma, T. Takeguchi and W. Ueda, *J. Catal.*, 2008, **259**, 183-189
- ¹⁰⁷ R. L. Wingad, P. J. Gates, S. T. G. Street, D. F. Wass, *ACS Catal.*, 2015, **5**, 5822-5826
- ¹⁰⁸ S. Chakraborty, P. E. Piszal, C. E. Hayes, R. T. Baker, W. Jones, *J. Am. Chem. Soc.*, 2015, **137**, 14264-14267
- ¹⁰⁹ G. Ertl, "Handbook of Heterogeneous Catalysis", Wiley-VCH, Weinheim-New York, 2008

2. Experimental and methods

2.1. Formula and expressions

Conversion:

$$X_{(Substrate)} = \frac{([Substrate]_0 - [Substrate]_t)}{[Substrate]_0} \times 100 \quad [Equation 2.1]$$

Yield:

$$Y_{(Product)} = \frac{[Product]_t}{[Substrate]_0} \times 100 \quad [Equation 2.2]$$

Selectivity:

$$S_{(Product)} = \frac{[Product]_t}{([Substrate]_0 - [Substrate]_t)} \times 100 \quad [Equation 2.3]$$

Carbon Balance:

$$C.B. = \frac{\sum Carbon_t}{\sum Carbon_0} \times 100 \quad [Equation 2.4]$$

Turnover Number:

$$TON = \frac{\text{moles of substrate converted}}{\text{moles of metal}} \quad [Equation 2.5]$$

Turnover Frequency:

$$TOF (h^{-1}) = \frac{\text{moles of substrate converted}}{\text{moles of metal} \times \text{time}} \quad [\text{Equation 2.6}]$$

Contact time:

$$CT (\text{min}) = \frac{\text{volume}_{\text{catalyst bed}}}{\text{flow rate}} \quad [\text{Equation 2.7}]$$

Space-time-Yield:

$$STY (g_{\text{product}} \text{ mL}^{-1} h^{-1}) = \frac{\text{mass}_{\text{product}}}{\text{time} \times \text{volume}_{\text{reactor}}} \quad [\text{Equation 2.8}]$$

2.2. Catalysts employed

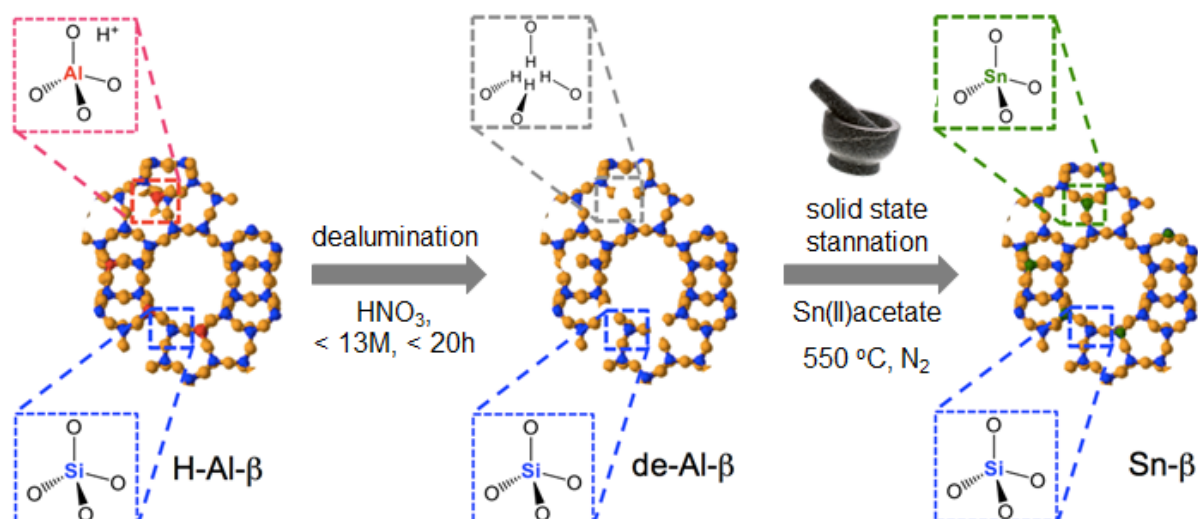
In this study two main kinds of heterogeneous catalysts were employed: Lewis acid silicalites and metal supported nanoparticles. Details for material preparations for all the catalysts presented in this work are described below.

2.2.1. Catalyst preparation

The catalysts listed in Section 2.2.1.1 and Section 2.2.1.2 were synthesised by Luca Botti and Ricardo Navar.

2.2.1.1. Solid state incorporation

Commercial zeolite Al- β ($\text{SiO}_2/\text{Al}_2\text{O}_3 = 38$) in its protonic form was first de-aluminated by treatment in a solution of HNO_3 (13 M HNO_3 , 100 °C, 20 mL g^{-1} zeolite) for a total of 20 h. The proton form of the Al- β zeolites (H-Al- β) was first obtained after treatment at 550 °C in a tubular furnace for 3 h under air flow.



Scheme 2.1: Graphical representation of the synthesis of Sn- β via solid state incorporation (SSI). Adapted from Hammond *et al.*¹

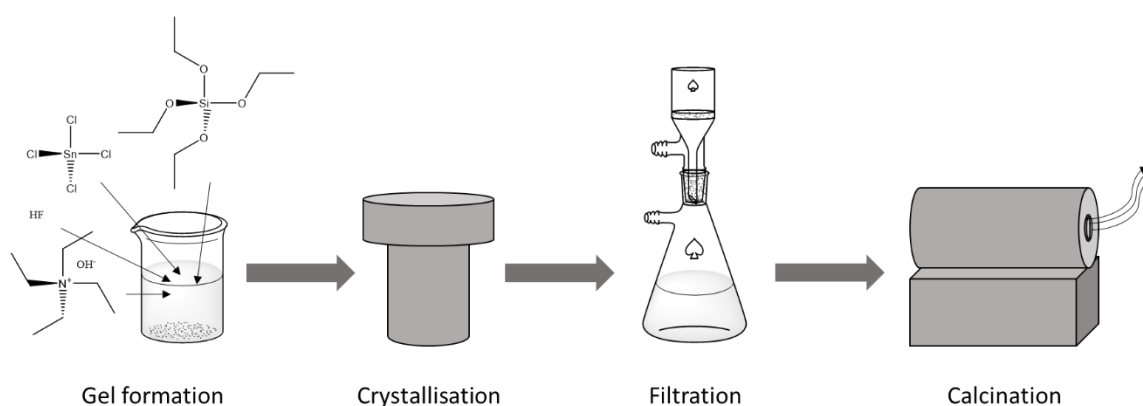
Solid State Incorporation (SSI) of Sn and Hf into de-aluminated zeolite β was performed by grinding the appropriate amount of metal precursor with the necessary amount of dealuminated zeolite for 10 min in a pestle and mortar. The catalysts employed in this work with metal loading of 1 wt.% were synthesised and named Sn- β SSI and Hf- β SSI respectively. Typically, to make 1 g of Sn- β 1 wt.%, 0.020 g of Sn(II)acetate and 0.990 g of de-aluminate β were mixed and ground together for 10 min. In the case of Hf- β , 0.018 g of Hf(IV)Cl₄ and 0.990 g of de-aluminate β were mixed and ground together for 10 min. Following this procedure, the sample was heated in a tubular combustion furnace (Carbolite MTF12/38/400) to 550 °C (10 °C min⁻¹ ramp rate) first in a flow of N₂ (3 h) and subsequently air (3 h) for a total of 6 h. Gas flow rates of 60 mL min⁻¹ were employed at all times.

List of chemicals used for this procedure: zeolite Al- β (Zeolyst®, NH₄-form), HNO₃ (70 %, Fisher scientific®), Sn(II)acetate (99 %, Sigma Aldrich®), Hf(IV)Cl₄ (98 %, Sigma Aldrich®).

2.2.1.2. Hydrothermal synthesis

The catalysts employed in this work with metal loading of 1 wt.% were synthesised and named Sn- β HDT, Hf- β HDT and Zr- β HDT respectively. Typically to synthesize Hf- β HDT, 30.6 g of tetraethyl orthosilicate (TEOS) were added to 33.1 g of tetraethylammonium hydroxide (TEAOH) (Sigma Aldrich®, 35 %) under careful stirring, forming a two-phase system. After 60–90 min, one phase was obtained and 0.235 g of HfCl₄ (Sigma Aldrich®, 98 %), dissolved in 2.0 mL of H₂O, was added to the solution dropwise. The solution was then left for several h

under stirring until a viscous gel was formed. The gel was analysed by the addition of 3.1 g HF in 1.6 g of demineralised H₂O, yielding a solid gel with the molar composition: 1.0Si: 0.005Hf: 0.02Cl⁻: 0.55TEA⁺: 0.55F⁻: 7.5H₂O. Sn-β and Zr-β were prepared with the same methodology changing the metal precursor. Purely siliceous β was prepared following the same route, only leaving out the addition of the metal source. All samples were then homogenised and transferred to a Teflon-lined stainless steel autoclave and heated statically at 140 °C for a duration of 7 days. The obtained solid was recovered by filtration and washed with ample amounts of deionised H₂O, followed by drying over-night at 80 °C in air. The synthesis was finalised by removing the organic template, by heating the sample at 2 °C min⁻¹ to 550 °C in static air and maintaining this temperature for 6 h.



Scheme 2.2: Graphical representation of the synthesis of Sn-β *via* Solid State Incorporation (SSI). Adapted from Hammond *et al.*¹

List of chemicals used for this procedure: TEOS (≥99 %, Sigma Aldrich®), TEAOH 35 %, Sigma Aldrich®), Hf(IV)Cl₄ (98 %, Sigma Aldrich®), Zr(IV)Cl₄ (99.9 %, Sigma Aldrich®), Sn(IV)Cl₄ (98 %, Sigma Aldrich®), HF (49 %, Sigma Aldrich®).

2.2.1.3. Ag/HT synthesis

To prepare the Ag/HT catalyst, 2 g of the hydrotalcite support (HT) was carefully added to 20 mL of AgNO₃ aqueous solution (0.5 M). The heterogeneous mixture was stirred for 1 h in air, submerged in an ice-water bath. The resulting slurry was filtered, washed thoroughly with deionised H₂O, and dried at room temperature to yield a white powder. To finalise the synthesis, the Ag/HT catalyst was subjected to a heat treatment in a tubular combustion

furnace (Carbolite MTF12/38/400) in reducing atmosphere ($10\text{ }^{\circ}\text{C min}^{-1}$, 30 min at $110\text{ }^{\circ}\text{C}$ in H_2).

List of chemicals used for this procedure: Hydrotalcite (synthetic, Sigma Aldrich®), AgNO_3 (>99 %, Sigma Aldrich®).

2.2.1.4. Commercial catalysts used throughout the thesis

In addition to the synthesised materials described above, these listed commercial catalysts were also employed in this work: Pd/C (5 Pd wt.% on activated C, Sigma Aldrich®), Pd/ Al_2O_3 (5 Pd wt.% on γ - Al_2O_3 , Sigma Aldrich®), $[\text{RuCl}_2(\eta^6\text{-}p\text{-cymene})]_2$ (dimer, Sigma Aldrich®) and 2-(diphenylphosphino)ethylamine ($\geq 95\%$, Sigma Aldrich®).

2.3. Kinetic evaluation

2.3.1. Batch Guerbet reaction of ethanol



Figure 2.1: Asynt PressureSyn high pressure autoclave reactor. Pictures retrieved from www.asynt.com.

Batch Guerbet reactions were carried out in a 125 mL stainless steel Asynt PressureSyn high pressure autoclave reactor, with aluminium heating mantle and magnetic stirring, connected to a vent line through a rupture disk. Appropriate amounts of the catalyst $[\text{RuCl}_2(\eta^6\text{-}p\text{-cymene})]_2$ (0.05 mol% Ru with respect to ethanol), biphenyl as internal standard (0.2 M) and EtONa (5 mol% with respect to ethanol) were added to a clean oven-dried glass liner, inserted

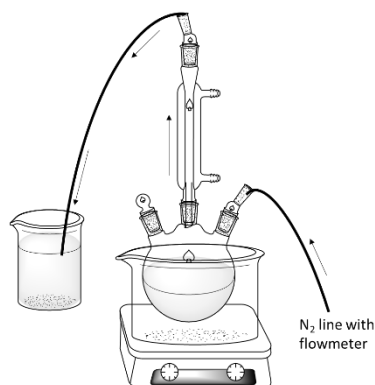
in the glovebox. In an inert atmosphere (N_2), 15 mL of ethanol and appropriate amounts of the ligand 2-(diphenylphosphino)ethylamine (typically, 0.05 mol% unless otherwise stated) were added. The glass liner was then sealed within the autoclave, before removal from the glovebox. The autoclave was then placed into the pre-heated (150 °C) aluminium heating block (Figure 2.1) and left to reach the appropriate temperature for 10 min. The reaction was then started by turning on the magnetic stirring and carried out at 750 rpm, for different times. After the reaction run time, the autoclave was cooled down in an ice-water bath. Subsequently, the autoclave was vented to remove any gas generated during the reaction. The liquid samples were removed, further dissolved in 135 mL of methanol and filtered through a short plug of Silica gel prior to injection into a gas chromatograph (GC). The GC employed was an Agilent 7820 equipped with a 25 m CP-Wax 52 CB capillary column and a Flame Ionisation Detector (FID), with He as carrier gas (5 mL min^{-1}). Reactants were quantified against biphenyl as internal standard. More details on this analytical technique can be found in Section 2.4.2.

List of chemicals used for these experiments: ethanol (absolute HPLC grade, Fisher scientific®), biphenyl ($\geq 95 \%$, Sigma Aldrich®), EtONa ($\geq 95 \%$, Sigma Aldrich®), methanol (absolute HPLC grade, Fisher scientific®).

2.3.2. Batch acceptorless dehydrogenation of 1-phenylethanol on glass reactor

Batch acceptorless dehydrogenation reactions were carried out in a three neck 100 mL round bottom flask equipped with a reflux condenser and glass cap adaptors. The system was connected to a N_2 line and the gas flow was controlled using a mass flow controller. The reaction temperature was controlled by immersion in a silicon oil bath (Scheme 2.3). The flask was charged at room temperature with 20 mL of a solution of 1-phenylethanol 0.2 M in *p*-xylene and various amounts of Pd/C catalyst (or Ag/HT where stated) in the range 0-1.25 mol% Pd/1-phenylethanol molar ratio (0-106.8 mg of Pd/C). For all reactions, the flask was purged with a N_2 flow of 50 mL min^{-1} for 6 min. Unless specified, the flow was then decreased to 10 mL min^{-1} of N_2 and the flask was introduced in the oil bath and pre-heated at the desired temperature, between 100-120 °C. The reaction was then initiated by switching on the magnetic stirring, typically 750 rpm, unless otherwise specified. After the reaction, the flask was cooled down to room temperature, the catalyst was recovered by filtration and each sample was prepared by adding 100 μL of reaction solution to 900 μL of a solution of biphenyl in toluene (0.01 M), which acts as external standard. The samples were analysed by the GC

system described in Section 2.3.1. The concentration of acetophenone and 1-phenylethanol were obtained by previous GC calibration with their respective standards. More details on this analytical technique can be found in Section 2.4.2.



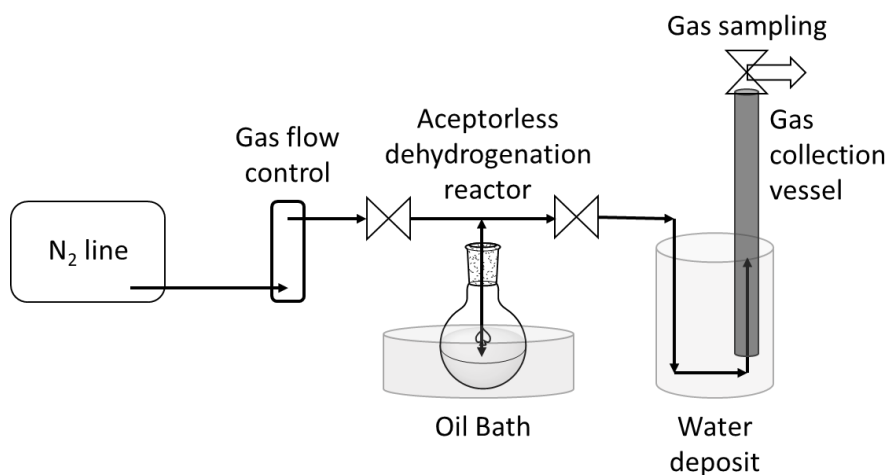
Scheme 2.3: Reaction scheme for 1-phenylethanol dehydrogenation in classic batch reactor.

List of chemicals used for these experiments: 1-phenylethanol (98 %, Sigma Aldrich®), *p*-xylene (99 %, Alfa Aesar®), toluene (99.5 %, Alfa Aesar®), biphenyl (≥ 95 %, Sigma Aldrich®).

2.3.3. Batch acceptorless dehydrogenation of 1-phenylethanol in stainless steel reactor body with a pressurised connection vessel

Batch acceptorless dehydrogenation reactions were carried out in a one necked 100 mL Ace round-bottom pressure flask with an Ace-Thread 15 PTFE front-seal plug. The flask was connected to a stainless-steel body reactor, connected to a burette (Scheme 2.4). This vessel was isolated from the atmosphere with a water tank. The system was connected to a N₂ line and the gas flow was controlled using a mass flow controller. The reaction temperature was controlled by immersion in a silicon oil bath, between 110-130 °C. The flask was charged at room temperature with 20 mL of a solution of 1-phenylethanol in *p*-xylene 0.2 M and appropriate amount of catalyst (typically Pd/C unless specified, 0.08 mol% Pd/1-phenylethanol molar ratio). For all reactions, the flask was purged with a flow of 50 mL min⁻¹ of N₂ for 10 min at room temperature. When a H₂ measurement was required, the flow was then stopped for the reaction to be carried out under static N₂ atmosphere. For experiments with N₂ flow, the reaction was carried out using a N₂ flow rate of 10 mL min⁻¹. The flask was introduced into the oil bath and pre-heated to the desired temperature for 15 min. The reaction was then initiated

by switching on the magnetic stirring (750 rpm). For kinetic studies, the gas produced during the reactions was collected in the burette allowing the quantification of the H₂ produced. Aliquots of gas sample were then collected and analysed by Mass Spectrometer (MS). More details on this analytical technique can be found in Section 2.4.1. Analyses of the liquid samples were performed analogously to the procedure described in Section 2.3.2. Theoretical volume of gas V , was calculated from the ideal gas equation, $PV = nRT$, considering n = mols of produced acetophenone, $T = 12\text{ }^{\circ}\text{C}$, $P = 1\text{ atm}$ and $R = 0.082\text{ L}\cdot\text{atm} / \text{K}\cdot\text{mol}$.



Scheme 2.4: Scheme of stainless steel body batch reactor for 1-phenylethanol dehydrogenation

List of chemicals used for these experiments: 1-phenylethanol (98 %, Sigma Aldrich®), *p*-xylene (99 %, Alfa Aesar®), toluene (99.5 %, Alfa Aesar®), biphenyl (≥ 95 %, Sigma Aldrich®).

2.3.4. Batch acceptorless dehydrogenation of benzyl alcohol, and deuterated and *p*-substituted analogues, in stainless steel reactor body with a pressurised connection vessel

The setup, methodology and analyses of the liquid samples were performed analogously to the procedure described in Section 2.3.3, charging the flask at room temperature with 20 mL of a solution of the desired substrate in *p*-xylene (0.2 M).

List of chemicals used for these experiments: benzyl alcohol (99,8 %, Sigma Aldrich®), 4-chlorobenzyl alcohol (99 %, Sigma Aldrich®), 4-methylbenzyl alcohol (98 %, Sigma Aldrich®), benzyl alcohol- α,α -d₂ (98 %, Sigma Aldrich®), *p*-xylene (99 %, Alfa Aesar®), toluene (99.5 %, Alfa Aesar®), biphenyl (≥ 95 %, Sigma Aldrich®).

2.3.5. Hot filtration experiment

Setup and analyses of the liquid samples were performed analogously to the procedure described in Section 2.3.3. During the first part of the hot filtration experiment, a general reaction with the solid catalyst, as described earlier in 2.3.3. was performed. After 5 min of reaction, the reaction mixture was withdrawn, and the solid catalyst was removed by filtration. The filtered reaction mixture was then added into another flask equipped with a magnetic stirrer, purged with a flow of 50 mL min⁻¹ of N₂ for 10 min at room temperature and heated again. The reaction was then continued by switching on the magnetic stirring, this time in the absence of the solid catalyst. After an appropriate length of time, the reaction solution was re-analysed to determine any differences in substrate conversion or product yield in the absence of the solid catalyst.

List of chemicals used for these experiments: 1-phenylethanol (98 %, Sigma Aldrich®), p-xylene (99 %, Alfa Aesar®), toluene (99.5 %, Alfa Aesar®), biphenyl (≥95 %, Sigma Aldrich®).

2.3.6. Batch hydrogenation of acetophenone and styrene

Batch hydrogenation reactions were carried out using a 100 mL Parr autoclave (Compact Mini Bench Top Reactor 5500) equipped with a glass liner and mechanical stirrer, connected to a Parr 4848 Reactor controller (Figure 2.2). For all the experiments, the vessel was charged with 20 mL of the desired substrate in toluene (0.2 M) along appropriate amounts of a Pd/C catalyst (0.08 mol% Pd/1-phenylethanol molar ratio) and sealed. The reactor was purged and charged with 2 bar of H₂ gas and subsequently heated to 130 °C. The reaction was started with magnetically stirring and carried out for 1h. After the reaction run time, the autoclave was cooled in an ice-water bath. The autoclave was subsequently vented to remove any gas left. Analyses of the liquid samples were performed analogously to the procedure described in Section 2.3.2.

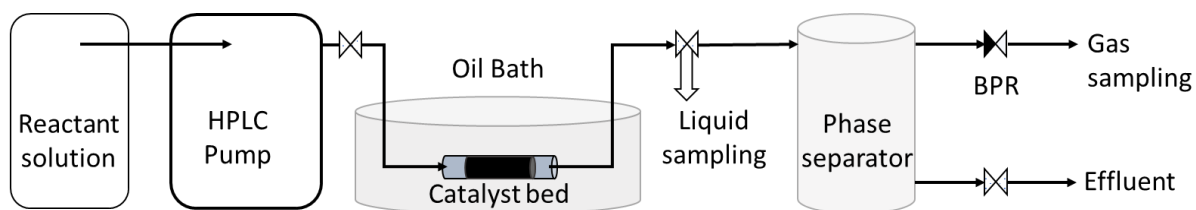


Figure 2.2: Compact Mini Bench Top Reactor 5500. Pictures from www.parrinst.com.

List of chemicals used for these experiments: acetophenone (99 %, Sigma Aldrich®), styrene (≥ 99 %, Sigma Aldrich®), p-xylene (99 %, Alfa Aesar®), toluene (99.5 %, Alfa Aesar®), biphenyl (≥ 95 %, Sigma Aldrich®).

2.3.7. Continuous flow: acceptorless dehydrogenation of 1-phenylethanol

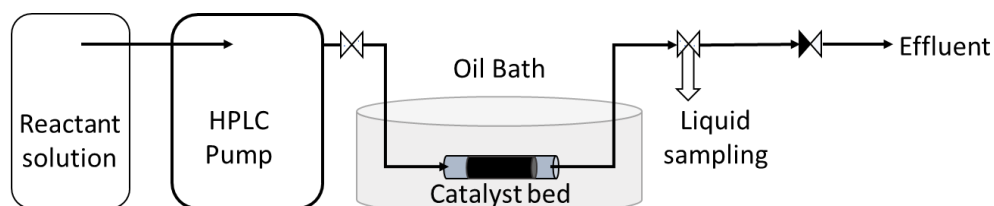
Continuous acceptorless dehydrogenation reactions were performed in a plug flow, stainless steel, tubular reactor (PFR). The reactor was connected to an HPLC pump (Agilent 1200) in order to regulate the reactant flow and allow operation at elevated pressures. The reactor was connected to a Swagelok TPED phase separator cylinder, to separate the gas produced (Scheme 2.5). The reactor temperature was controlled by immersion in an oil bath, and the pressure (10 bar) was controlled by means of a back pressure regulator. The reactant used was a solution of 1-phenylethanol in toluene (0.2 M). The catalyst, Pd/C (0.08 g) was placed in between two plugs of quartz wool and densely packed into a 1/4 inch stainless steel tube (3.8 mm ID), and a frit (0.5 mm) was placed at the end of the bed to avoid any loss of material. A contact time of 0.45 min and temperature of 130 °C were typically employed. Aliquots of the reaction solutions were taken periodically from a sampling valve placed after the reactor. Analyses of the liquid samples were performed analogously to the procedure described in Section 2.3.2.



Scheme 2.5: Scheme of plug flow reactor for 1-phenylethanol dehydrogenation in continuous flow.

List of chemicals used for these experiments: 1-phenylethanol (98 %, Sigma Aldrich®), toluene (99.5 %, Alfa Aesar®), biphenyl (≥ 95 %, Sigma Aldrich®).

2.3.8. Continuous flow: Aldol condensation of benzaldehyde with acetone



Scheme 2.6: Scheme of plug flow reactor for benzaldehyde and acetone Aldol condensation in continuous flow.

Continuous acceptorless dehydrogenation reactions were performed in a stainless steel PFR. The reactor was connected to an HPLC pump (Agilent 1200) in order to regulate the reactant flow and allow operation at elevated pressures (Scheme 2.6). The reactor temperature was controlled by immersion in an oil bath, and the pressure (10 bar) was controlled by means of a back pressure regulator. The reactant used was a solution of benzaldehyde (0.1 M) and acetone (0.3 M) in toluene. The selected catalyst was placed in between two plugs of quartz wool and densely packed into a 1/4 inch stainless steel tube (3.8 mm ID), and a frit (0.5 mm) was placed at the end of the bed to avoid any loss of material. A contact time of 3.5 min and temperature of 160 °C were typically employed, otherwise specified. Aliquots of the reaction solutions were taken periodically from a sampling valve placed after the reactor. Analyses of the liquid samples were performed analogously to the procedure described in Section 2.3.2.

List of chemicals used for these experiments: benzaldehyde ($\geq 99\%$, Sigma Aldrich®), acetone (HPLC grade, Fisher scientific®), toluene (99.5 %, Alfa Aesar®), biphenyl ($\geq 95\%$, Sigma Aldrich®).

2.3.9. Continuous flow: Meerwein–Ponndorf–Verley transfer hydrogenation of furfural

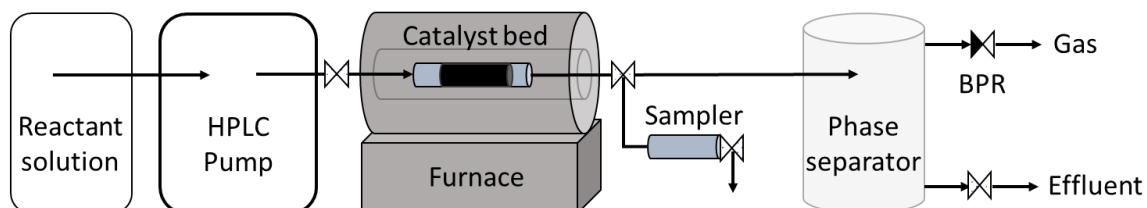
Continuous Meerwein-Ponndorf-Verley (MPV) reaction of furfural was performed using the same PFR setup described in 2.3.8. The reactant used was a solution of furfural (0.1 M) in 2-butanol. The selected catalyst was placed in between two plugs of quartz wool and densely packed into a 1/4 inch stainless steel tube (3.8 mm ID), and a frit (0.5 mm) was placed at the end of the bed to avoid any loss of material. A contact time of 3.5 min and temperature of 100 °C were typically employed. Aliquots of the reaction solutions were taken periodically from a sampling valve placed after the reactor. Analyses of the liquid samples were performed analogously to the procedure described in Section 2.3.2.

List of chemicals used for these experiments: furfural (99 %, Sigma Aldrich®), 2-butanol ($\geq 99\%$, Fisher scientific®), toluene (99.5 %, Alfa Aesar®), biphenyl ($\geq 95\%$, Sigma Aldrich®).

2.3.10. Continuous flow: Acceptorless dehydrogenation of 2-butanol and ethanol

Continuous acceptorless dehydrogenation reactions were performed in a stainless steel PFR. The reactor was connected to an HPLC pump (Agilent 1200) in order to regulate the reactant flow and allow operation at elevated pressures (Scheme 2.7). The reactor temperature was controlled by using a Carbolite tubular furnace and the pressure was controlled by means of a back pressure regulator (33 bar). The reactant used was a solution of the desired alcohol 0.5 M in toluene. The reactor was connected to a Swagelok TPED phase separator cylinder, to separate the gas produced. 0.1 g of Pd/C catalyst was placed in between two plugs of quartz wool and densely packed into a 1/4 inch stainless steel tube (3.8 mm ID), and a frit (0.5 mm) was placed at the end of the bed to avoid any loss of material. The reactions were carried out in a range of temperatures between 130 to 290 °C. Aliquots of the reaction solutions were taken periodically from a sampler consist in a tub of stainless steel equipped with two valves,

placed after the reactor. The sampler can be filled opening the first valve, keeping the system isolated from the atmosphere and avoiding big changes of pressure. Once full and the first valve closed, the collected sample can be cooled down inserting the sampler in an ice bath. The frozen sample can be then collected for analysis by opening the second valve of the sampler. Analyses of the liquid samples were performed analogously to the procedure described in Section 2.3.2.



Scheme 2.7: Scheme of plug flow reactor for acceptorless dehydrogenation of 2-butanol and ethanol in continuous flow.

List of chemicals used for these experiments: ethanol (HPLC grade, Fisher scientific®), 2-butanol ($\geq 99\%$, Fisher scientific®), toluene (99.5%, Alfa Aesar®), biphenyl ($\geq 95\%$, Sigma Aldrich®).

2.3.11. Continuous flow: Guerbet reaction of ethanol

Continuous Guerbet reaction of ethanol was performed using the same PFR described in Section 2.3.9:

- 1- For reactions using Pd/C, 0.1 g of Pd/C 5 wt.% and 0.1 g of Hf- β 1 wt.% HDT were used.
- 2- For reactions using Pd/Al₂O₃, 0.2 g of Pd/Al₂O₃ 5 wt.% and Hf- β 1 wt.% HDT in the range of 0-5 by mass Hf/Pd (0-1 g of Hf- β).

The selected catalysts were manually ground together for 5 min until homogenisation of the mixture. The resultant was placed in between two plugs of quartz wool and densely packed into a 1/4 inch stainless steel tube (3.8 mm ID), and a frit (0.5 mm) was placed at the end of the bed to avoid any loss of material. The reactant used was a solution of ethanol (1 M) in toluene. The reactions were carried out in temperatures between 200 and 290 °C. Aliquots of

the reaction solutions were taken periodically analogously to the procedure described in Section 2.3.10. Analyses of the liquid samples were performed analogously to the procedure described in Section 2.3.2.

List of chemicals used for these experiments: ethanol (HPLC grade, Fisher scientific®), toluene (99.5 %, Alfa Aesar®), biphenyl (≥95 %, Sigma Aldrich®).

2.4. Analytical methods

Analytical details of the qualitative and quantitative analyses of the reactions reported in the whole project, are provided in this section.

2.4.1. Mass spectroscopy

Mass Spectrometry (MS)² is an analytical technique that measures the mass-to-charge ratio of ions and is a widely used procedure to identify unknown analytes. In a typical MS procedure, a sample, which may be solid, liquid, or gaseous, is ionised, for example by bombarding it with electrons. This may cause some of the sample's molecules to break into charged fragments or simply become charged without fragmenting. These ions are then separated according to their mass-to-charge ratio, for example by accelerating them and subjecting them to an electric or magnetic field. In this way, ions of the same mass-to-charge ratio will undergo the same amount of deflection. The ions are detected by a mechanism capable of detecting charged particles, such as an electron multiplier. Results are displayed as spectra of the signal intensity, for detected ions, as a function of the mass-to-charge ratio. The atoms or molecules in the sample can be identified by correlating known masses from standard samples, to the masses identified during analysis, or by comparing a characteristic fragmentation pattern.

2.4.1.1. Experimental details

For acceptorless dehydrogenation reactions, kinetic studies were performed collecting the gas produced in a burette as is described in Section 2.3.3. Gas samples were obtained from the burette using a 100 mL SGE gas tight syringe and analysed by a mass spectrometer (Hiden Analytical Quadrupole Gas Analyzer (QGA)) equipped with an inert quartz capillary with a

consumption rate of 16 mL min^{-1} and Faraday electron multiplier detector capable of detecting concentrations between 0.1 ppm to 100 %. QGA Professional Software was used to quantify the partial pressures as a function of the m/z ratio.

2.4.2. Chromatography

The analytical technique known as chromatography is a commonly used method to separate a mixture of substances into its components. The samples analysed by chromatography are dissolved in a fluid, called mobile phase, carrying the samples through a fixed structure, which contains the so-called stationary phase. In this technique the separation occurs depending on the affinity of the single components carried by the mobile phase to bind with the stationary phase.

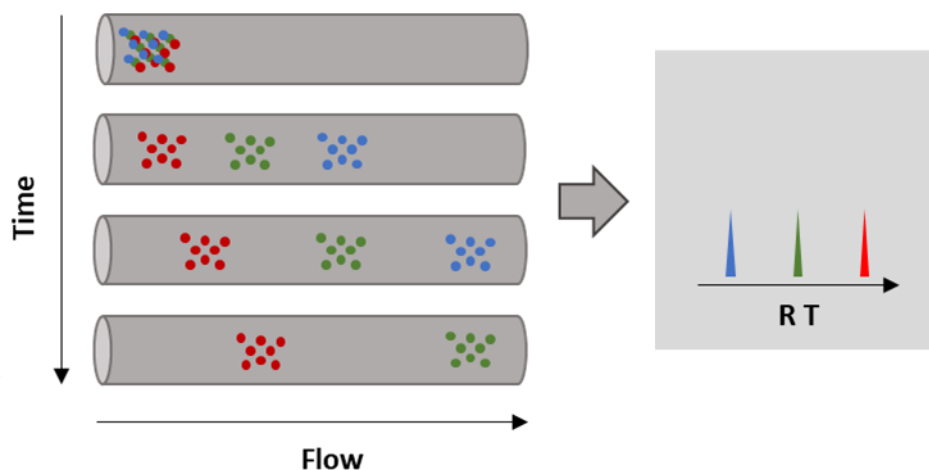
2.4.2.1. Gas Chromatography (GC)

Gas Chromatography (GC) is one type of chromatography used to analyse compounds that can be vaporised without decomposition. In this technique, an inert gas (He typically) is used as mobile phase to carry the mixture through the system. This fluid is continuously carried through a capillary column coated with a polymeric film (known as chromatographic column), which acts as the stationary phase. The substances transported by the mobile phase have different interactions with the stationary phase, causing their separation and eluding from the column at different times (retention times, RT). In this way, the molecules with stronger interactions with the column will have longer RT. In established conditions, the RT are characteristic for every substance (Scheme 2.8).

A GC instrument is generally composed for the same common elements. The injector, maintained at high temperatures ($100\text{-}300 \text{ }^\circ\text{C}$), vaporises the sample and adds it to the eluent gas, being carried through the chromatographic column, which itself is held in an oven. This allows the separation process to work at different temperatures and allows the introduction of temperature ramps to facilitate separation, which is highly dependent of the temperature and the type of stationary phase. To finalise the process, the separated analytes arrive to the detector and generate a response proportional to the amount of substance that arrives. This signal results in Gaussian peaks whose areas can be used for quantification of the analytes. The signal series, in form of different peaks, is known as a chromatogram. The type of detector used depends on sensitivity to towards the analytes and its ability to generate appropriate signals. The Flame Ionisation Detector (FID), is widely used for the detection of organic

molecules such as alcohols, ethers, acids, hydrocarbons and ketones. It employs a hydrogen flame to burn the analytes, producing a flow of ions that are collected, which then generates a current that is transformed into the chromatographic signal.

Gas chromatography can be also combined with mass spectroscopy (GC-MS) to identify the different components from a test sample.



Scheme 2.8 :Representation of a chromatographic separation.

2.4.2.1.1. Quantification of Guerbet products

The evolution of the Guerbet reaction and its different steps were monitored using a GC (Agilent 7820 equipped with a 25 m CP-Wax 52 CB column) equipped with an FID (at 250 °C) and using He (5 mL min⁻¹) as carrier gas. The quantification of the analytes was carried out against a biphenyl external standard, calibrated prior to measurement of all the analytes of interests. Calibrations were performed by preparation of accurate solutions of the analytes at different concentrations in toluene with a fixed concentration of biphenyl. The area of the analytes and standard were obtained by integration of the corresponding signals in the chromatograph. The GC method employed was previously optimised to ensure proper separation of all components. In this case, the method used was: starting at 40 °C, holding that temperature for 5 min, then start a ramp of 20 °C min⁻¹ until 210 °C, and finally holding that temperature for 5 min. Table 2.1 shows the representative example of the calibration of ethanol.

Table 2.1: Concentration and GC areas obtained for ethanol calibration

<u>Ethanol</u>		<u>Biphenyl</u>	
Concentration (M)	Area	Concentration (M)	Area
0.25	4055.9	0.01	1194.4
0.20	3269.7	0.01	1082.5
0.15	2432.7	0.01	1162.2
0.10	1661.2	0.01	1193.5
0.05	843.4	0.01	1167.3

The calibration curve was then generated by plotting the ratio of the concentration of the analyte and biphenyl against the ratio of the corresponding areas (Figure 2.3) obtained by the chromatogram (Equation 2.9):

$$\frac{[EtOH]}{[Bp]} = CF \frac{\int EtOH}{\int Bp} \quad [Equation 2.9]$$

The calibration factor (CF) was obtained by calculating the slope of the fitting curve of the calibration points, and it was used to obtain the unknown concentrations of each analyte during the reaction. For example, the CF obtained for ethanol was 7.13. CFs for the rest of the products involved in this reaction were calculated following the procedure described above and their CF as well as RT are compiled in Table 2.2.

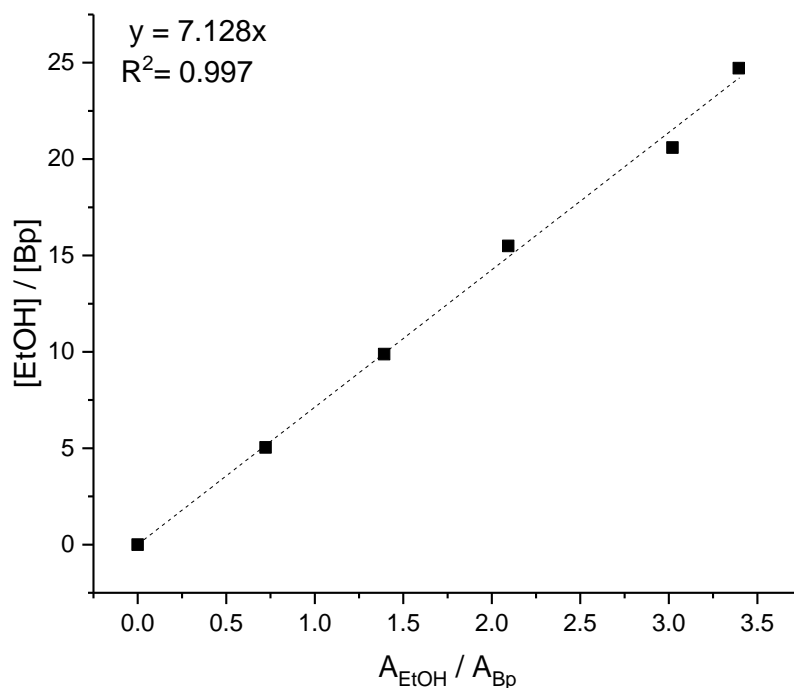


Figure 2.3: Calibration plot obtained by GC areas for ethanol against biphenyl as standard.

Table 2.2: CF and RT for products of Guerbet reaction of ethanol obtained by GC-FID.

<u>Analyte</u>	<u>CF</u>	<u>RT (min)</u>
Diethyl ether	3.85	1.5
Acetaldehyde	34.94	1.8
Butyraldehyde	3.85	4.0
Acetal	2.92	4.3
Ethanol	7.13	5.5
2-Butanol	3.51	7.2
Crotonaldehyde	3.77	7.5
n-Butanol	3.66	8.6
Crotyl alcohol	3.45	9.4
2-Ethyl-1-butanol	1.90	10.1

n-Hexanol	2.18	10.4
2-Ethyl-1-hexanol	1.56	11.4
n-Octanol	1.58	11.8

2.4.2.1.2. Quantification of acceptorless dehydrogenation products

The evolution of products from the acceptorless dehydrogenation reaction were monitored by the same GC instrument, following the same experimental and GC method described in Section 2.4.1.1. CF and RT of the analytes involved are compiled in Table 2.3.

Table 2.3: CF and RT for products of acceptorless dehydrogenation of different alcohols obtained by GC-FID.

<u>Analyte</u>	<u>CF</u>	<u>RT (min)</u>
2-Butanone	3.84	4.5
1-phenylethanol	1.51	13.4
Acetophenone	1.61	12.6
Styrene	1.44	9.8
Ethylbenzene	1.54	8.6
Benzyl alcohol	1.79	13.8
Benzaldehyde	1.94	11.9
Benzyl alcohol- α,α -d ₂	1.79	13.8
Benzaldehyde- α -d ₁	1.95	11.9
4-chlorobenzyl alcohol	2.11	17.2
4-chlorobenzaldehyde	2.27	17.1
4-methylbenzyl alcohol	1.52	14.4
4-methylbenzaldehyde	1.66	12.7

2.4.2.1.3. Quantification of Aldol condensation and MPV reaction products

The evolution of products from the acceptorless dehydrogenation was monitored by the same GC instrument, following the same experimental and GC method described in Section 2.4.1.1. CF and RT of the analytes involved are compiled in Table 2.4.

Table 2.4: CF and RT for products of Aldol condensation of benzaldehyde with acetone and MPV reaction of furfural with 2-butanol obtained by GC-FID.

<u>Analyte</u>	<u>CF</u>	<u>RT (min)</u>
Benzaldehyde	1.77	12.0
Benzalacetone	1.37	13.6
Furfural	3.81	11.4
Furfuryl alcohol	3.38	12.5
2-(Butoxymethyl)furan	1.50	12.1

2.2.4.1.4. Identification of unknown products

GC-MS was used in tandem with the described quantifications of products for the different reactions listed in this work. A GC (Agilent 6890N equipped with a 25 m CP-Wax 52 CB column) equipped with an MS detector (Agilent 5973) and using He (5 mL min⁻¹) as carrier gas was used. The GC method employed was the same described in Section 2.4.1.1.

2.5. Catalyst characterisation techniques

To better understand catalytic performance, and to correlate the structure of the catalysts to their activity, multiple characterisation techniques were adopted in this study. Structural and textural analyses were performed with powder X-ray Diffraction and porosimetry, respectively, and the morphology of each material studied with Scanning Electron Microscopy and Transmission Electron Microscopy, while the nature of the active species in metal supported nanoparticles was investigated by X-Ray Photoelectron Spectroscopy. The combination of these techniques provides a deeper understanding of the structure - activity relationships observed in the catalytic systems studied in this thesis. The theoretical background of each

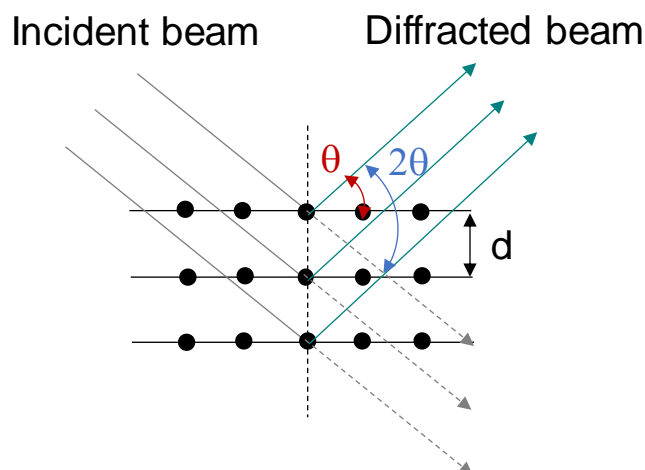
characterisation technique and experimental details associated with the use of each method are presented in the following sections.

2.5.1. Powder X-Ray Diffraction (XRD)

X-Ray Diffraction (XRD) is a technique used to analyse the crystalline structure of materials and to confirm phase purity by examination of their diffraction patterns.³ Crystalline solid materials are spatially arranged in a highly ordered manner that is repeated in the three dimensions of space. Hence, diffraction occurs when the incident X-ray beam interacts with their structure at certain angles that satisfy Bragg's Law,⁴ which provides information on the crystalline lattice:

$$n\lambda = 2d\sin\theta \quad [\text{Equation 2.10}]$$

Where n is an integer number, λ is the wavelength of the X-ray radiation, d is the spacing between the planes and θ is the angle between the diffracted beam and the sample. A schematic of the X-ray diffraction process is shown in Scheme 2.9.



Scheme 2.9: Scheme of diffraction phenomenon generated by the incidence of a monochromatic radiation into a crystalline structure according to the Bragg's law.

An XRD instrument is commonly composed of an X-Ray generator, a sample holder and a detector. The X-Ray beam is generated by irradiating a copper foil with a high-energy electron beam and is filtered by a monochromator that selects the typical CuK_α radiation (1.54 Å) to

converge upon the sample. The detector moves around the sample through an arc, collecting the diffracted radiation at a determined range of angles. The resulting diffractogram shows the intensity of the diffracted beam against the diffraction angle 2θ . By comparison of the obtained XRD patterns with reference patterns on a data base, the phase or phases present in each sample can be identified, alongside the crystal planes corresponding to each main diffraction peak. Furthermore, it allows comparison of crystallinity between samples by measuring parameters such as the full width half maximum intensity.

2.5.1.1 Experimental details

In this work, a Panalytical X'PertPRO X-ray diffractometer was employed for powder XRD analysis. A $\text{CuK}\alpha$ radiation source (40 kV and 30 mA) was employed and diffraction patterns were recorded between $5\text{--}80^\circ 2\theta$ (step size 0.0167° , time/step = 150 s). In case of the zeolite materials, patterns were compared with references on the data base, *i.e.* "Collection of simulated XRD powder patterns for zeolites".⁵

2.5.2. Surface area and porosimetry analysis

Porosimetry is an analytical technique used to determine the porous properties of solid materials including pore diameter, total pore volume and surface area. It consists in the gradual physical adsorption of an inert gas (N_2 , Ar or Kr) at low temperature on the material surface, first forming a mono-layer and then subsequent multi-layers, generating an isotherm which is a function of the volume of gas adsorbed (v) against the relative pressure (P/P_0).⁶

One of the most relevant parameters studied by this technique is the surface area, commonly calculated by the Brunauer-Emmett-Teller (BET) method:⁷

$$\frac{1}{v[(P/P_0) - 1]} = \frac{c - 1}{v_m c} \left(\frac{P}{P_0}\right) + \frac{1}{v_m c} \quad [\text{Equation 2.11}]$$

Where v is the volume of adsorbed gas at a pressure P , P_0 is the saturation pressure, v_m is the molar volume of gas needed to make monolayer of adsorbed gas and C is the BET constant. According to the BET theory, it should be possible to obtain a straight line if the equation is applied in the relative pressure range of $0.05 - 0.35 P/P_0$. The slope calculated by this line contains the value of v_m and the specific surface area can be calculated as:

$$S_{BET} = \frac{v_m N s}{V a} \quad [Equation 2.12]$$

Where N is the Avogadro number, s is the adsorption cross-section of the adsorbing gas, V is the molar volume of the adsorbing gas and a is the mass of the solid.

The total pore volume can be directly extrapolated from the isotherm at partial pressure $P/P_0 = 0.99$, assuming all pores are filled with adsorbate. The pore size distribution is usually determined by the Barrett-Joyner-Halenda (BJH) model,⁸ a procedure for calculating pore size distributions from experimental isotherms using the Kelvin model of pore filling. BJH can only be correctly applied to mesopores and small macropores. The microporous volume and external surface area can be calculated by the t-plot,⁹ based on standard isotherms and thickness curves, which describes the statistical thickness of the film of adsorptive on a non-porous reference surface. The difference between the total pore volume and the micropore volume (obtained by t-plot) gives the mesopore volume.

2.5.2.1. Experimental details

Porosimetry analysis of all materials used in this work were carried out on a Quantachrome Quadrasorb, with N_2 as adsorbate, and the isotherms were collected at 77 K. Samples were degassed accordingly prior the N_2 adsorption measurements, depending on the kind of sample analysed. Zeolite based catalyst were degassed at 277 °C for 16 h using a FLOVAC Degasser, while the metal supported nanoparticles were degassed at 120 °C for 6 h.

2.5.3. Electron Microscopy

Electron microscopy is a technique that uses a beam of accelerated electrons as a source of illumination to irradiate the sample and obtain detailed images at a very small scale. In catalysis, this technique is typically employed to obtain information on the morphology of solid samples.¹⁰

2.5.3.1. Transmission electron microscopy (TEM)

Transmission Electron Microscopy (TEM) is a powerful microscopy technique. A high energy beam of electrons is passed through a very thin sample, allowing features such as crystal

structure, grain boundaries and dislocations to be observed due to the interactions between the electrons and the atoms.

In a TEM instrument, the electron gun generates the electron beam that hits the sample, and transmitted electrons are magnified by electromagnetic lenses. The optics bring the scattered electron from the same point in the sample to the same point in the image. The image recorder transforms the electron signals into a form perceivable by the human eye. While other techniques work on the topological and compositional structure of a surface, TEM obtains information from the electron beam as it interferes with the mass in a two-dimensional image.

This technique is especially useful to characterise metal supported nanoparticles, since usually particle with a diameter > 1 nm can be observed. The processing of several images of each sample allows a statistical analysis to be performed, allowing the particle size distribution and the average particle size of the supported nanoparticles to be determined.

2.5.3.1.1. Experimental details

Samples were prepared by dispersing the catalyst powder in ethanol *via* ultra-sonication. 50 μ L of the suspension was dropped on to a holey C film supported by a 300-mesh copper TEM grid, followed by evaporation at room temperature. TEM images were obtained using a JEOL JEM-1200EX, operating at 300 kV.

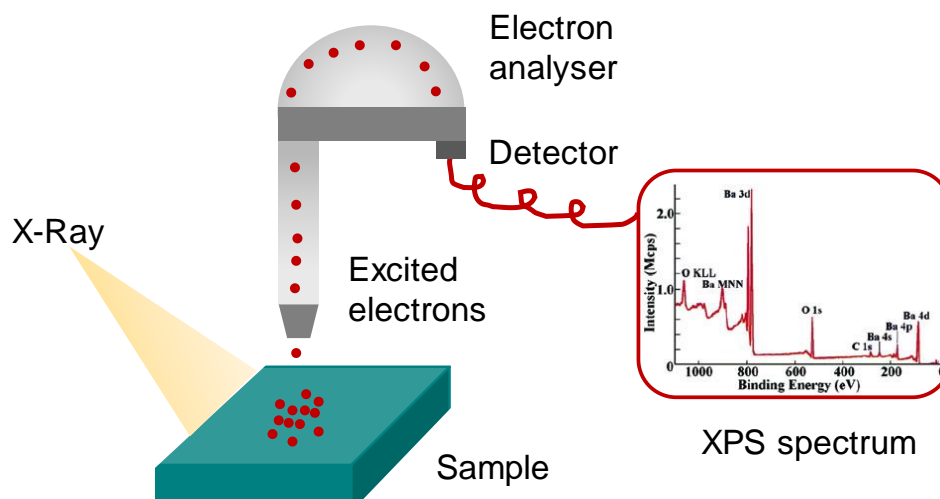
The analysis of the particle size distribution of each sample was carried out by measuring 300 particles and performing statistical analysis of this data set to build a histogram. This permitted the particle size distribution, the average particle size and the standard deviation of the sizes to be determined.

2.5.4. X-Ray Photoelectron Spectroscopy (XPS)

X-ray Photoelectron Spectroscopy (XPS) is a surface-sensitive quantitative spectroscopic technique that measures the elemental composition at the parts per thousand range. It also allows the empirical formula, chemical state and electronic state of the elements that exist within a material to be identified.

A surface is irradiated with X-rays (commonly Al K_{α} or Mg K_{α}) in vacuum. When an X-ray photon hits and transfers its energy to a core-level electron, it is emitted from its initial state with a kinetic energy dependent on the incident X-ray, and the binding energy of the atomic orbital from which it has been originated. The energy and intensity of the emitted

photoelectrons are analysed to identify and determine the concentrations of the elements present in the analysed material. These photoelectrons originate from a depth of < 10 nm; therefore, this technique provides only information about the elements present within this depth. An XPS instrument is commonly composed of a high vacuum system, a source of radiation, an ionisation chamber, an electron analyser (typically hemispherical) and an electron detector, which transforms the signal accordingly to generate the corresponding XPS spectrum.



Scheme 2.10: Schematic of a typical XPS instrument.

The interpretation of an XPS spectrum is based on the fact that each element possesses characteristic binding energies depending on its chemical state. For instance, metallic Pd has a binding energy of 335.0 eV, whilst Pd oxide has a binding energy of 336.7 eV. The deconvolution of the bands characteristic of each element allows determination and quantification of the oxidation state of the metal(s) present on the samples, giving valuable information on the chemical nature of the metal supported nanoparticles. This technique is also very useful to analyse the changes that occurs after a certain treatment (*i.e.* reduction heat treatments) or after a reaction.

2.5.4.1. Experimental details

XPS analyses were performed on a Thermo Scientific K-alpha⁺ spectrometer by Davide Motta. Samples were analysed using a monochromatic Al X-ray source operating at 72 W (6 mA x 12 kV), with the signal averaged over an oval-shaped area of approximately 600 x 400 microns. Data was recorded at pass energies of 150 eV for survey scans and 40 eV for high

resolution scan with a 1eV and 0.1 eV step size respectively. Charge neutralisation of the sample was achieved using a combination of both low energy electrons and argon ions (less than 1 eV), which gave a C (1s) binding energy of 284.8 eV. All data was analysed using CasaXPS (v2.3.17 PR1.1) software using Scofield sensitivity factors and an energy exponent of -0.6 by Davide Motta.

References

- ¹ C. Hammond, D. Padovan, G. Tarantino, *R. Soc. Open. Sci.*, 2018, **5**, 2, 171315
- ² E. Hoffmann, V. Stroobant, *“Mass spectroscopy: Principles and Applications”*, **2002**
- ³ C. Suryanarayana, M. Grant Norton, *“X-Ray Diffraction: A practical Approach”*, New York; London: Plenum Press, **1998**
- ⁴ W.H. Bragg, W.L. Bragg, *Proc. R. Soc. Lond. A.*, 1913, **88** (605), 428–38
- ⁵ M.M.J. Treacy, J.B. Higgins, *“Collection of Simulated XRD Powder Patterns for Zeolites”*, 5th Edition Elsevier Science, **2007**
- ⁶ J. Gregg, K. S. W. Sing, *“Adsorption, Surface area and Porosity”*, 2nd edition Academic Press, **1982**
- ⁷ S. Brunauer, P. H. Emmett, E. Teller, *J. Am. Chem. Soc.*, 1938, **60**, 309-319
- ⁸ E. P. Barrett, L. G. Joyner, P. P. Halenda, *J. Am. Chem. Soc.*, 1951, **73**, 373 380
- ⁹ B. C. Lippens, B. G. Linsen, J. H. de Boer, *J. Catal.*, 1965, **3**, 319-323
- ¹⁰ Y. Lin, J. A. McCarthy, K. R. Poeppelmeier, L. D. Marks, *“Applications of Electron Microscopy in Heterogeneous Catalysis”*, **2015**

3. Upgrade of ethanol by Guerbet reaction

3.1. Introduction

As previously discussed in Chapter 1, the interest in finding renewable energy sources able to replace conventional fossil fuels has greatly increased in the last decades. The pressing problem of global warming, combined with shortage in oil reserves, forces human civilization to find other ways to meet their needs, both in terms of energy production for transportation and daily life, and for the C based chemical industry. In this context, biomass is considered to be one of the most favourable renewable sources able to satisfy the human necessities for fuels and chemical industry. For instance, biomass can be used as raw material for a range of products, such as the family of alcohols. Over the last decade, alcohols have been identified as a green energy source and a promising alternative to fossil fuels. The use of bioalcohols, derived from plants, will allow to use C from the atmosphere, recycled by photosynthesis, resulting in a renewable energy source.¹

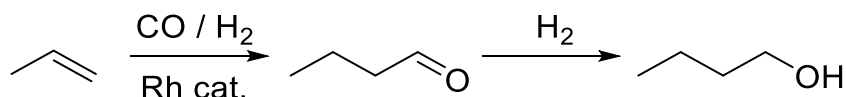
Currently, ethanol is one of the most promising bioalcohols. As described in Chapter 1, ethanol can be obtained from different sources, including direct fermentation of sugar containing crops, a remarkable example being its production from corn in Brazil.² Nevertheless, the competition with food production, clearly indicates the unsuitability of this route for the generation of bioethanol. For this reason, other biological sources of ethanol such as cellulosic material^{3,4} and algae,^{5,6} amongst others⁷ have been developed. Nonetheless, although ethanol has already been efficiently employed as a satisfactory alternative to conventional gasoline and

as an additive to conventional fuels, several inconveniences prohibit greater implementation of this alcohol for energy production, especially in the transport sector:⁸

- 1- Ethanol possesses only 70 % of the energy density of gasoline.
- 2- It can be corrosive for transportation engines.
- 3- It easily absorbs significant quantities of H₂O, resulting in problems for its separation and transportation.

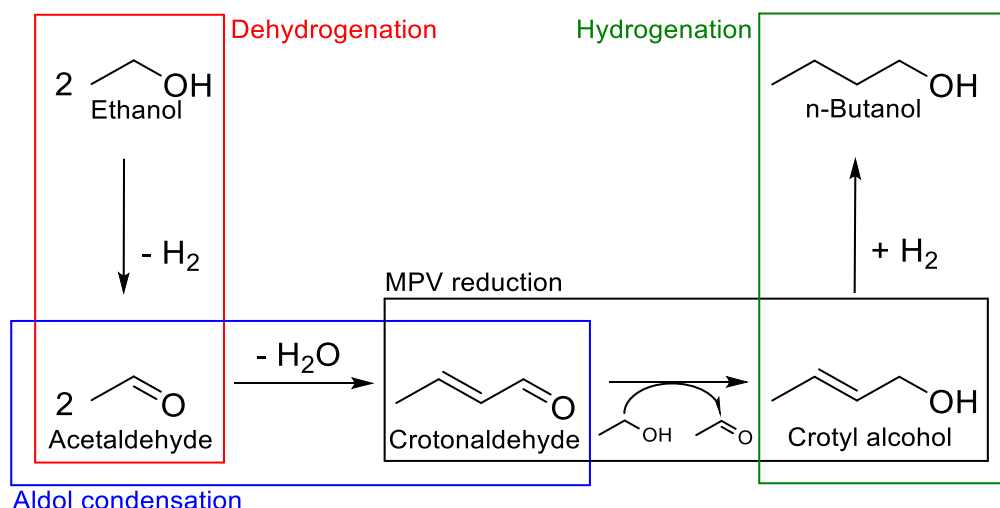
For all these reasons, higher alcohols may be more adequate as fuels, with n-butanol identified as a desirable substitute. In contrast to ethanol, n-butanol possesses 90 % of energy density compared with gasoline, it is noncorrosive and do not present the same water-related problems. Furthermore, n-butanol shows interesting applications for paints, adhesives, coatings, cosmetics, cleaning solvents, artificial flavours, plasticisers and lubricants and as bulk chemical to produce valuable industrial chemicals like butyl acrylate, butyl acetate, butyl glycol ethers and butyl esters.^{9,10}

The current way for the industrial production of n-butanol is called oxo process¹¹ (Scheme 3.1). In this reaction, propylene, derived from petroleum, undergoes hydroformylation, using a homogenous rhodium catalyst, forming butyraldehyde which is then hydrogenated to form n-butanol.



Scheme 3.1: Basic scheme for oxo process of propylene to butyraldehyde followed by hydrogenation to n-butanol.

However, this complicated process is associated with high capital and operational costs. Interestingly, before the 1940, the production of n-butanol was based on Acetone-Butanol-Ethanol (ABE) fermentation,¹² where the action of anaerobic bacteria over glucose leads to the formation of the three products that give name to this system. Nevertheless, this option was extensively abandoned for the more profitable oxo process. Therefore, as described in Chapter 1, due to the abundance and the increasing production of ethanol, the condensation of two molecules of ethanol to form n-butanol would be an economically attractive option. This is possible through the Guerbet reaction (Scheme 3.2).



Scheme 3.2: General reaction scheme for the Guerbet reaction of ethanol.

This reaction, first published in 1899 by Marcell Guerbet in the French journal *Comptes Rendus*,¹³ is a well-known industrial process where a short chain primary or secondary alcohol can be condensed with the same or another alcohol, to form a longer chain alcohol with the release of H_2O . Despite the real pathway of the Guerbet reaction still being subject to discussion, the most accepted mechanism applied to n-butanol production consists in an initial dehydrogenation of ethanol to acetaldehyde, which undergo a self-aldol condensation, yielding crotonaldehyde. At that point, crotonaldehyde is reduced to crotyl alcohol and subsequently hydrogenated to form the desired n-butanol.

Unfortunately, the Guerbet reaction is a difficult process when ethanol is used as substrate, with the most challenging problem being the selectivity.¹⁴ In fact, due to the high reactivity of acetaldehyde, the Aldol condensation step (Scheme 3.2) is hard to control, leading to a range of oligomeric and polymeric by-products. Depending upon the reaction conditions, n-butanol can also act as a substrate, yielding higher alcohols like n-hexanol and n-octanol. In a similar way, any long chain alcohol produced can suffer cross condensation with the initial ethanol, yielding isomeric products such as 2-ethyl-1-butanol. Some examples of these competitive reactions are the Cannizzaro reaction, where two aldehyde molecules produce alcohols *via* deprotonation, or the Tishchenko reaction, which produces esters from aldehydes. It should be noted the interestingly related reaction that is the Lebedev process. This system shows an identical pathway to the Guerbet reaction except for the last step. Instead of the specific Guerbet re-hydrogenation, for the Lebedev reaction, the long chain products of the Aldol condensation undergo dehydration, yielding the final alkenes. With the Lebedev reaction, a highly interesting monomer for industrial purposes can be obtained, that is 1,3-butadiene. The

Guerbet reaction is a complex process which needs a system that exhibits acidic, basic, dehydrogenating and hydrogenating properties at the same time.

Due to the interest that the upgrade of ethanol has gained, both for fuels and the chemical industry, and its challenging issues, the production of n-butanol through ethanol condensation *via* Guerbet reaction will be the focus of this chapter.

3.2. Results and discussion

3.2.1. The catalyst

Since Marcell Guerbet published his work using sodium alkoxides, heterogeneous and homogenous catalysts have been used for the condensation of different alcohols. In the specific case of ethanol, some advances have been made in the last years using homogeneous catalysts based on metals like Ir or Ru. Hence, in order to gain experience with the Guerbet chemistry, a first approach using a mixture of $[\text{RuCl}_2(\eta^6\text{-}p\text{-cymene})]_2$ and 2-(diphenylphosphino)ethylamine ligand, in basic conditions, was applied to the Guerbet condensation of ethanol, following the results found in literature.¹⁵ The choice of this catalyst was based on the reportedly high levels of activity (25.1%) and selectivity (91.1) exhibited, thus allowing all further studies to be compared to this benchmark catalyst in the literature.

Due to the highly volatile nature of ethanol and the Guerbet reaction products, gas chromatography (GC) was chosen as principal analytical technique to detect and quantify these products, using methanol as solvent and biphenyl as internal standard. Details of this technique are presented in Section 2.4.2.

3.2.2. Investigation on the catalytic runs

A preliminary test was carried out following literature conditions ($[\text{RuCl}_2(\eta^6\text{-}p\text{-cymene})]_2$, 0.05 mol%; 2-(diphenylphosphino)ethylamine, 0.1 mol%; and EtONa, 5 mol% at 150 °C)¹⁶ in a Parr autoclave, however, the system reached excessive pressure and the run was aborted after 30 min. The production of H_2 is a key element of this reaction, and therefore to reduce the pressure of the system for safety reasons, the starting conditions were modified ($[\text{RuCl}_2(\eta^6\text{-}p\text{-cymene})]_2$, 0.025 mol%; 2-(diphenylphosphino)ethylamine, 0.05 mol%; and EtONa, 5 mol% at

150 °C) in order to avoid explosive conditions. As detailed in Section 2.3.1, the Parr autoclave was then substituted with a bigger Asynt PressureSyn autoclave equipped with a gas release valve to ensure safer working conditions.

With the new reactor and methodology, catalytic runs were carried out with reaction times between 0.5 and 4 h to analyse the impact of reaction time on catalyst activity and product distribution (Figure 3.1).

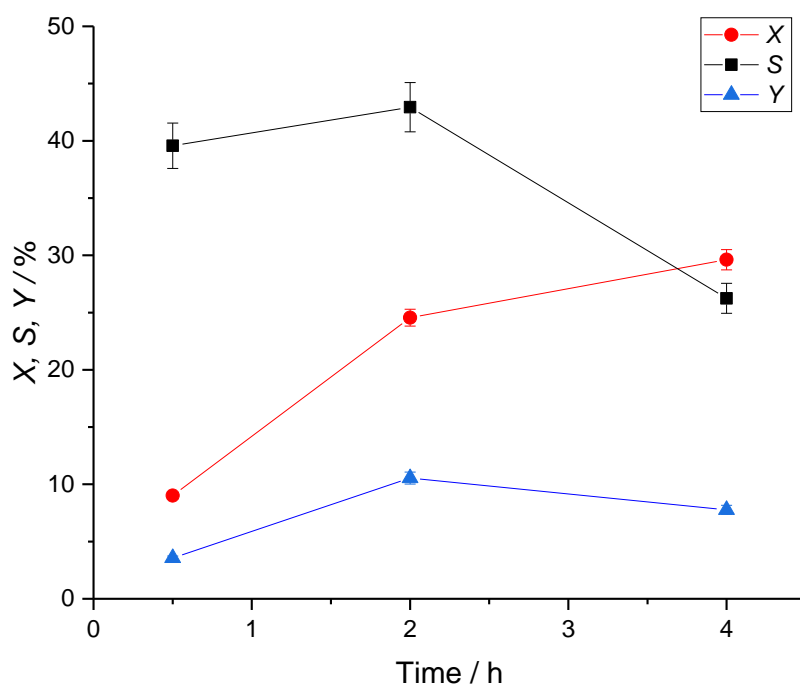


Figure 3.1: Conversion (X) of ethanol (red circles), Selectivity (S) for n-butanol (black squares) and Yield (Y) of n-butanol (blue triangles) over time. **Reaction conditions:** 125 mL stainless steel autoclave reactor, 15 mL of ethanol, $[\text{RuCl}_2(\eta^6\text{-}p\text{-cymene})_2]$ (0.025 mol%), 2-(diphenylphosphino)ethylamine (0.05 mol%), biphenyl (11.7 mol%) and EtONa (5 mol%), 150 °C and magnetic stirring of 750 rpm.

For all the experiments, n-butanol was found as a product, ensuring that the Guerbet reaction is an effective route to obtain n-butanol from upgrade of ethanol. As shown in Figure 3.1, the selectivity to n-butanol falls after 2 h of reaction. The products obtained from these experiments presented black colour and an oil-like texture with some solid residues, which were successfully dissolved in methanol. GC-FID analysis of these products showed great number of peaks, ranging between 40 and 60. The formation of higher alcohols, both linear and branched, was confirmed, being 2-ethyl-1-butanol and n-hexanol the principal by products, amongst others.

With the evidence that the use of the Asynt PressureSyn autoclave system is an effective and reasonably safe way to carry out the Guerbet reaction to n-butanol, two more tests were performed, increasing the amount of $[\text{RuCl}_2(\eta^6\text{-}p\text{-cymene})]_2$ used to match the conditions found in literature.¹⁶ For the first of this new series of experiments, the amount of homogeneous ligand, 2-(diphenylphosphino)ethylamine, was also increased following the literature method ($[\text{RuCl}_2(\eta^6\text{-}p\text{-cymene})]_2$, 0.05 mol%; 2-(diphenylphosphino)ethylamine, 0.1 mol%; and EtONa, 5 mol% at 150 °C). Alternatively, in a second test, no 2-(diphenylphosphino)ethylamine was used to understand its role in the reaction. Considering the levels of conversion and selectivity to n-butanol observed, 2 h was selected as reaction time for further experiments. The results, presented in Figure 3.2, show the key role of the ligand in the reaction: the selectivity to n-butanol is improved when using 2-(diphenylphosphino)ethylamine, for comparable levels of conversion of ethanol.

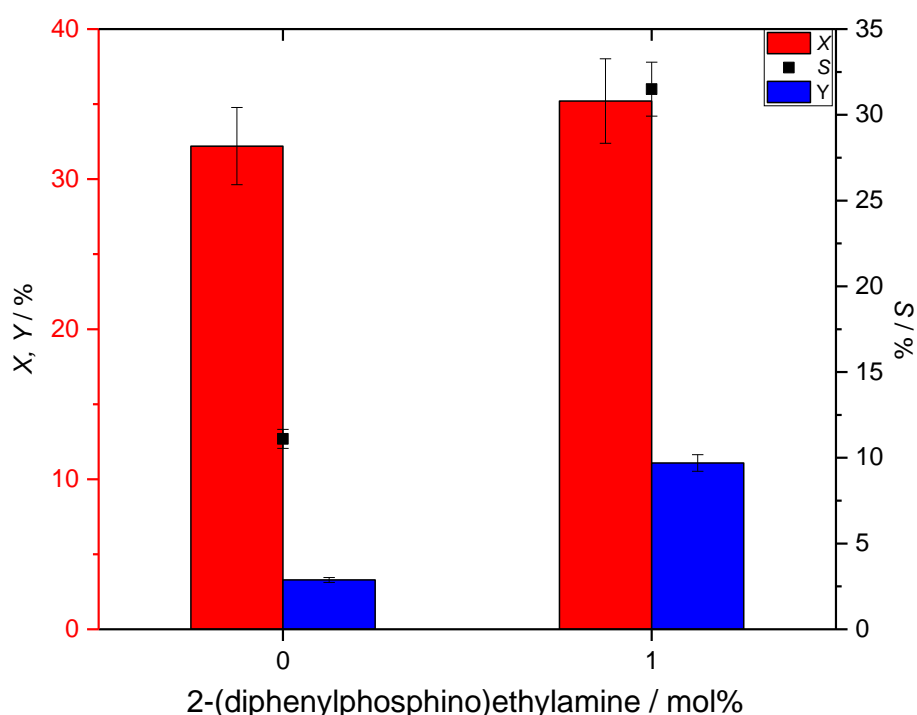


Figure 3.2: Conversion (X) of ethanol (red bars), Selectivity (S) for n-butanol (black squares) and Yield (Y) of n-butanol (blue bars) over 2-(diphenylphosphino)ethylamine mol% (mols of ligand / mols of substrate x100). **Reaction conditions:** 125 mL stainless steel autoclave reactor, 15 mL of ethanol, $[\text{RuCl}_2(\eta^6\text{-}p\text{-cymene})]_2$ (0.05 mol%), biphenyl (11.7 mol%) and EtONa (5 mol%) 150 °C and magnetic stirring of 750 rpm, 2 h.

Considering the data obtained, it is clear that the decreased selectivity in Figure 3.1 for n-butanol at high conversion is caused by the production of higher alcohols and other unidentified products. This hypothesis is supported by the appearance of more peaks at higher

retention times in the chromatograms obtained by GC-FID. Ligands such as 2-(diphenylphosphino)ethylamine may improve the selectivity for n-butanol (Figure 3.2); however, the effect of (diphenylphosphino)ethylamine seems to be insufficient to stop what some authors describe as a “cascade of reactions”.¹⁶ At high conversion, the selectivity drops and higher alcohols among other products are produced, as described in Section 3.1. This effect is in line with the results presented in Figure 3.1 and Figure 3.2 and summarised in Table 3.1. As can be seen the higher activity caused by the increased amount of catalyst entails loss of selectivity, although this effect may also be caused by the degradation of the ligand.

Table 3.1: Catalytic performance for Guerbet reaction to n-butanol at different amounts of catalyst.

[RuCl₂(η^6-p-cymene)]₂ (mol%) ^[a]	X (%) ^[b]	S (%) ^[c]
0.025	24.6	42.9
0.050	35.2	31.5

[a] Reaction conditions: 125 mL stainless steel autoclave reactor, 15 mL of ethanol, [RuCl₂(η^6 -p-cymene)]₂, biphenyl (11.7 mol%) and EtONa (5 mol%), 150 °C and magnetic stirring of 750 rpm, 2 h. **[b]** Conversion (X) of ethanol. **[c]** Selectivity (S) for n-butanol.

3.2.3. General considerations

The upgrading of ethanol to more valuable products via the Guerbet reaction is a promising route for the generation of sustainable energy. In this context, the Guerbet reaction seems to be an efficient strategy to obtain a desirable product such as n-butanol from ethanol. However, its selectivity is the main obstacle to overcome. The Guerbet upgrade of ethanol to n-butanol is shown to be possible with the use of Ru based homogeneous catalysts but this system has several drawbacks:

- 1- Despite the excellent results reported in literature (25% of ethanol conversion with 91% of selectivity for n-butanol),¹⁶ the use of [RuCl₂(η^6 -p-cymene)]₂ catalyst leads to comparable levels of conversion of ethanol (24-35%) and low levels of selectivity for n-butanol (32-43%).

- 2- The ligand 2-(diphenylphosphino)ethylamine is air sensitive¹⁷ and cannot be used in open air. This chemical also shows high viscosity, resulting in difficulties with respect to its collection and measurement.
- 3- The combination of strong basic conditions, necessary for the reaction, with the reaction products results in the deterioration of several parts of the autoclave.
- 4- The homogeneous Ru catalyst does not stop the mentioned “cascade of reactions”.

Therefore, the homogeneous strategy was abandoned. In addition to the mentioned Ru catalysts and other noble metals (Ir),¹⁸ several reports of heterogeneous systems can be found in literature. A first example is the use of MgO, which can catalyse the reaction at elevated temperatures due its basicity but showing poor selectivity.^{19,20} Hydrotalcites derived and related Mg/Al mixed oxides have been also used as catalysts for this reaction, where their different acid-base site distribution seem to favour n-butanol production.²¹⁻²³ Other materials such as hydroxyapatites and substituted hydroxyapatites, with unique structure, showing both, acid and basic sites in a single crystal, can perform the ethanol upgrade exhibiting higher yields than the rest of catalysts, depending on their Ca/P ratios.²⁴⁻²⁶ All these materials, however, present the same weakness of poor selectivity for n-butanol at high conversions, since the Guerbet reaction is a complex process with a wide variety of possible side reaction. This fact underlines the difficulty to imagine a single material able to catalyse efficiently all its steps.

The preliminary benchmarking experiments with Ru permit some interesting initial ideas to be formed. Dehydrogenating agents such Ru and Ir can perform H₂ generation; however, under strong basic conditions the reaction cannot limit the mentioned “cascade of reactions”. Alternatively, materials such as Lewis acid-based catalysts can perform the reaction with poor activity or selectivity. Accordingly, in this thesis a different strategy for Guerbet reaction will be explored. Having in mind the theoretical pathway of the Guerbet reaction (Scheme 3.2) different blocks can be identified,

- 1- Dehydrogenation of the initial alcohol.
- 2- Condensation of the carbonyl product
- 3- A reduction to form the final long chain product.

Thus, instead of treating the upgrading of ethanol as a single reaction, this work will target the different parts of the Guerbet reaction, with each being studied separately through model reactions, with the aim to find the best catalyst for every step. Subsequently, combining these catalysts into a single catalytic system will be explored.

3.3. Conclusions

The Guerbet reaction is an effective way to form n-butanol through the upgrade of ethanol; however, control of the reaction selectivity is challenging. Furthermore, although stated to be highly active and selective, the combination of $[\text{RuCl}_2(\eta^6\text{-}p\text{-cymene})]_2$ and the homogenous ligand 2-(diphenylphosphino)ethylamine results in low n-butanol yields at the reported literature conditions.¹⁶

Considering the potential list of candidates, none of them seems to be able to satisfy all the aspects necessary for this purpose. Thus, the focus of the next chapters will be the study of the individual steps of the Guerbet reaction, performing model reactions with more adequate catalysts for every step, with the ultimate aim of combining the optimised catalysts into one system of improved performance.

References

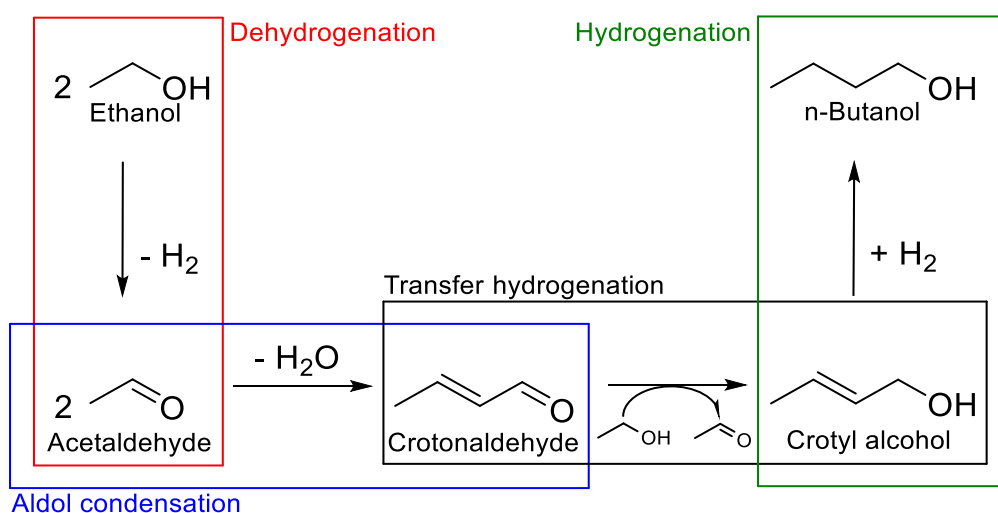
- ¹ T. L. Jordison, C. T. Lira, D. J. Miller, *Ind. Eng. Chem. Res.*, 2015, **54**, 10991–11000
- ² C. A. Cardona, Ó. J. Sánchez, *Bioresour. Technol.*, 2007, **98**, 2415–2457
- ³ L. Jayakody, J. J. Liu, E. J. Yun, T. Turner, E. J. Oh, Y. Jin, *Biotechnol. Bioeng.* 2018, **115**, 2859–2868
- ⁴ R. Yamada, Y. Nakatani, C. Ogino, A. Kondo, *Amb Express*, 2013, **3**, 34–41
- ⁵ Sulfahri, Ni'matuzahroh, S. Manuhara, *Biotechnol. Bioeng.*, 2017, **8**, 367–372
- ⁶ B. İnan, D. Özçimen, *Chem. Biochem. Eng. Q.*, 2019, **33**, 133–140
- ⁷ J. J. Spivey, A. Egbebi, *Chem. Soc. Rev.*, 2007, **36**, 1514–1528
- ⁸ S. Atsumi, A. F. Cann, M. R. Connor, C. R. Shen, K. M. Smith, M. P. Brynildsen, K.J.Y. Chou, T. Hanai, J. C. Liao, *Metab. Eng.*, 2008, **10**, 305–311
- ⁹ J. Wang, H. Pan, A. Wang, X. Tian, X. Wu, Y. Wang, *Catal. Commun.*, 2015, **62**, 29–33
- ¹⁰ C. Jina, M. Yaoc, H. Liuc, C. F. Lee, J. Ji, *Renew. Sust. Energ. Rev.*, 2011, **15**, 4080–4106
- ¹¹ M. Uyttebroek, W. Van Hecke, K. Vanbroekhoven, *Catal. Today*, 2015, **239**, 7–10
- ¹² D. Cai, H. Chen, C. Chen, S. Hu, Y. Wang, Z. Chang, Q. Miao, P. Qin, Z. Wang, J. Wang, T. Tan, *Chem. Eng. J.*, 2016, **287**, 1–10
- ¹³ M. Guerbet, *C. R. Hebd, Séances Acad. Sci.*, 1899, **128**, 511–513
- ¹⁴ C. Carlini, M. Di Girolamo, A. Macinai, M. Marchionna, M. Noviello, A. M. Raspolli, G. J. Sbrana, *Chem.*, 2003, **200**, 137–146

- ¹⁵ R. L. Wingad, P. J. Gates, S. T. G. Street, D. F. Wass, *ACS Catal.*, 2015, **5**, 5822–5826
- ¹⁶ T. Moteki, A. Rowley, D. Flaherty, *ACS Catal.*, 2016, **6**, 7278–7282
- ¹⁷ R. Edmundson, "Dictionary of Organophosphorus Compounds" CRC Press, **1987**
- ¹⁸ K. Koda, T. Matsu-ura, Y. Obora, Y. Ishii, *Chem. Lett.*, 2009, **38**, 838–839
- ¹⁹ W. Ueda, T. Kuwabara, T. Ohshida, Y. Morikawa, *J. Chem. Soc., Chem. Commun.*, 1990, 1558–1559
- ²⁰ A.S. Ndou, N. Plint, N.J. Coville, *Appl. Catal. A.*, 2003, **251**, 337–345
- ²¹ M. León, E. Díaz, S. Ordóñez, *Catal. Today*, 2011, **164**, 436–442
- ²² D. Carvalho, R. de Avillez, L. Borgesa, L. Appel, *Appl. Catal. A.*, 2012, **415–416**, 96–100
- ²³ K. Ramasamy, M. Gray, H. Job, D. Santosa, X. Li, A. Devaraj, Y. Wang, *Top Catal.*, 2016, **59**, 46–54
- ²⁴ T. Tsuchida, S. Sakuma, T. Takeguchi, W. Ueda, *Ind. Eng. Chem. Res.*, 2006, **45**, 8634–8642
- ²⁵ S. Ogo, A. Onda, K. Yanagisawa, *Appl. Catal. A.*, 2011, **402**, 188–195
- ²⁶ S. Hanspal, Z. Young, H. Shou, R. Davis, *ACS Catal.*, 2015, **5**, 1737–1746

4. Acceptorless alcohol dehydrogenation

4.1. Introduction

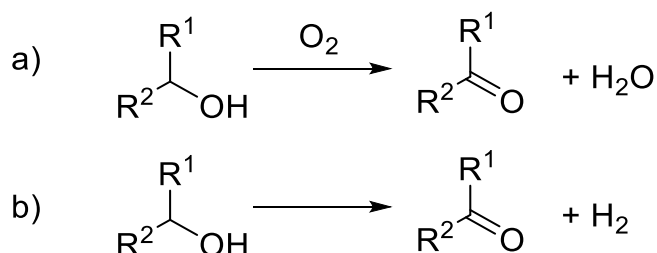
As described in Chapter 3, the first step of the Guerbet reaction is the dehydrogenation of the initial alcohol, followed by condensation of the carbonyl product *via* Aldol condensation and re-hydrogenation to form the desired long chain alcohol. Always keeping the upgrade of ethanol in mind as main goal, the dehydrogenation of alcohols as a separate system will be the focus of this chapter.



Scheme 4.1: General reaction scheme for the Guerbet reaction of ethanol.

The formation of carbonyl compounds is one of the most important chemical reactions in organic synthesis, due to the key role played by ketones and aldehydes as building block intermediates for a wide range of value-added compounds and for the synthesis of polymers.^{1,2} Despite the importance of this process for synthetic applications, alcohol oxidation is typically performed by use of stoichiometric equivalents of toxic oxidising agents,^{3,4} such as Cr(VI) based species like ditertiary butyl chromate, tetrakis(pyridine) silver dichromate and tripropyl ammonium fluorochromate.⁵ Evidently, the use of oxidants dramatically affects the sustainability of these processes, due to the co-production of stoichiometric amounts of toxic inorganic waste. To increase the sustainability of this reaction, over the last decades much effort has been focused on the development of catalysts able to convert alcohols to the corresponding carbonyl compounds using O₂, *i.e.* removing the need for the already mentioned Cr inorganic salts.⁶⁻⁸ In parallel with this strategy, another approach that has received less attention is the development of catalysts able to catalyse alcohol dehydrogenation under inert conditions, which is referred as acceptorless dehydrogenation (Scheme 4.2), producing H₂ as by-product.⁹⁻¹¹ Although less explored, this second route is especially desirable because it includes the parallel production of H₂, which is a highly valuable as a sustainable source of energy,¹² and because the increased selectivity towards the carbonyl compounds, often subjected to overoxidation to the corresponding carboxylic acids in the presence of O₂.⁷

Gunanathan *et. al.* have recently demonstrated that acceptorless dehydrogenation can also be employed to achieve a broader range of organic reactions, following further reactivity of the carbonyl compounds with nucleophiles such as amines and terminal alkenes (one pot synthesis *via* acceptorless dehydrogenative coupling).¹¹



Scheme 4.2: General reaction scheme for: **a)** dehydrogenation in presence of oxygen, and **b)** acceptorless dehydrogenation.

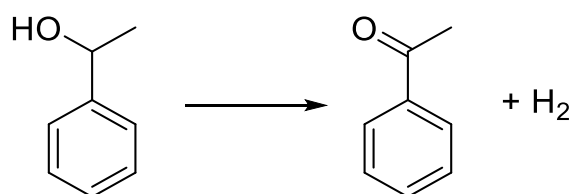
Due to the substantial increase of sustainability achieved *via* this route, several efforts have been focused on performing acceptorless alcohol dehydrogenation with heterogeneous catalysts, including supported noble metal nanoparticles (Cu,¹³ Ag,¹⁴ Au¹⁵), with the best

catalytic performances exhibited by Ag nanoparticles supported on hydrotalcite.¹⁶ Notably, although displaying lower activities, examples of supported Ni,^{17,18} Co,¹⁹ Pt,²⁰ Re²¹ and Ru^{22,23} have also been reported in the literature.

Despite notable breakthroughs, alcohol dehydrogenation still suffers from several major drawbacks including:

- 1- Scarce catalytic activity.
- 2- The reactors employed for this reaction generally prohibit time online measurement of the H₂ produced during the chemical reaction, which limits full kinetic investigation of the chemical process under study.
- 3- The reaction mechanism is still not clear (thus preventing critical/rigorous optimisation studies of the catalysts).
- 4- The viability of this reaction in continuous mode still must be efficiently achieved.

The limited knowledge of continuous operations on acceptorless alcohol dehydrogenation, catalysed by heterogeneous catalyst, strongly limits the industrial applicability of this route, which is highly desirable from a sustainability standpoint. Therefore, the dehydrogenation of 1-phenylethanol (Scheme 4.3) as model reaction was investigated in order to study the first step of the Guerbet process. This reaction was chosen for two main reasons: 1-phenylethanol is a more activated substrate compared to ethanol and more likely to react at lower temperatures; and the product, acetophenone is easier to handle than its analogue acetaldehyde, which presents a high reactivity and very low boiling point (20 °C).



Scheme 4.3: General reaction scheme for dehydrogenation of 1-phenylethanol to acetophenone with formation of H₂.

4.2. Results and Discussion

4.2.1. The catalyst, preliminary kinetic measurements

As reported in Section 4.1, several examples of alcohol dehydrogenation reactions using heterogeneous catalysts based on noble metals deposited nanoparticles, can be found in literature, where Ag supported on hydrotalcite (HT) stands out with the best catalytic performance (full conversion of 1-phenylethanol with a selectivity >99 % after a period of 16 h).¹⁶ In order to properly understand the catalytic properties of dehydrogenating agents, Ag/HT was synthesised as described in Section 2.2.1.3. This catalyst was tested for the dehydrogenation of 1-phenylethanol in batch under N₂ flow (10 mL min⁻¹) as described in Section 2.3.2. 21.7 % of conversion of 1-phenylethanol was recorded with 73.1 % of selectivity for acetophenone were achieved following 3 h of reaction at 120 °C. To minimise side reactions, it is essential to find a catalyst highly selective towards acceptorless dehydrogenation and therefore other catalysts were tested.

Given the few options present in literature, similar reaction systems were considered. Previous work on formic acid dehydrogenation,²⁴ had shown that commercial Pd on C (Pd 5 wt.% on activated C (Pd/C), Sigma Aldrich®) exhibited the best catalytic performance for H₂ generation, and therefore Pd/C was identified as a suitable choice to perform 1-phenylethanol dehydrogenation to acetophenone. Herein, as shown in Table 4.1, Pd/C exhibits a superior catalytic activity compared with Ag/HT, under identical reaction conditions.

Table 4.1: Catalytic performance of Ag/Hydrotalcite and Pd/C.^[a]

<u>Catalyst</u>	<u>X</u> (%) ^[b]	<u>S</u> (%) ^[c]
Ag/HT	21.7	73.1
Pd/C	93.8	95.9

[a] Reaction conditions: 20 mL of a solution 0.2 M of 1-phenylethanol in *p*-xylene, 0.1 g of catalyst, 120 °C. Reaction carried out under N₂ flow of 10 mL min⁻¹. **[b]** Conversion of 1-phenylethanol. **[c]** Selectivity for acetophenone.

Kinetic studies were carried out using Pd/C as catalyst in N₂ atmosphere. Preliminary time online analyses are presented in Figure 4.1. As can be seen, experiments performed at a Pd/substrate ratio of 1/80 (1.25 mol%), show conversion of 90 % of the 1-phenylethanol into

the desired product after 3 h of reaction. Notably, an acetophenone selectivity of more than 95 % is observed throughout the reaction period, indicating that the dehydrogenation of 1-phenylethanol can efficiently be catalysed by Pd/C in N₂ atmosphere. The acceptorless dehydrogenation of alcohols is usually performed using He as inert gas but, in addition to its high activity and stability, the described reaction can be efficiently performed in N₂, leading to increased economic viability.

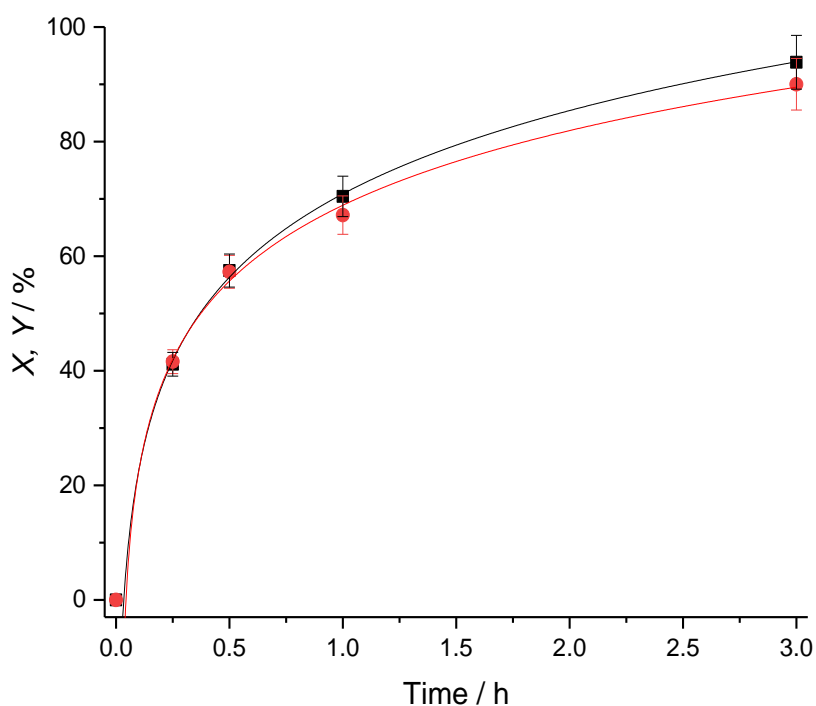


Figure 4.1: Conversion (X, black squares) of 1-phenylethanol and yield (Y, red circles) of acetophenone over Pd/C catalyst, over time. **Reaction conditions:** 20 mL of a solution 0.2 M of 1-phenylethanol in *p*-xylene, 120 °C. Reaction carried out under N₂ flow of 10 mL min⁻¹, 1.25 mol% Pd/Substrate molar ratio.

Herein, selectivity improvement is investigated through optimisation of parameters such as mass of catalyst, stirring rate and reaction temperature.

4.2.2. Impact of temperature

The first parameter investigated was the effect of temperature on the system. The reaction was carried out in a range of temperatures between 100-120 °C as described in Section 2.3.2 based on literature¹⁶⁻²⁰. Through the results shown in Figure 4.1, a loss in selectivity to

acetophenone can be appreciated at extended reaction time. Based on that observation, and with the aim of maximising the production of H₂, subsequent reactions were carried out for 0.5 h (Figure 4.2).

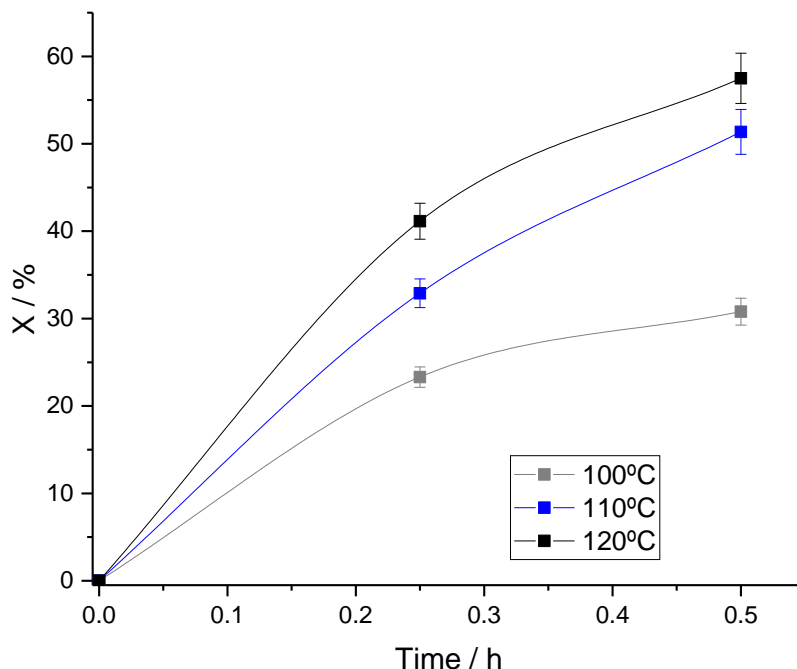


Figure 4.2: Conversion (X) of 1-phenylethanol obtained in the temperature range of 100-120 °C over time. **Reaction conditions:** 20 mL of a solution 0.2 M of 1-phenylethanol in *p*-xylene, 1.25 mol% Pd/Substrate molar ratio. Reaction carried out under N₂ flow of 10 mL min⁻¹.

As can be seen in Figure 4.2, the conversion per unit time decreases when lower temperature is employed. For instance, the conversion reached at 100 °C is 46 % lower than the obtained at 120 °C. However, no changes on reaction selectivity occur over the range tested. Kinetic constant obtained from each reaction for first order reaction adjustment can be used to calculate the activation energy of the reaction using the Arrhenius equation (Equation 4.1):

$$\ln k = \ln A - \frac{E_{act}}{RT} \quad [Equation 4.1]$$

Interestingly, constructing an Arrhenius plot (Figure 4.3), with the rate of the reaction between 100 and 120 °C, results in an activation energy of only 31 kJ/mol, a value far lower than E_{act} found in literature^{25,26}. Considering that the cleavage of a C(sp³)-H bond should be involved in the reaction mechanism, the obtained data show an extremely low barrier. This low activation energy can indicate a thermodynamic control but may also indicate contribution from other factors, particularly mass transfer. Therefore, further studies were performed to ensure that the amount of catalyst employed was low enough to carry out the reaction under the kinetic regime.

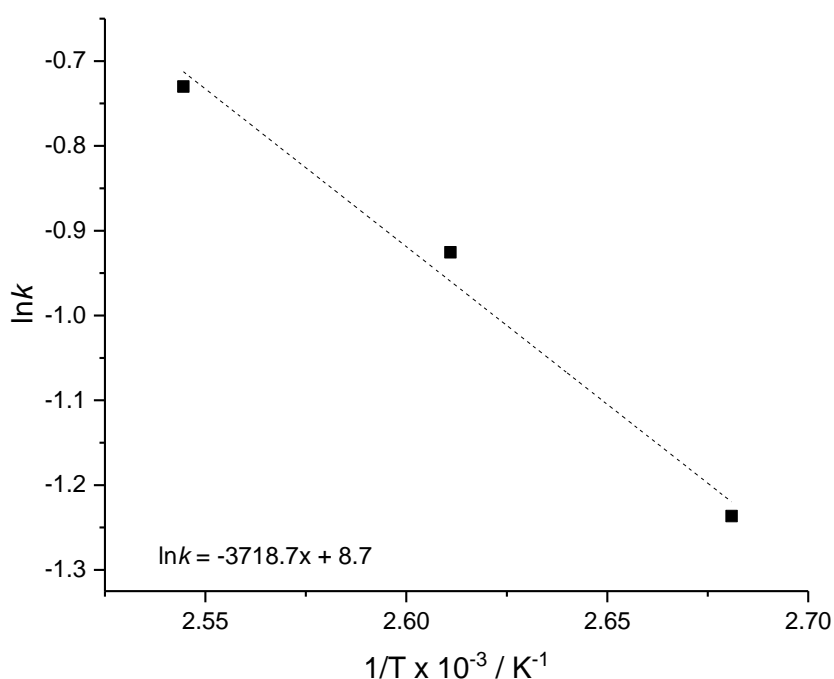


Figure 4.3: Arrhenius plot obtained in a temperature range of 100-120 °C.

4.2.3. Impact of catalyst/substrate ratio and stirring rates

Being in the kinetic regime, *i.e.* under catalyst control, is of great importance to obtain reliable catalytic data free of interferences such as mass transfer limitations, which can occur when the limiting reaction step is the diffusion of the reactants to the active sites of the catalyst, instead of being the reaction itself. Therefore, the effect of the mass of catalyst employed was investigated in order to ensure performance in a purely kinetic system.

Accordingly to the results obtained in Section 4.2.2, a series of experiments were carried out at identical conditions, where the amount of Pd relative to 1-phenylethanol was varied from 0

to 1.25 (mol%). As can be seen in Figure 4.4, although a linear relationship between activity and the quantity of Pd exists at low metal molar ratios, deviation from the initial linearity occurs above 0.1 %, leading to a different regime. Thus, to maintain kinetic integrity, 0.08 mol% was chosen as the amount of catalyst molar ratio for catalytic reactions.

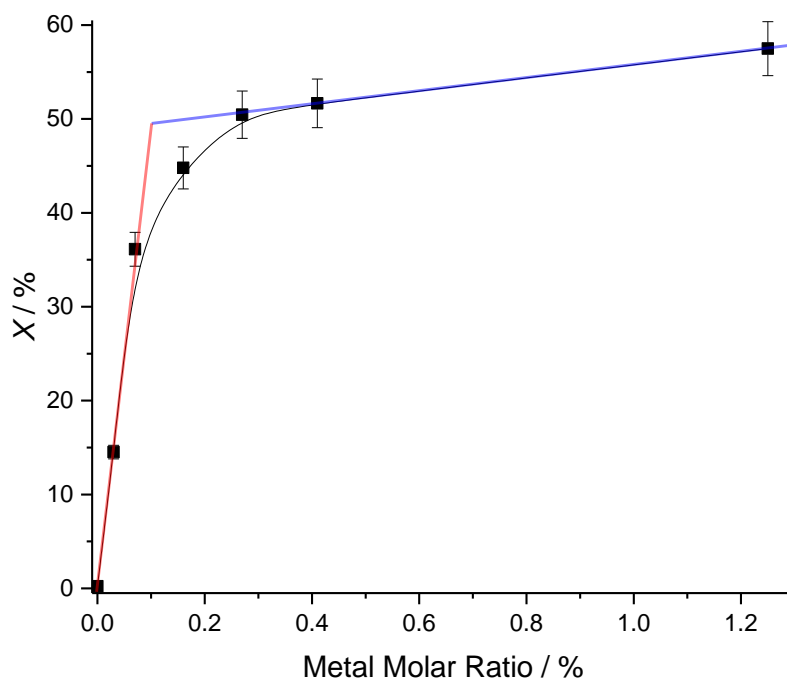


Figure 4.4: Conversion (X) of 1-phenylethanol over metal molar ratio. **Reaction conditions:** 20 mL of a solution 0.2 M of 1-phenylethanol in *p*-xylene, 120 °C, 10 min. Reaction carried out under N_2 flow of 10 mL min^{-1} . External standard 0.01 M biphenyl in toluene.

Having identified the optimal amount of catalyst needed, additional optimisation experiments were performed varying the stirring rate to ensure the kinetic regime and avoid mass transfer. As can be seen in Figure 4.5, gradual improvement on catalytic performance is observed with increasing stirring rate from 250 to 750 rpm, suggesting that stirring rates equal or above 750 rpm is also essential to avoid mass transfer limitations. Given the higher levels of activity and selectivity, 750 rpm was chosen as the stirring rate to be used for the rest of the study.

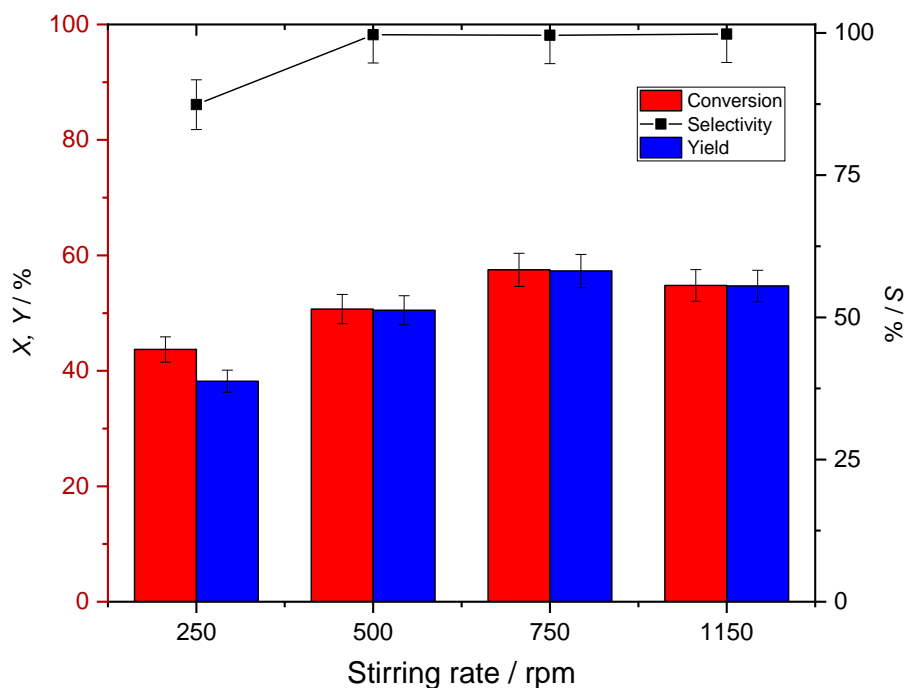


Figure 4.5: Conversion (X) of 1-phenylethanol (red bars), Yield (Y) of acetophenone (blue bars) and Selectivity (S) for acetophenone at different stirring rates. **Reaction conditions:** 100 mL round-bottom flask, 20 mL of a solution 0.2 M of 1-phenylethanol in *p*-xylene and 0.08 mol% of Pd/substrate molar ratio (7.2 mg Pd/C 5 wt.%), 130 °C, 30 min. External standard 0.01 M biphenyl in toluene. Purged 6 min with a flux of 50 mL min⁻¹ of N₂ and preheated for 15 min prior reaction. Reaction carried out in a N₂ flow of 10 mL min⁻¹.

4.2.4. Optimisation of the reactor

Acceptorless alcohol dehydrogenation is particularly desirable over other alcohol dehydrogenation strategies due to the beneficial co-production of H₂. In fact, H₂ represents a particularly green and sustainable source of energy compared to typical non-renewable fossil sources. Therefore, accurate analysis of the gas produced throughout 1-phenylethanol dehydrogenation is essential to perform thorough kinetic and mechanistic studies of alcohol dehydrogenation and confirm both, the formation of H₂ as reaction product and that the reaction is truly acceptorless.

Under typical literature conditions *i.e.* in conventional borosilicate batch reactors, technical challenges need to be faced. To achieve the acceptorless dehydrogenation the absence of O₂ is indispensable. As such, the reactions presented in this chapter were carried out under N₂ flow, which regrettably prevents accurate collection and quantification of the gas produced during the reaction. Attempt to seal the system would lead to dangerous scenarios such as

increase of pressure for the gas produced and explosive atmosphere buildings. To overcome these problems and allow accurate analyses of the gaseous products, a novel reactor was developed. The reactor consisted of an Ace round-bottom pressure flask with an Ace-Thred 15 PTFE front-seal plug, with a tolerance of 8 bar, coupled to a stainless steel reactor body, which is connected to a volumetric glass vessel, isolated from the atmosphere through water, that acts as collection vessel. Equipped with this setup, the experiments can be carried out in static N₂ atmosphere; the volume of the gas formed during reaction was periodically monitored at three different temperatures in a range 110-130 °C. In all cases, the amount of gas collected during the first 10 min of reaction was in good agreement to the theoretical amount of gas that should be produced, based on the mols of 1-phenylethanol converted (Table 4.2). This observation confirms that appropriate time online measurements can be achieved by measuring the gas evolution during the reaction. In addition to achieving time online analysis by measuring the amount of H₂ produced, analysis of the liquid phase could also be achieved following termination of the reaction, allowing substrate conversion and product yields to also be determined for all liquid products by Gas Chromatography (GC) analysis. Small quantities of ethylbenzene and styrene were identified as side products.

Table 4.2: Catalytic performance of Pd/C at different temperatures. ^[a]

<u>I</u> (°C) ^[a]	<u>X</u> (%) ^[b]	<u>Y</u> (%) ^[c]	<u>S</u> (%) ^[d]	<u>C. B.</u> (%) ^[e]	<u>T.V. Gas</u> (mL) ^[f]	<u>C.V. Gas</u> (mL) ^[g]
130	29.6	28.8	97.6	99.4	26.1	25
120	23.6	23.6	99.9	100	22.0	20
110	15.4	15.4	99.9	100	14.4	15

[a] Reaction conditions: stainless steel reactor body with 100 mL pressurised round bottom flask. 0.2 M of 1-phenylethanol in *p*-xylene, 0.08 mol% of Pd/substrate molar ratio, static N₂ atmosphere, 0.16 h. **[b]** Conversion of 1-phenylethanol. **[c]** Yield of acetophenone. **[d]** Selectivity for acetophenone. **[e]** Carbon balance. **[f]** Theoretical volume of gas. **[g]** Collected volume of gas.

4.2.5. Analysis of gas products

In addition to allowing the kinetic parameters to be verified from both the gaseous and liquid phases, this approach with the new reactor also permits the acceptorless nature of the dehydrogenation reaction to be confirmed. The gas produced during the dehydrogenation of 1-phenylethanol was collected over a reaction time of 1 h (43 mL of gas collected) and analysed *via* mass spectrometry. As can be seen in Table 4.3, compositional analysis indicates 24.4 mol% of H₂ to be present into the gas mixture. To ensure that the produced H₂ derives from dehydrogenation of the substrate, a control experiment was performed, conducting the reaction under typical reaction conditions, albeit in the absence of the substrate. As expected, only trace amounts of H₂ were detected (0.08 mol%), indicating 1-phenylethanol to be the source of H₂.

Table 4.3: Gas composition analysis for 1-phenylethanol dehydrogenation with and without 1-phenylethanol.^[a]

Gas Composition (mol%)	<u>N</u>₂	<u>H</u>₂	<u>O</u>₂
General reaction	74.12	24.73	1.15
Without 1-phenylethanol ^[b]	99.20	0.08	0.72

[a] Reaction conditions: stainless steel reactor body with 100 mL pressurised round bottom flask. 0.2 M of 1-phenylethanol in *p*-xylene, 0.08 mol% of Pd/substrate molar ratio, static N₂ atmosphere, 1 h. **[b]** No 1-phenylethanol.

The relatively high molar percentage of H₂ detected in the gas phase, in addition to the good catalytic performances exhibited by the catalyst, strongly indicates that acceptorless alcohol dehydrogenation can efficiently be catalysed by commercial Pd/C in N₂ atmosphere. Notably, the employment of an inert gas dramatically reduces the overoxidation problems typically observed during aerobic alcohol oxidation,⁸ leading to higher selectivity values for the carbonyl compounds.

4.2.6. Side reactions and impact of H₂ accumulation

As demonstrated previously in this chapter, Pd/C shows remarkable catalyst activity for the acceptorless dehydrogenation of 1-phenylethanol in N₂ atmosphere with outstanding selectivity to acetophenone in the tested conditions. Accordingly, a reaction was carried out

for an extended period under optimised reaction conditions. As compiled in Table 4.4, performing the reaction for prolonged time (18 h) under optimised reaction conditions results in a drop in selectivity from 97.6 to 69.0 %. This phenomenon was not observed in the preliminary tests under N₂ flow, thus suggesting the presence of side reactions affected by different levels of H₂ in the reaction medium. In parallel to the drop of selectivity, the amount of substrate converted at extended periods is lower than anticipated based on the initial rate of reaction (from 29.6 % conversion of 1-phenylethanol at 10 min to only 51.0 % at 2.5 h). This result is in agreement with previous reports, suggesting the reversibility of the process,^{27,28} through regeneration of the substrate following the hydrogenation of acetophenone.

Table 4.4: Effect of N₂ on 1-phenylethanol dehydrogenation catalysed by Pd/C.^[a]

Time (h)	X (%)^[b]	Y (%)^[c]	S (%)^[d]	C. B. (%)^[e]
0.16	29.6	28.8	97.6	100
2.5	51.0	40.8	80.0	100
18	85.2	58.8	69.0	100
2.5 ^[f]	72.7	71.5	98.4	100

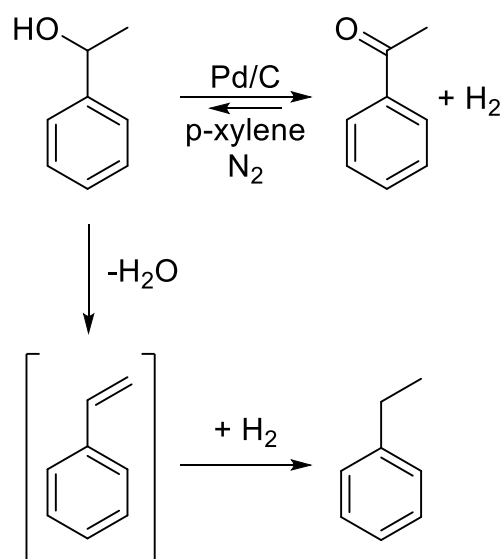
[a] Reaction conditions: stainless steel reactor body with 100 mL pressurised round bottom flask. 0.2 M of 1-phenylethanol in *p*-xylene. 0.08 mol% of Pd/substrate molar ratio, static N₂ atmosphere. **[b]** Conversion of 1-phenylethanol. **[c]** Yield of acetophenone. **[d]** Selectivity for acetophenone. **[e]** Carbon balance. **[f]** Reaction performed in N₂ flow (10 mL min⁻¹).

Subsequently, to study the negative effect of H₂ accumulation on the reaction, experiments were performed with a static N₂ atmosphere was replaced with N₂ flow, to remove the H₂ from the reaction mixture following its formation. Performing the reaction under N₂ flow (10 mL min⁻¹) dramatically increases 1-phenylethanol conversion and acetophenone yield, and boosts selectivity to acetophenone up to 98.4 %, strongly indicating that excessive quantities of H₂ are detrimental for selectivity at high conversion.

4.2.7. Side reactions and 1-phenylethanol stability

The results presented in the previous section indicate the presence of two different processes affecting the selectivity for acceptorless dehydrogenation of alcohols catalysed by Pd/C (Scheme 4.4):

- The reversibility of the dehydrogenation, where excess H_2 in the mixture results in rehydrogenation of acetophenone to 1-phenylethanol.
- The dehydration of 1-phenylethanol to styrene with a consecutive hydrogenation to ethylbenzene.



Scheme 4.4: Proposed reaction pathways, reporting the reversibility of the direct reaction and the side reactions.

Therefore, closer attention was considered for dehydrogenation of 1-phenylethanol at high conversions. Detailed GC analyses of the liquid phase, shown in Figure 4.6, reveal that the quantity of acetophenone lost under static N_2 atmosphere is comparable to the amount of ethylbenzene formed.

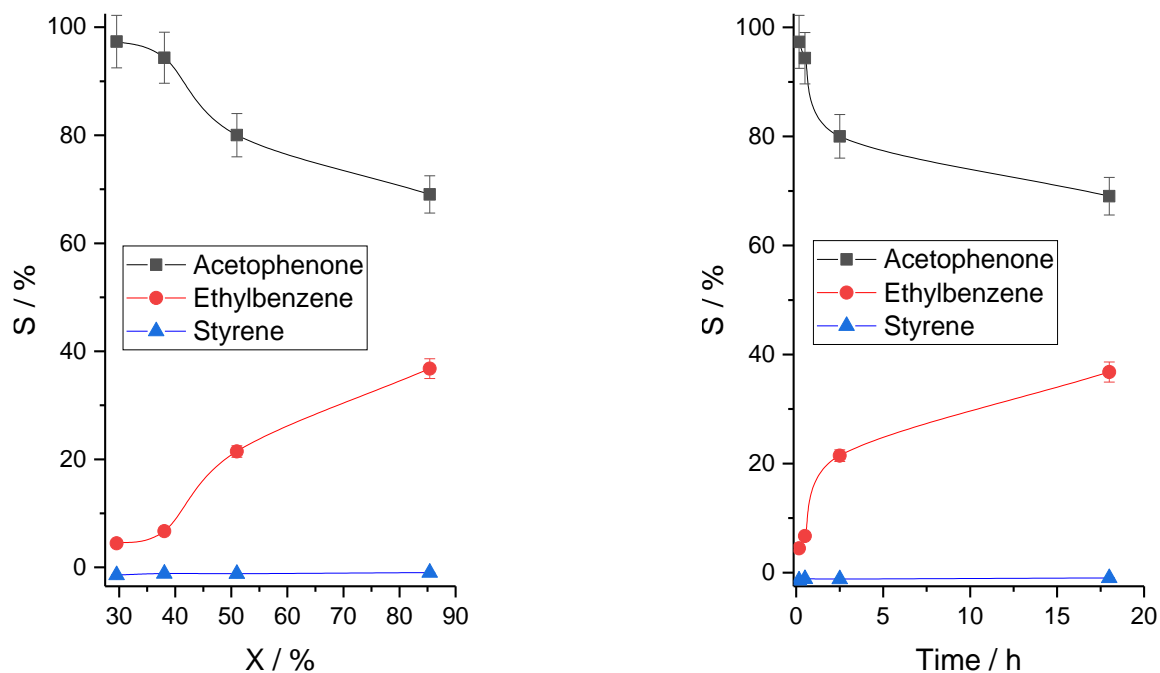
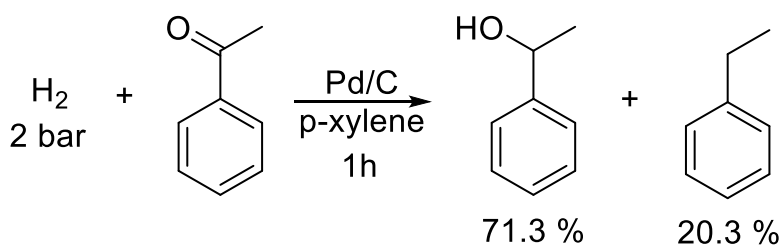


Figure 4.6: Left. Selectivity (S) for; i) acetophenone (squares), ii) ethylbenzene (circles), and iii) styrene (triangles) over 1-phenylethanol conversion (X). Right. Time online profile of selectivity for i) acetophenone (squares), ii) ethylbenzene (circles), and iii) styrene (triangles). **Reaction conditions:** stainless steel reactor body with 100 mL pressurised round bottom flask. 20 mL of a solution 0.2 M of 1-phenylethanol in *p*-xylene, 0.08 mol% of Pd/substrate molar ratio, static N₂ atmosphere.

To further explain these observations, reactant stability studies were conducted by the hydrogenation of acetophenone and styrene (Scheme 4.5) in an autoclave filled with H₂ (2 bar) and Pd/C as catalyst under optimised condition, as is described in Section 2.3.6.

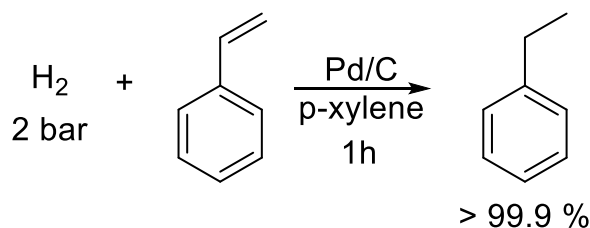


Scheme 4.5: Acetophenone hydrogenation catalysed by Pd/C. Autoclave reactor (Parr® 5500) with 100 mL glass liner. **Reaction conditions:** 20 mL of a solution 0.2 M of acetophenone in toluene and 0.08 mol% of Pd/substrate molar ratio, 130 °C. Reaction performed with 2 bar of H₂.

Following 1 h of hydrogenation, a yield of 71.3 % of 1-phenylethanol, and 20.3 % of ethylbenzene were detected when employing acetophenone as substrate. This result is in

agreement with the previous section, indicating that at high quantities of H₂, the reverse hydrogenation of acetophenone occurs, accompanied by the formation of 1-phenylethanol.

Although no styrene was found into this last reaction mixture, it may still be involved in the reaction mechanism as an intermediate (Scheme 4.6) with a short lifetime, *i.e.* this compound may be formed from the dehydration of 1-phenylethanol and rapidly undergoes hydrogenation to yielding ethylbenzene.



Scheme 4.6: Styrene hydrogenation catalysed by Pd/C. Autoclave reactor (Parr® 5500) with 100 mL glass liner. **Reaction conditions:** 20 mL of a solution 0.2 M of styrene in toluene and 0.08 mol% of Pd/substrate molar ratio, 130 °C. Reaction performed with 2 bars of H₂.

To validate this hypothesis, analogous stability studies were performed using styrene as substrate. Reaction conditions are detailed in Section 2.3.6. As detailed in Scheme 4.6, after 1 h of reaction full conversion of styrene into ethylbenzene is reached, indicating that Pd/C is also an effective catalyst for hydrogenation of styrene in the presence of H₂. These side reactions indicate the detrimental effect that excessive quantities of H₂ exert on the reaction. Hence, working under conditions that remove H₂ from the reactor, and/or working at low conversion conditions, is beneficial for the overall reaction. Based on these mechanistic observations, all further kinetic studies were performed at short reaction times and lower conversion levels, to limit the contribution of the side reactions to the kinetic parameters and catalyst optimisation studies. Moreover, experiments were performed under static conditions to continue to permit measurement of the gaseous phase of the reaction.

4.2.8. Hot filtration test

To ensure that the reaction is truly heterogeneously catalysed, *i.e.* that no contribution to the reaction rate derives from homogeneous species leached into the reaction mixture, a “hot filtration” experiment was performed (Figure 4.7) as is described in Section 2.3.5.

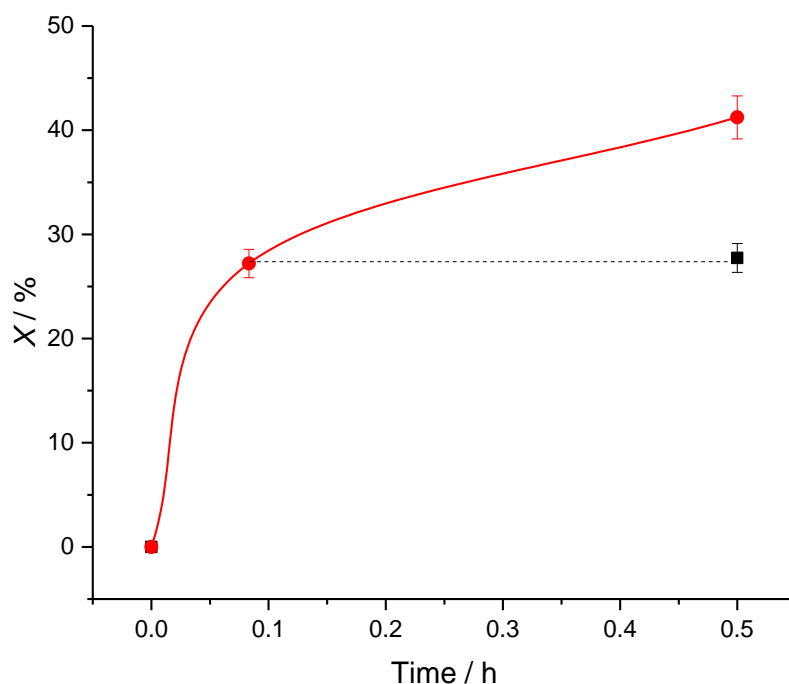


Figure 4.7: Conversion (X) of 1-phenylethanol over time (h) for: i) hot filtration experiment (black square), ii) normal 1-phenylethanol dehydrogenation (red circles). **Reaction conditions:** stainless steel reactor body with 100 mL pressurised round bottom flask. 20 mL of a solution 0.5 M of 1-phenylethanol in *p*-xylene and 0.08 mol% of Pd/substrate molar ratio, 130 °C. External standard 0.01 M biphenyl in toluene. Purged 30 min with a flux of 50 mL min^{-1} of N_2 and preheated for 15 min prior reaction. Reaction carried out in static N_2 atmosphere.

As can be seen in Figure 4.7, following filtration of the solid catalyst, no further changes to the solution are observed, indicating termination of the reaction by removal of the catalyst and, hence, demonstrating that the reaction is truly heterogeneously catalysed.

4.2.9. Optimised kinetic studies

Having identified the optimal kinetic regime of the reaction and ensuring a negligible contribution of side reactions to the reaction network, an accurate Arrhenius plot can be obtained. Monitoring the reaction by the gas production, allows the measure of the initial rate of the reaction (k) in the linearity range ($t < 3.5$ min) at different temperatures (110-130 °C, Figure 4.8) for a first order kinetic adjustment (Equation 4.2, PE: 1-phenylethanol)).

$$\ln [PE] = \ln [PE]_0 - kt \quad [\text{Equation 4.2}]$$

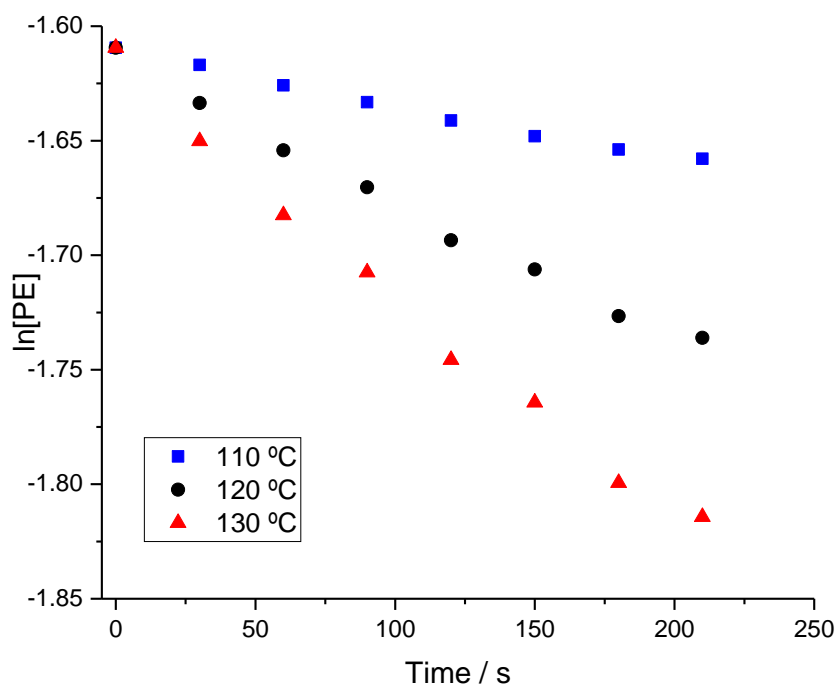


Figure 4.8: \ln of [1-phenylethanol] over time at different temperatures (110-130 °C). **Reaction conditions:** stainless steel reactor body with 100 mL pressurised round bottom flask. 20 mL of a solution 0.2 M of 1-phenylethanol in *p*-xylene, 0.08 mol% of Pd/substrate molar ratio, static N_2 atmosphere.

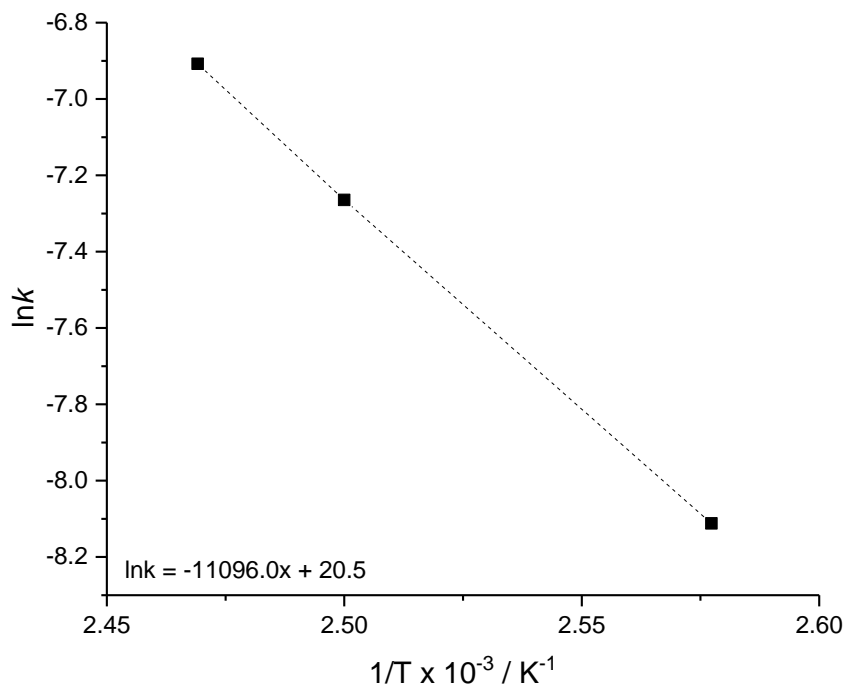
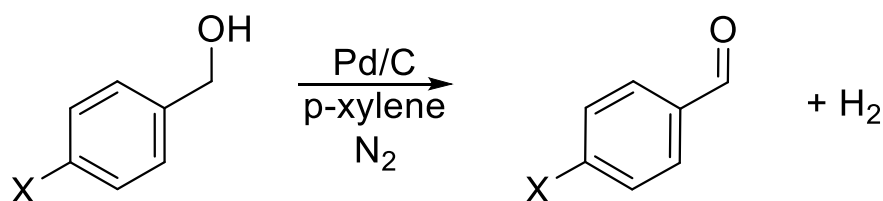


Figure 4.9: Arrhenius plot obtained in a temperature range of 110-130°C.

At true kinetic conditions, after a full optimisation to discard that the limiting step is the diffusion of the substrate to the active sites, a higher activation energy of 92 kJ/mol is determined (Figure 4.9), in better agreement to the nature of the reaction and in line with previous reports.^{8,29}

4.2.10. Mechanistic studies

Following these kinetic insights, more detailed attention was paid to the mechanism of the reaction, since very little is known about acceptorless dehydrogenation chemistry. As such, mechanistic studies were performed *via* Hammett correlation and determination of Kinetic Isotope Effects (KIEs). Due the lack of adequate commercial 1-phenylethanol derivatives, benzyl alcohol was selected as a new model compound.



Scheme 4.7: General reaction scheme for dehydrogenation of *p*-substituted benzyl alcohols to their corresponding aldehydes with liberation of H₂.

In order to identify the nature of the intermediate species involved in the reaction mechanism, a Hammett correlation was obtained, using substituted benzyl alcohols as substrates for acceptorless dehydrogenation from Pd/C, due to greater commercial availability of substituted benzylic alcohols. Purely electronic effects can be studied by using the Hammett equation, which describes a linear Gibbs free energy relationship relating the changes in equilibrium or rate constant with the presence of substituent groups. The basics of this equation (Equation 4.3) rely on the linear change of rate of reaction observed depending on the electron donating/withdrawing ability of the substituent involved:

$$\log \frac{kR}{kH} = \sigma \rho \quad [\text{Equation 4.3}]$$

Where k_R is the reaction rate involving the substituted reactant, k_H is the reaction rate involving unsubstituted reactant ($R = H$), σ is the Hammett constant determined for each R and ρ is the reaction constant which depends only on the type of reaction.

A great variety of organic substituent groups have their Hammett constant value assigned depending on their electron donating ($\sigma < 1$) or electron withdrawing ($\sigma > 1$) capabilities, differentiating also the substituent position (*ortho*, *meta*- or *para*-).^{30,31}

As can be seen (Figure 4.10) the acceptorless dehydrogenation of benzyl alcohol and its *p*-substituted analogues, 4-methylbenzyl alcohol and 4-chlorobenzyl alcohol, indicates that electron donating substituents, such as $-\text{CH}_3$, lead to increased activity. On the other hand, electron withdrawing groups, such as $-\text{Cl}$, exhibit a negative impact on the reaction rate. The negative slope of the Hammett plot strongly indicates the formation of a positively charged reaction intermediate, suggesting the formation of a carbo-cationic intermediate during the reaction mechanism.

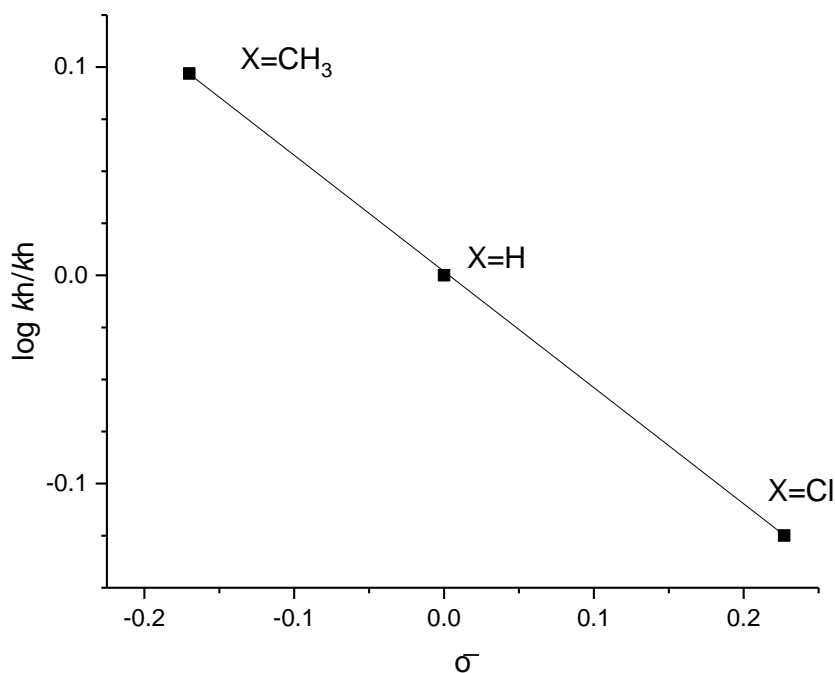
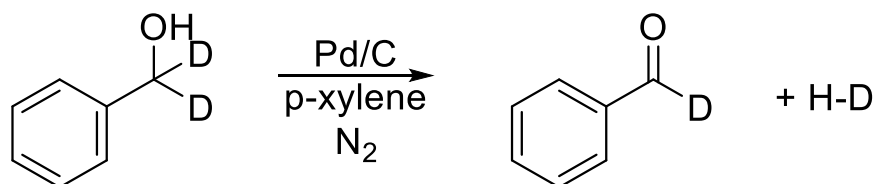


Figure 4.10: Hammett plot obtained from substituted benzyl alcohol dehydrogenation to acetophenone over Pd/C
Reaction conditions: stainless steel reactor body with 100 mL pressurised round bottom flask. 20 mL of a solution 0.2 M of substrate in *p*-xylene, 0.08 mol% of Pd/substrate molar ratio, 0.16 h, 130 °C, static N_2 atmosphere.

Additional mechanistic insights on the reaction mechanism were obtained by deuteration of the benzylic H-atoms of the substrate, and thereby studying its Kinetic Isotope Effect (KIE). A KIE is the change in the reaction rate of a chemical reaction when one of the atoms in

the reactants is replaced by one of its isotopes.³² Formally, it is the ratio of rate constants for the reactions involving the light (k_H) and the heavy (k_D) isotopically substituted reactants (isotopologues).



Scheme 4.8: General reaction scheme for dehydrogenation of α deuterated benzyl alcohol.

This change in reaction rate is a mechanical effect that primarily results from heavier isotopologues having lower vibrational frequencies compared to their lighter counterparts. In most cases, this implies a greater energetic input needed for heavier isotopologues to reach the transition state, and consequently, a slower reaction rate.

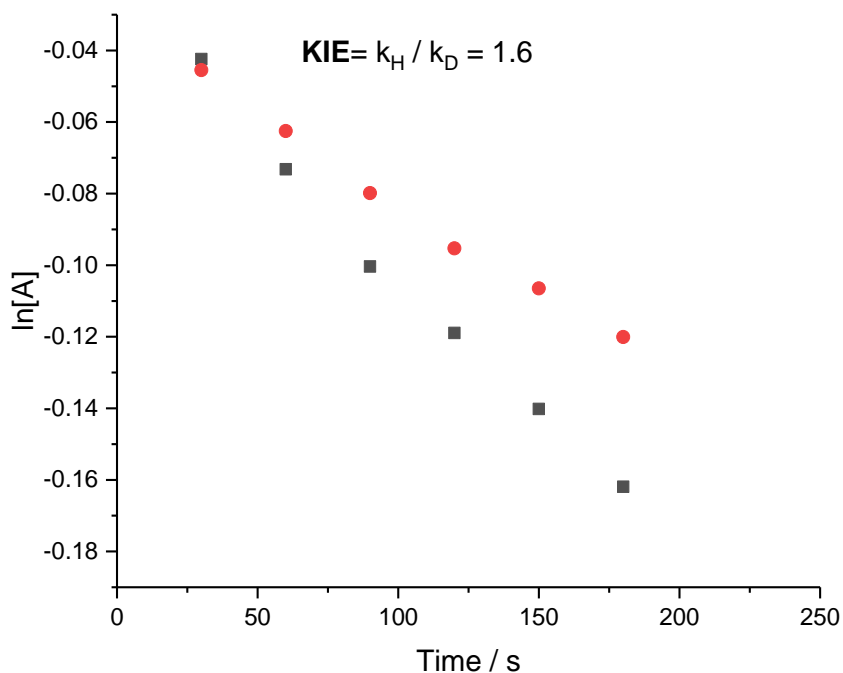


Figure 4.11: Reaction rate for benzyl alcohol (black squares) and α,α -deuterated benzyl alcohol (red circles). **Reaction conditions:** stainless steel reactor body with 100 mL pressurised round bottom flask. 20 mL of a solution 0.2 M of substrate in *p*-xylene, 0.08 mol% of Pd/substrate molar ratio, 0.16 h, 130 °C, static N₂ atmosphere.

As can be seen in Figure 4.11, a lower reaction rate was observed when benzylic C-D bonds are present over C-H bonds. KIEs greater than 1 usually indicate that cleavage of that bond is involved in the rate determining step of the reaction, which indicates that cleavage of the benzylic C-H/D bond may be rate limiting. However, it is notable that the observed KIE is lower than that typically observed for reactions limiting by the rate of C-H bond cleavage.^{33,34}

This could be due to second order effects, where the H/D substitution in question is not directly involved in the rate limiting step, or the involvement of the H/D atom in a different rate limiting step, such as elimination of the H/D atom (H-D formation) from the Pd surface to regenerate the active site. Nevertheless, the negative Hammett correlation coupled with a KIE > 1 indicates that the acceptorless dehydrogenation reaction possesses similarities to classical beta-hydride elimination mechanisms, often observed during aerobic alcohol oxidation.³⁵

4.2.11. Optimisation of the catalyst

Having identified a promising catalyst candidate, optimisation of its activity was undertaken. In the aforementioned studies of formic acid decomposition,¹² it has been reported that different Pd species in the catalyst impact catalytic activity. As such, preliminary catalyst optimisation studies were performed by examining the effect of the oxidation state of the metal (Pd) on the reaction rate.

To do so, the catalyst was subjected to a series of heat treatments under reducing atmosphere (5 % H₂ in Ar), or under oxidising conditions (in air) in a range of temperatures between 200 and 400 °C. These treated samples were tested for the acceptorless dehydrogenation of 1-phenylethanol at the optimised conditions (Figure 4.12). Notably, although treatments in H₂ performed at 400 °C did not affect the C support, the analogous treatment in air at 400 °C led to decomposition of the support, where the physical aspect of the catalyst changes radically, from a fine black powder (fresh catalyst), to a reddish solid, with a more evident loss of volume. Therefore, the appropriate temperatures were concluded to be 400 °C for the H₂ treatment and 300 °C for the air treatment.

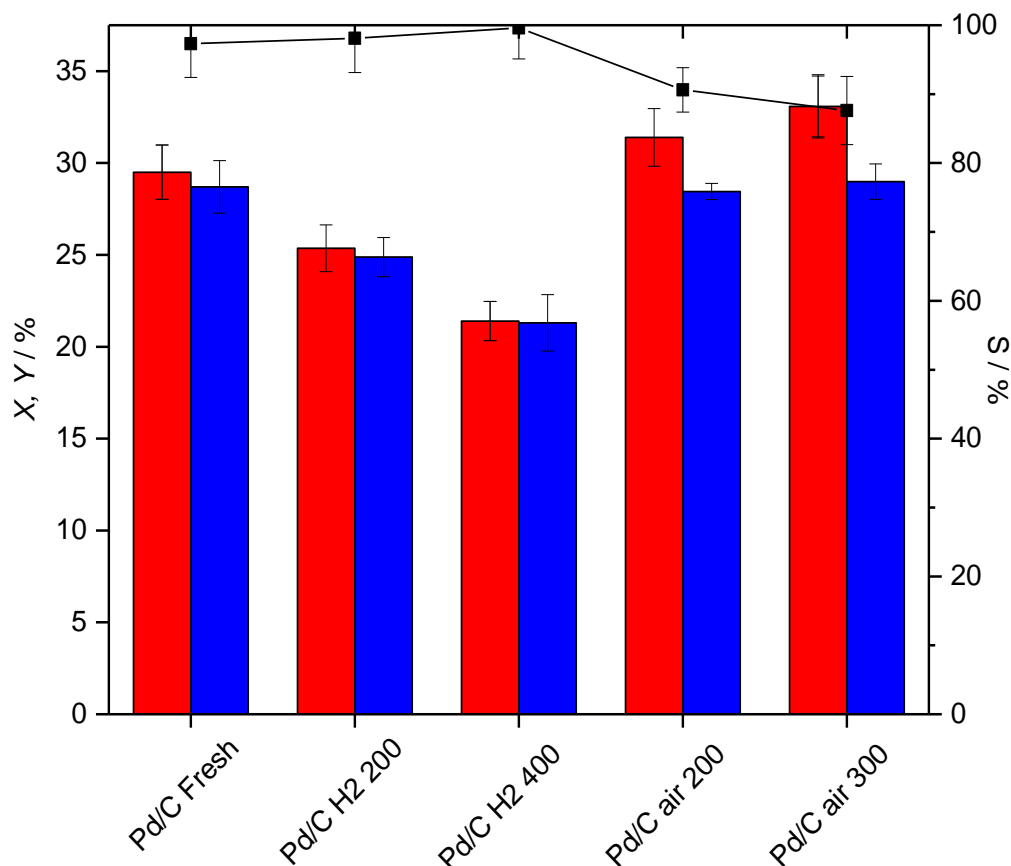


Figure 4.12: Conversion (X) of 1-phenylethanol (red bars), yield (Y) of acetophenone (blue bars) and selectivity (S) for acetophenone (black squares) for: a) fresh Pd/C (*i.e.* not treated), Pd/C heated in 5 % H₂ in Ar for 2 h (ramp rate 10 °C min⁻¹) b) at 200 °C and c) at 400 °C, and Pd/C heated under air for 2 h (ramp rate 10 °C min⁻¹) d) at 200 °C and e) at 300 °C. **Reaction conditions:** stainless steel reactor body with 100 mL pressurised round bottom flask. 20 mL of a solution 0.2 M of 1-phenylethanol in *p*-xylene, 0.08 mol% of Pd/substrate molar ratio, 130 °C, static N₂ atmosphere, 0.16 h.

As shown in Figure 4.12, although a beneficial effect on the catalytic performance of Pd/C is observed by treating the catalyst in air for 2 h at 300°C (from 29.5 % to 33.1 % of 1-phenylethanol conversion), loss in selectivity for acetophenone occurs (from 97.3 % to 87.6 %). An opposite effect can be observed calcining the catalyst under reducing atmosphere (10 °C min⁻¹, 2 h at 400 °C or 200 °C in 5 % H₂ in Ar), with lower conversion values achieved but full selectivity (>98 %) toward the desired product, acetophenone. However, these differences may also be (partially) related to the natural conversion vs. selectivity relationship of the reaction, where higher selectivity is observed at lower levels of conversion for a lower influence of side reactions.

4.2.12. Characterisation of Pd/C

To correlate the observed trends in selectivity and activity with differences in Pd speciation and material properties, selected catalysts were characterised *via* X-Ray Diffraction (XRD), X-ray Photoelectron Spectroscopy (XPS), Transmission Electron Microscopy (TEM) and Brunauer-Emmett-Teller (BET) analysis.

4.2.12.1. X-Ray diffraction

XRD analyses of the fresh Pd/C catalyst before and after the mentioned heat treatments were performed to evaluate the effect of these processes over the original structure. As can be seen in Figure 4.13, all XRD patterns presented the same characteristic diffraction peak of the C support, and showed comparable intensity, demonstrating the preservation of the structure. However, changes to the Pd peaks are observed depending on the oxidative/reducing conditions of the heat treatment applied to the selected sample.

Moreover, the decomposition of the catalyst by treatment in air at 400 °C is confirmed with the XRD results presented in Figure 4.14, where the diffraction peak of the C support disappears leaving only the pattern of different Pd species.

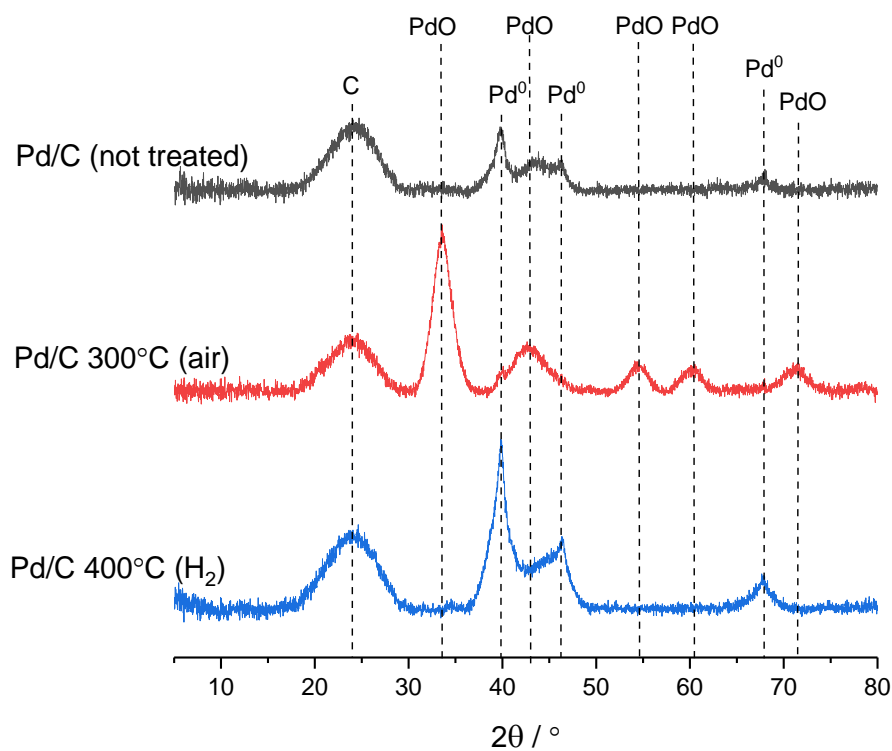


Figure 4.13: pXRD pattern of: fresh Pd/C (*i.e.* not treated, black), Pd/C heated at 300 °C under air for 2 h (ramp rate 10 °C min⁻¹, red), and Pd/C heated at 400 °C in 5 % H₂ in Ar for 2 h (ramp rate 10 °C min⁻¹, blue).

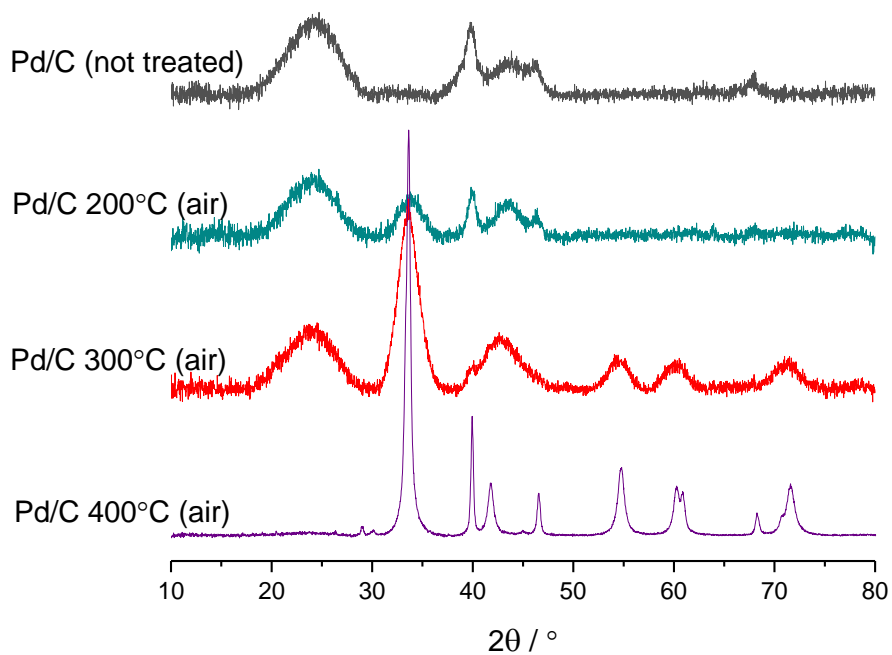


Figure 4.14: pXRD pattern of: fresh Pd/C (*i.e.* not treated, black), and Pd/C heated in air for 2 h (ramp rate 10 °C min⁻¹) at 200 °C (blue), 300 °C (red), and 400 °C (purple).

4.2.12.2. X-ray Photoelectron Spectroscopy

To analyse the Pd speciation, XPS analysis was performed. Although a mix of oxidation states were in the untreated Pd/C (37.1 % Pd^{II}, 62.9 % of Pd⁰), predominance of Pd^{II} was found on Pd/C heated in air at 300 °C (73.9 % Pd^{II}, 26.1 % of Pd⁰) whilst mostly Pd⁰ was found on Pd/C heated in H₂ at 400 °C (1.7 % Pd^{II}, 98.3 % of Pd⁰).

Interestingly, although large differences in Pd speciation were observed in this series of catalysts, each of these materials exhibits good activity for 1-phenylethanol dehydrogenation. This may be due to both oxidation states being active for this reaction and/or interconversion between Pd^{II} and Pd⁰ occurs in the reaction mixture, however, comparison of the initial rates of each reaction obtained by monitoring the gas evolution with time, show that lower initial rates (*k*) are observed for catalysts possessing higher initial percentages of Pd⁰ (Table 4.5), indicating that Pd⁰ may catalyse 1-phenylethanol dehydrogenation to a lower degree than Pd^{II}. XRD analysis is in good agreement to the XPS results (Figure 4.15), showing different distribution between metallic Pd and Pd oxide to be present on these catalysts, in analogy with the results displayed in Table 4.5.

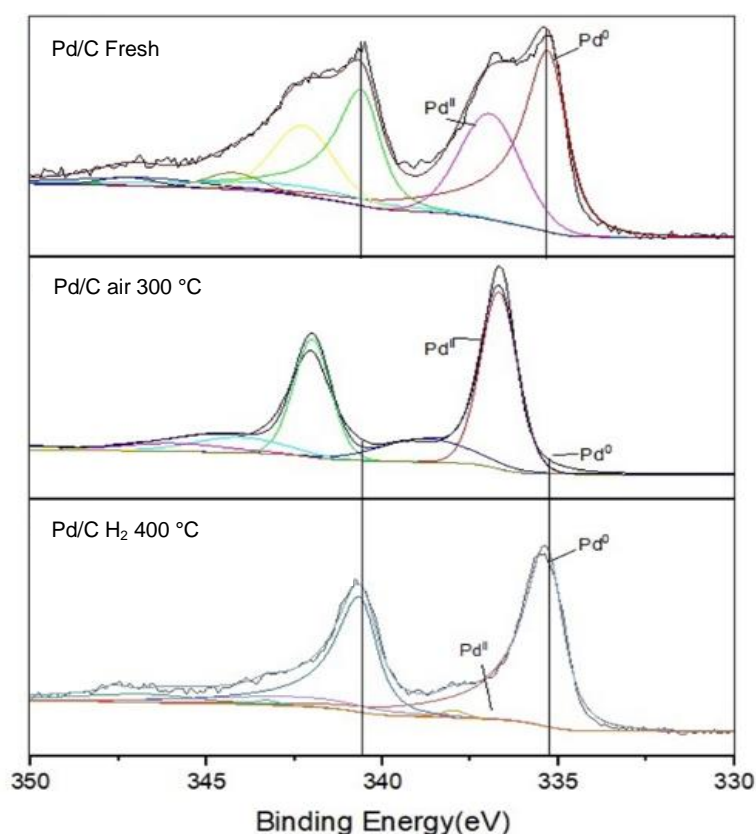


Figure 4.15: XPS analysis for: fresh Pd/C (*i.e.* not treated), Pd/C heated at 300 °C under air for 2 h (ramp rate 10 °C min⁻¹), and Pd/C heated at 400 °C in 5 % H₂ in Ar for 2 h (ramp rate 10 °C min⁻¹).

Table 4.5: Amount of Pd⁰ and initial rate for 1-phenylethanol dehydrogenation over Pd/C fresh (*i.e.* non-treated) and following different heat treatments.

Catalyst	Pd⁰ (%) ^[a]	$k \times 10^{-3} \text{ (s}^{-1}\text{)}$ ^[b]
Pd/C Fresh	62.9	1.09
Pd/C H ₂ 200 °C	78.1	0.90
Pd/C H ₂ 400 °C	98.3	0.82
Pd/C air 200 °C	49.1	1.13
Pd/C air 300 °C	26.1	1.14

[a] Relative percentage of Pd⁰ on the overall Pd, measured *via* deconvolution of XPS spectra **[b]** Initial reaction rate

4.2.12.3. Impact of structural change

In addition to oxidation state, variation in activity may also arise from several other parameters related to the support material surface, as well as variations of the Pd particle size. In fact, heat treatments have often been reported to affect the particles size distribution of the metals, due to agglomeration of the particles.⁸ Accordingly, TEM analysis was also performed on this series of heat treated catalysts.

TEM allows high-resolution images of every sample to be acquired, which can be processed with image analysis programs to measure the Pd size and distribution over the C support. As can be seen in Figure 4.16 and Figure 4.17, an increase in the Pd particles size was found for the heat treated samples. Although there is a net agglomeration of Pd in both heat-treated catalysts, the extent of agglomeration is comparable in both H₂ and air atmospheres and cannot explain the different kinetic capabilities of these samples.

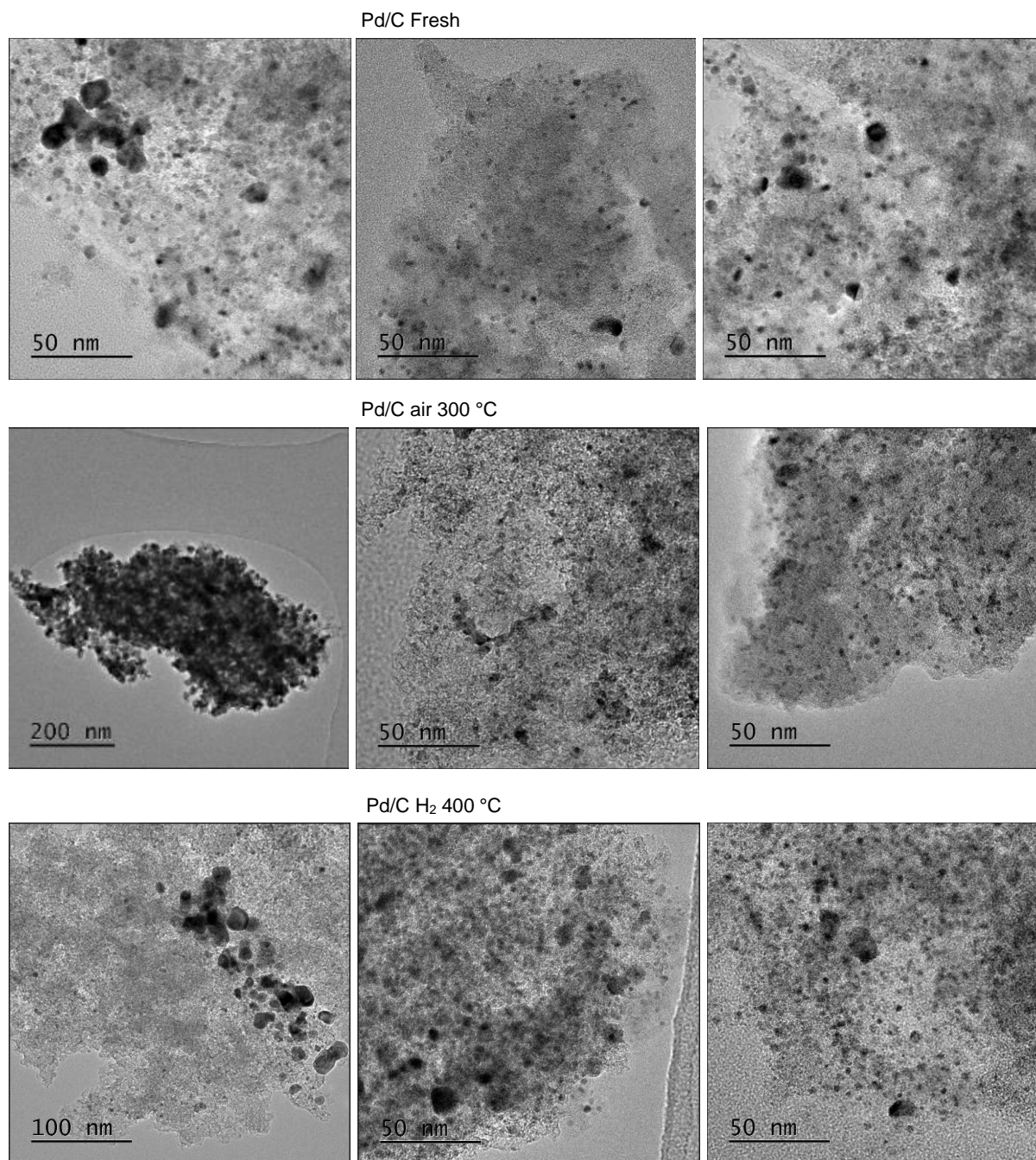


Figure 4.16: TEM images for: fresh Pd/C (*i.e.* not treated), Pd/C heated at 300 °C under air for 2 h (ramp rate 10 °C min⁻¹), and Pd/C heated at 400 °C in 5 % H₂ in Ar for 2 h (ramp rate 10 °C min⁻¹).

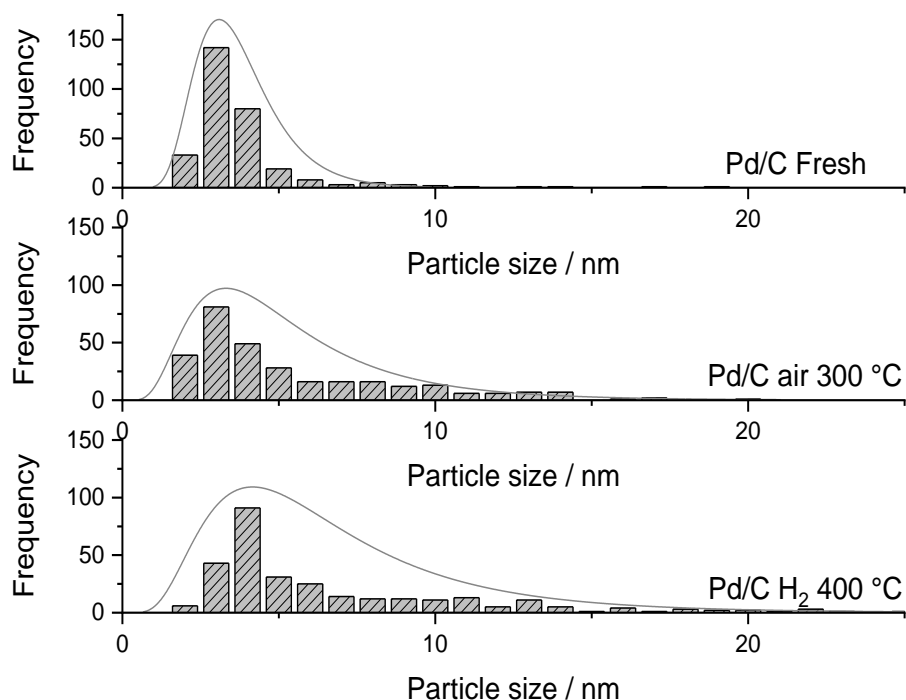


Figure 4.17: Particles size distribution for: fresh Pd/C (*i.e.* not treated), Pd/C heated at 300 °C under air for 2 h (ramp rate 10 °C min⁻¹), and Pd/C heated at 400 °C in 5 % H₂ in Ar for 2 h (ramp rate 10 °C min⁻¹),

To further investigate structural changes potentially occurring on the surface of the catalyst, porosimetry analysis was also performed. Using the BET method, surface areas of the analysed samples were obtained, as presented in Table 4.6. This data reveals that no major variation to the catalyst surface area occurs following the different heat treatments. These results, combined with the TEM analysis, suggest that the difference in activity for the different heat treatments is not due to significant physical changes in the catalyst.

Table 4.6: Specific surface area of: fresh Pd/C (*i.e.* not treated), Pd/C heated at 300 °C under air for 2 h (ramp rate 10 °C min⁻¹), Pd/C heated at 400 °C in 5 % H₂ in Ar for 2 h (ramp rate 10 °C min⁻¹)

Catalyst	Specific Surface Area (m² g⁻¹)
Pd/C Fresh	973
Pd/C air 300 °C	885
Pd/C H ₂ 400 °C	959

4.2.13. Stability of the catalyst over time

In addition to activity and selectivity, the durability of a heterogeneous catalyst plays a key role in its potential industrial applicability. In order to perform an accurate investigation of the durability of the material, and hence understand the industrial feasibility of this process, the catalytic performance of Pd/C was studied under continuous flow conditions using a Plug Flow Reactor (PFR) under otherwise analogous conditions to the batch experiments as described in Section 2.3.7. Continuous flow operation allows the productivity of a system to be increased, as well as allowing the stability of a catalyst to be identified, which plays an important role for all industrial processes and is vital to ensure the success of the catalytic reaction. A PFR offers major advantages over a batch reactor, including: i) improved process control and safety, ii) excellent mass- and heat-transfer, iii) smaller reactor volumes and iv) scalability.

In particular, a PFR results especially appropriate for the acceptorless dehydrogenation of 1-phenylethanol for two main reasons: First, the characteristics of the PFR reactor isolates the reaction from the atmosphere, where the reactant flows through the catalyst, thus avoiding the presence of undesired O₂. Secondly, the constant flow removes the H₂ produced in situ from the catalyst bed which, as described in Section 4.2.6, improves the selectivity for acetophenone. When employed in continuous mode, Pd/C displayed good activity for 1-phenylethanol dehydrogenation with acetophenone selectivity > 80 % (Figure 4.18). Although some losses in activity are observed over the first 24 h on stream, the system reaches steady state conditions, thereafter indicating the longer term durability of Pd/C for continuous operations.

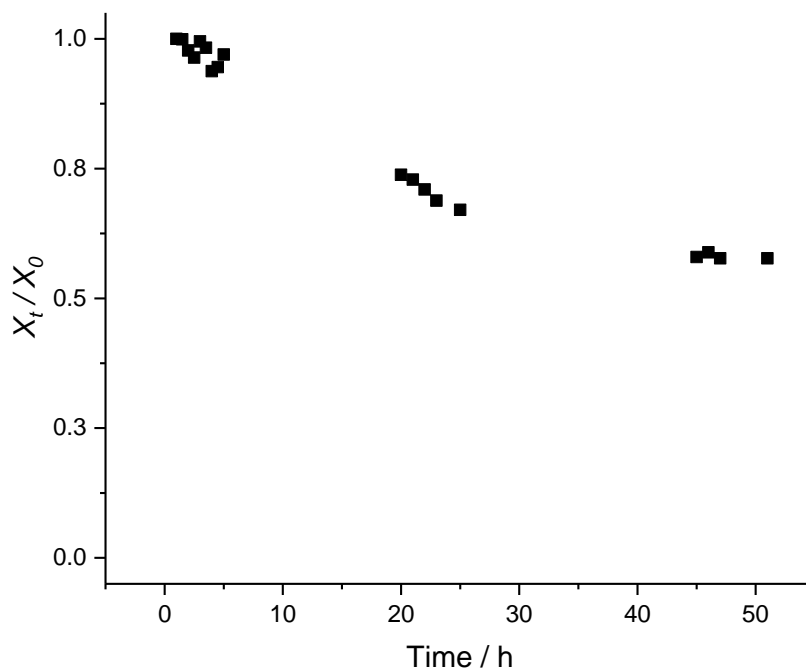


Figure 4.18: Continuous 1-phenylethanol dehydrogenation reactions in PFR. Relative performance for Pd/C-catalysed 1-phenylethanol (X_t/X_0) over time on stream. **Reaction conditions:** 0.1g Pd/C, 1-phenylethanol 0.5 M in toluene, 130 °C, 0.5 min contact time.

XPS analysis of the used sample indicates that the relative content of Pd⁰ increases from 62.9 % (fresh sample) to 88.6 % during the reaction, indicating that reduction of Pd occurs *in situ*, potentially contributing to the initial loss of activity observed over the initial stage of the reaction. However, several other phenomena such as poisoning, pore fouling and active site reorganisation, may also contribute to the initial drop of activity. In any case, these studies indicate that long term dehydrogenation is clearly feasible, even in the absence of acceptors and bases, and is accompanied by the continuous production of high purity H₂.

Notably, as shown in Table 4.7, this preliminary result presents in a maximum space-time-yield (STY) of 0.683 g_(product) mL⁻¹ h⁻¹ being achieved, which is over two orders of magnitude higher than the ones calculated for the best catalysts reported in the literature (Ag/hydrotalcite), indicating the high viability of Pd/C as a heterogeneous catalyst for alcohol dehydrogenation. Preliminary experiments on the general applicability of the system were also performed by substituting of 1-phenylethanol with a smaller, non-aromatic substrate, 2-butanol. Pd/C was also able to continuously perform 2-butanol dehydrogenation to 2-butanone in the continuous regime (Table 4.7); however, higher temperatures (200 °C) are necessary to obtain comparable levels of conversion (16 % conversion of 2-butanol). Alongside 1-

phenylethanol and the substituted benzylic alcohols, this substrate further indicates the general suitability of Pd/C-catalysed dehydrogenation in continuous operational mode.

Table 4.7: Relative performance of Pd/C and Ag/hydrotalcite.

Catalyst	Substrate	STY (g_(product) mL⁻¹ h⁻¹)^[a]
Ag/hydrotalcite ¹⁷	1-phenylethanol	2.2x10 ⁻³ [b]
Pd/C	1-phenylethanol	0.683
Pd/C	2-butanol ^[c]	0.010

[a] STYs calculated at maximum conversion as grams of reactant converted per mL (reactor volume), per h. Volume of catalyst bed used as the reactor volume. **[b]** Only the liquid volume was used as the reactor volume. **[c]** Reaction condition identical to the ones used for 1-phenylethanol, albeit at 200 °C.

4.3. Conclusions

The successful results presented in this chapter confirm that the commercially available 5 wt.% Pd/C is a suitable catalyst for the acceptorless dehydrogenation of alcohols, such as 1-phenylethanol, in inert atmosphere (N₂). The acceptorless nature of the reaction is confirmed and results in the co-production of molecular H₂, a clean energy source.

Full kinetic analysis of all the reaction products and kinetic parameters, including the gaseous product, was achieved following design of a novel batch reactor. After optimisation, accurate kinetic analyses were performed, and an activation energy of 92 kJ/mol was found, alongside a negative Hammett correlation and a Kinetic Isotope Effect > 1, indicating that the reaction possesses mechanistic similarities to beta-hydride elimination.

In addition to that, the hydrogenation capability of the Pd is also evidenced through the reversibility of the dehydrogenation and the side reactions, establishing Pd as an effective catalyst for both, dehydrogenation of alcohols and hydrogenation of carbonyl groups in presence of H₂.

Preliminary structure-activity relationships, performed with kinetics, XPS, XRD, TEM and BET, reveal that the heat treatment of the catalyst lead to differences in catalytic performance, with Pd/C calcined in air at 300 °C being the optimal catalyst for acceptorless dehydrogenation.

Finally, experiments in the continuous regime evidence the durability of the catalyst over 50 h on stream, at space-time-yields up to 0.683 g_(product) mL⁻¹ h⁻¹, over two orders of magnitude higher than the ones found in literature up to date.

These promising results set the basis to evaluate the mixture of different solid catalysts to the full system of the Guerbet reaction. In Chapter 5, attention is focused on the exploration of the next steps of the upgrading of ethanol, those being the Aldol condensation and the Meerwein–Ponndorf–Verley (MPV) reduction.

This chapter contributed to the following paper:

G. Nicolau, G. Tarantino, C. Hammond, *ChemSusChem*, 2019, **22**, 4953 – 4961

References

- ¹ R. A. Sheldon, J. K. Kochi, “Metal-Catalyzed Oxidations of Organic Compounds”, Academic Press, New York, **1981**
- ² K. Banerji, “Organic Reaction Mechanisms”, Wiley, Chichester, **2012**
- ³ D. G. Lee, U. A. Spitzer, *J. Org. Chem.*, 1970, **35**, 3589–3590
- ⁴ J. Muzart, *Chem. Rev.*, 1992, **92**, 113–140
- ⁵ S. A. Katz, H. Salem, *J. Appl. Toxicol.* 1992, **13**, 217–224
- ⁶ K. Mori, T. Hara, T. Mizugaki, K. Ebitani, K. Kaneda, *J. Am. Chem. Soc.*, 2004, **126**, 10657–10666
- ⁷ K. Yamaguchi, N. Mizuno, *Chem. Eur. J.*, 2003, **9**, 4353–4361
- ⁸ T. Mallat, A. Baiker, *Chem. Rev.*, 2004, **104**, 3037–3058.
- ⁹ S. Chakraborty, P. O. Lagaditis, M. Förster, E. A. Bielinski, N. Hazari, M. C. Holthausen, W. D. Jones, S. Schneider, *ACS Catal.*, 2014, **4**, 11, 3994–4003
- ¹⁰ R. Kawahara, K.-i. Fujita, R. Yamaguchi, *J. Am. Chem. Soc.*, 2012, **134**, 3643–3646
- ¹¹ C. Gunanathan, D. Milstein, *Science*, 2013, **341**, 249
- ¹² J. A. Turner, *Science*, 2004, **305**, 972–974
- ¹³ T. Mitsudome, Y. Mikami, K. Ebata, T. Mizugaki, K. Jitsukawa, K. Kaneda, *Chem. Commun.*, **2008**, 4804–4806
- ¹⁴ K. Shimizu, K. Sugino, K. Sawabe, A. Satsuma, *Chem. Eur. J.*, 2009, **15**, 2341–2351
- ¹⁵ W. Fang, J. Chen, Q. Zhang, W. Deng, Y. Wang, *Chem. Eur. J.*, 2011, **17**, 1247–1256
- ¹⁶ T. Mitsudome, Y. Mikami, H. Funai, T. Mizugaki, K. Jitsukawa, K. Kaneda, *Angew. Chem. Int. Ed.*, 2008, **47**, 138–141
- ¹⁷ K. Shimizu, K. Kon, K. Shimura, S. S. M. A. Hakim, *J. Catal.*, 2013, **300**, 242–250
- ¹⁸ H. Chen, S. He, M. Xu, M. Wei, D. G. Evans, X. Duan, *ACS Catal.*, 2017, **7**, 2735–2743
- ¹⁹ K. Shimizu, K. Kon, M. Seto, K. Shimura, H. Yamazaki, J. N. Kondo, *Green Chem.*, 2013, **15**, 418–424
- ²⁰ K. Kon, S. M. A. H. Siddiki, K. Shimizu, *J. Catal.*, 2013, **304**, 63–71
- ²¹ J. Yi, J. T. Miller, D. Y. Zemlyanov, R. Zhang, P. J. Dietrich, F. H. Ribeiro, S. Suslov, M. M. Abu-Omar, *Angew. Chem. Int. Ed.*, 2014, **53**, 833–836
- ²² J. H. Choi, N. Kim, Y. J. Shin, J. H. Park, J. Park, *Tetrahedron Lett.*, 2004, **45**, 4607–4610
- ²³ W. H. Kim, I. S. Park, J. Park, *Org. Lett.*, 2006, **8**, 2543–2545
- ²⁴ F. Sanchez, D. Motta, A. Roldan, C. Hammond, A. Villa, N. Dimitratos, *Top. Catal.*, 2018, **61**, 254–266
- ²⁵ S. Chakraborty, P. O. Lagaditis, M. Förster, E. A. Bielinski, N. Hazari, M. C. Holthausen, W. D. Jones, S. Schneider, *ACS Catal.*, 2014, **4**, 3994–4003
- ²⁶ M. Farrukh, M. Nielsen, *J. Chem. Kinet.*, 2018, 91–110
- ²⁷ E. Buckley, E. F. G. Herington, *Trans. Faraday Soc.*, 1965, **61**, 1618–1625
- ²⁸ H. Esaki, R. Ohtaki, T. Maegawa, Y. Monguchi, H. Sajiki, *J. Org. Chem.*, 2007, **72**, 2143–2150
- ²⁹ A. A. Tolstopyatova, P. Pi-Hsiang, A. A. Balandin, *Russ. Chem. Bull.*, 1962, **11**, 8, 1242–1249

³⁰ C. D. Johnson, C. D Johnson, "The Hammett Equation", CUP Archive, **1973**

³¹ P. Zanello, "Inorganic Electrochemistry: Theory, Practice and Application", Royal Society of Chemistry, **2007**

³² P. Atkins P, J. de Paula," Atkins' Physical Chemistry" (8th ed.). Oxford University Press, **2006**

³³ H. Knözinger, A. Schengllila, *J. Catal.*, 1970, **17**, 252-263

³⁴ B. Shi, H. A. Dabbagh, B. H. Davis, *Top. Catal.*, 2002, **18**, 259–264

³⁵ A. Abad. A. Corma. H. García. *Chem. Eur. J.*, 2008, **14**, 212–222

5. Aldol condensation & Meerwein-Ponndorf-Verley reduction

5.1. Introduction

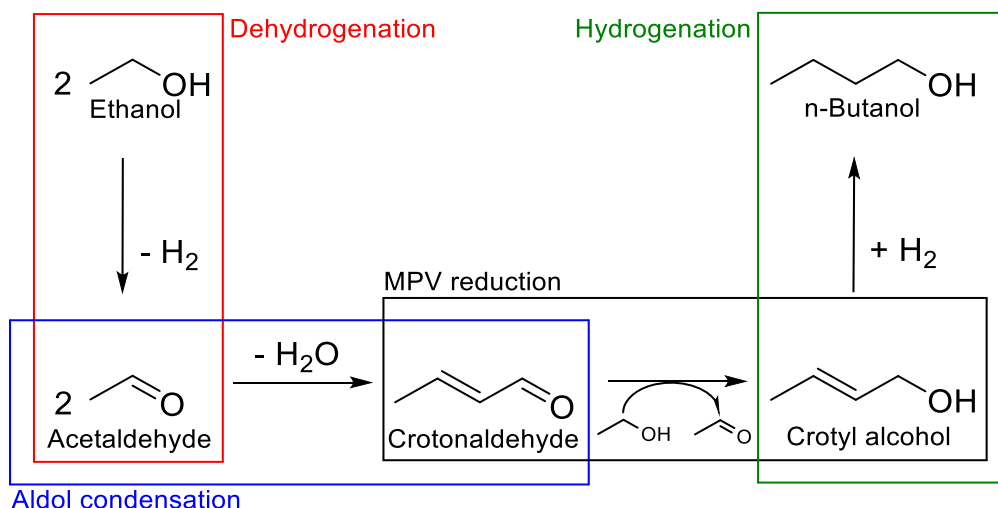
5.1.1. Next steps of the Guerbet reaction

As has been described in previous chapters, this study explores a different approach for the upgrading of ethanol. In Chapter 3, the state of the art approach for the conversion of ethanol to n-butanol through the Guerbet reaction was explored. Unfortunately, several problems were identified, including the inability of the homogeneous catalytic system to contain the “cascade of reactions”, resulting in low levels of selectivity towards the desired product. For that reason, a new strategy was adopted, separating the process into its different steps, with the aim of developing a catalytic system capable of performing all the individual steps of the Guerbet reaction at improved levels of selectivity.

In Chapter 4, the first step of the Guerbet reaction was tested and studied in depth. Known as acceptorless dehydrogenation, it is a relatively new process and few reports can be found in the open literature, making a strict and detailed analysis necessary. Commercial Pd/C 5 wt.% was found to be an excellent catalyst for that purpose. Accurate kinetic analysis for the reaction was provided and experiments to investigate the durability of the catalyst demonstrate the potential of Pd/C for continuous operations.

However, acceptorless dehydrogenation is simply the first step of the reaction network. As can be seen (Scheme 5.1), the generally accepted pathway of the Guerbet reaction shows the

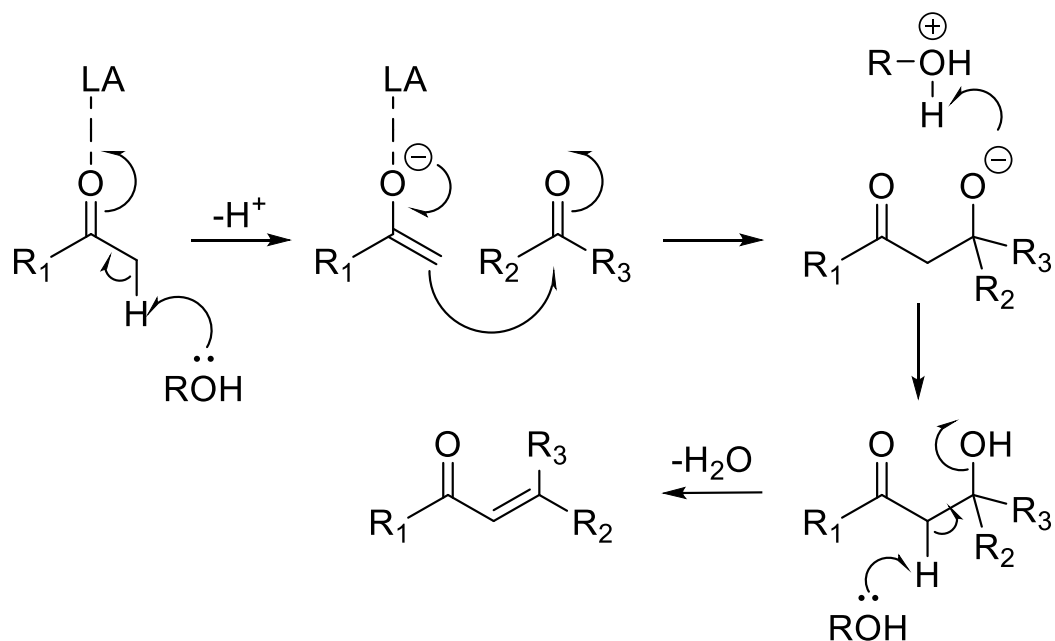
dehydrogenation of ethanol to acetaldehyde, followed by formation of crotonaldehyde, which is then reduced to crotyl alcohol and finally hydrogenated to n-butanol. Always keeping the upgrade of ethanol in mind as the main goal of this work, the Aldol condensation and the MPV reaction will be the focus of this chapter.



Scheme 5.1: General reaction scheme for the Guerbet reaction of ethanol, with its different steps.

The first of the mentioned steps is the Aldol condensation, a well known reaction that is especially important in organic synthesis as it is a favourable method of C-C bonds formation.¹² The reaction combines two carbonyl compounds to form a new β -hydroxy carbonyl compound. The products are known as aldols, from the **aldehyde** and **alcohol** components. Once formed, the aldol product releases a molecule of H_2O to form the final enal. Typically, this reaction is performed in strong basic conditions, with bases such as EtONa or NaOH being routinely employed. The use of strong bases results in several critical issues including corrosion, non-recyclability and high cost of neutralising the generated wastewater streams. In addition to these disadvantages, as has been discussed in Chapter 3, the condensation of ethanol is non-selective in basic conditions, particularly at high levels of conversion, leading to the aforementioned “cascade of reactions”.

To avoid all the problems originating from the use strong basic conditions, a different approach to catalyse the Aldol condensation with heterogeneous catalysts acting as Lewis acids. A proposed mechanism for the Aldol condensation catalysed by Lewis acids is presented in Scheme 5.2. Anion-exchange resins, metal oxides and mixed oxides, all presenting Lewis acidity, have been shown to be active materials for Aldol condensation reactions according to reports.³⁻⁷ These materials do still have some significant disadvantages, such as high sensitivity to CO_2 in air and poor stability on stream.



Scheme 5.2: General reaction scheme for the Aldol condensation reaction over Lewis acids (LA).⁸

Alternatively, Lewis acidic zeolites are a final option that have seen special attention in the recent times, and which do not present the same disadvantages of other heterogeneous catalysts, can be found with. Zeolites are inorganic silicates with three dimensional networks, and show several interesting properties including: high surface area, high and controllable adsorption capacity, high stability, active site isolation and possibility of adjusting electronic properties of active sites. Due their unique properties, zeolites have been widely applied to different processes and, in particular the Sn containing zeolite, Sn- β , has gained great attention in the recent years. Sn- β shows excellent catalytic performance for a large number of processes such as Baeyer-Villiger Oxidation (BVO),^{9,10} which converts ketones to lactones using hydrogen peroxide as green oxidant; glucose isomerisation and methyl lactate synthesis, reactions with high industrial interest;^{11,12} etherification of alcohols^{13,14} and epoxide ring opening,¹⁵ in addition to the aforementioned Aldol condensation. With its high activity and stability, Sn- β is a promising material to catalyse the Aldol condensation of acetaldehyde.

In addition, another important application of Sn- β is in the third step of the Guerbet reaction (Scheme 5.1), namely the Meerwein–Ponndorf–Verley (MPV) reduction.^{16,17} In this reaction, ketones and aldehydes are reduced to their respective alcohols in presence of a sacrificial alcohol that acts as hydrogen donor. Therefore, in the particular case of the Guerbet reaction, Sn- β could act as a catalyst for the Aldol condensation and the MPV reduction. For all this, Sn- β may be a good candidate to combine with a dehydrogenating and hydrogenating agent (Pd) to perform the upgrading of ethanol.

Hydrothermal synthesis (HDT) is typically the method employed to synthesise a fully Lewis acidic Sn- β . This method was the first employed to prepare Sn- β and involves several steps.¹⁸ Firstly the main components of the zeolite are dissolved with mineralising agents, typically inorganic anions (OH⁻ or F⁻) and a key component of the synthesis, the structure directing agent (SDA), whose role is to direct the synthesis toward a precise zeolite structure. When the gel is formed, it is then transferred into an autoclave and treated at high temperature and under autogenic pressure until the crystallisation of the zeolite is complete. After filtration and washing the crystallised zeolite with clean solvent, the powder is calcined in order to remove residues of the SDA from the inorganic porous crystalline material. The main disadvantages of this method are the necessary use of toxic species such as HF and the long synthesis times required, varying from 2 to 60 days depending on the Sn loading.¹⁹

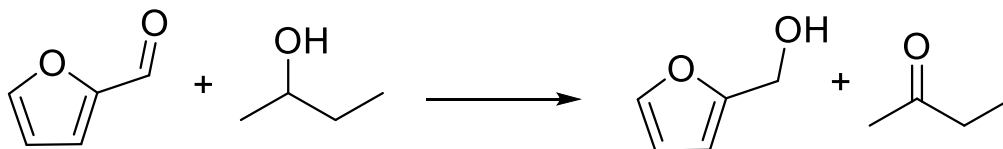
An alternative approach to synthesise Sn- β involves the use of post-synthetic methods, which start from readily made aluminosilicate zeolite of the desired structure. Here, the aluminium is extracted, typically by acid treatment, and Sn is successively inserted into the vacant framework sites. In this regard, an efficient and rapid method to prepare Sn- β is the Solid State Incorporation method (SSI).²⁰ In this preparation, a suitable Sn precursor is mechanically mixed with the dealuminated zeolite in order to form a homogeneous solid-solid precursor of Sn- β . After the solid-solid mixture is prepared, the catalyst undergoes a heat treatment to obtain the final Sn- β . These two described methodologies (HDT and SSI) have also been successfully used to incorporate several metals with Lewis acid properties other than Sn, such as Hf and Zr,^{21,22} resulting in new β zeolites as interesting candidates to perform the upgrading of ethanol.

5.1.2. Model reactions

The focus of this chapter is to explore the catalytic properties of different β zeolites containing Sn, Hf and Zr and for the Aldol condensation and MPV reduction reactions, comparing their activity and stability in order to find the most appropriated material to be used in the upgrade of ethanol. Analogously to the procedure presented in Chapter 4, the next steps of the Guerbet reaction (Aldol condensation and MPV transfer hydrogenation) were tested through model reactions in order to simplify the methodology and analytics.

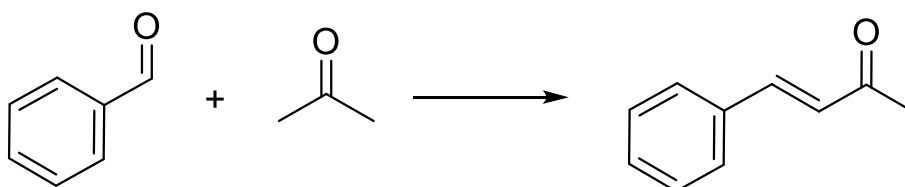
Analogously to the methodology presented in Chapter 4, bigger molecules were chosen to avoid the problems related with the use of acetaldehyde (hard to handle and to quantify due to low boiling point and high reactivity). The MPV reduction of furfural to furfuryl alcohol

(Scheme 5.3) and the Aldol condensation of benzaldehyde with acetone (Scheme 5.4) were chosen for this purpose. Reports of Sn- β being a successful catalyst for these two reactions can be found in literature.^{18,23}



Scheme 5.3: General reaction scheme for MPV reduction of furfural to furfuryl alcohol with 2-butanol.

The transfer hydrogenation of furfural is an interesting process by its own right, as furfural is one of the most common chemicals derived from biomass, with a production of more than 200 kt per annum.²⁴ The hydrogenation of furfural to furfuryl alcohol is a typical industrial process, since furfuryl alcohol is used for the production of resins, as high-quality cores and moulds for metal casting in the foundry industry; as a reactive solvent for phenolic resins in the refractory industry; as a viscosity reducer for epoxy resins, in the manufacture of polyurethane foams and polyesters; and as a chemical building block for the synthesis of tetrahydrofurfuryl alcohol, pharmaceuticals such as antiulcer ranitidine, and in the manufacture of fragrances.^{25,26} Moreover, it also represents a useful example of an intermolecular hydride transfer hydrogenation.

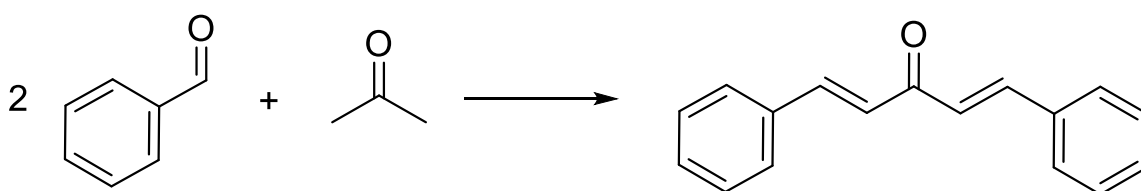


Scheme 5.4: General reaction scheme for Aldol condensation of benzaldehyde with acetone to form benzalacetone.

A different case was chosen as the Aldol condensation model reaction. Even if benzaldehyde is one of the most useful chemicals from the aromatic aldehyde family, which can be obtained from oxidation of toluene,²⁶ the Aldol condensation with acetone by itself does not have the same industrial relevance as the transfer hydrogenation of furfural. However, this particular reaction is adequate for the purposes of this study.

As has been described in Chapter 1 and Chapter 3, one of the main challenges for the upgrade of ethanol is to control the called “cascade of reactions”, where the over condensation leads

to longer chain products. In fact, as demonstrated in Chapter 3 the cascade for the reaction of ethanol occurs when using bases such as EtONa. Similarly, the over condensation of benzaldehyde to dibenzylideneacetone (Scheme 5.5) is a known reaction in basic conditions^{27,28} and has also been reported over heterogeneous catalysts.²⁹ However, the potential shape selectivity presented by Sn- β and other zeolites may prevent the over condensation to large products, preventing in this way the “cascade of reactions”.^{30,31} As such, this model reaction is useful from both a purely kinetic aspect, and also a selectivity aspect.



Scheme 5.5: General reaction scheme for Aldol condensation of benzaldehyde with acetone to form benzalacetone with subsequent condensation to dibenzylideneacetone.

5.2. Results and Discussion

5.2.1. Meerwein–Ponndorf–Verley reduction

As discussed in Section 5.1, Sn- β and the analogous Hf and Zr containing β zeolites were chosen as possible candidates to perform the MPV reaction of furfural with 2-butanol. To avoid excessive synthesis times (7 days) and to enable a strict comparison to be made between preparation methods, zeolites containing only 1 wt.% metal were targeted. In particular, Sn- β , Hf- β and Zr- β prepared by HDT method were selected as potential suitable catalysts for both model reactions.

5.2.1.1 Characterisation of hydrothermal β zeolites

Initially, characterisation of the synthesised catalysts was performed, in order to verify the successful synthesis of each material. Diffraction (XRD) analyses of fresh materials were performed to confirm that β crystalline zeolite structure was achieved for each material following HDT synthesis. As can be seen in Figure 5.1, all the materials prepared possess the characteristic pattern of β zeolite, without presenting any peaks corresponding to the pure

oxide species (also analysed by XRD), indicating the correct formation of the desired crystalline structures. In the same way, porosimetry analysis shown in Table 5.1 presents specific surface areas (between 391 to 433 m² g⁻¹) for the zeolites synthesised by HDT method. Loadings of 1 wt.% of each metal were also checked by Inductively Coupled Plasma Atomic Emission Spectroscopy (ICP-AES). The values presented are in agreement with levels found in literature.³² In this way, the correct structure and loading of the β zeolites were confirmed prior the testing for MPV reduction of furfural and Aldol condensation of benzaldehyde with acetone.

Table 5.1: Porosimetry data for Sn- β , Hf- β and Zr- β (HDT).

<u>Catalyst</u>	<u>Specific surface area</u> (m² g⁻¹) [a]	<u>Micropore volume</u> (cm³ g⁻¹) [a]	<u>Metal loading</u> (wt.%) [b]
H- β	498	0.23	N/A
Sn- β	391	0.19	1.0
Hf- β	433	0.22	1.1
Zr- β	404	0.19	1.1

[a] Specific surface areas were obtained by using BET equation and micropore volumes were obtained from t-plot method. **[b]** Metal loadings were obtained by ICP-AES analysis.

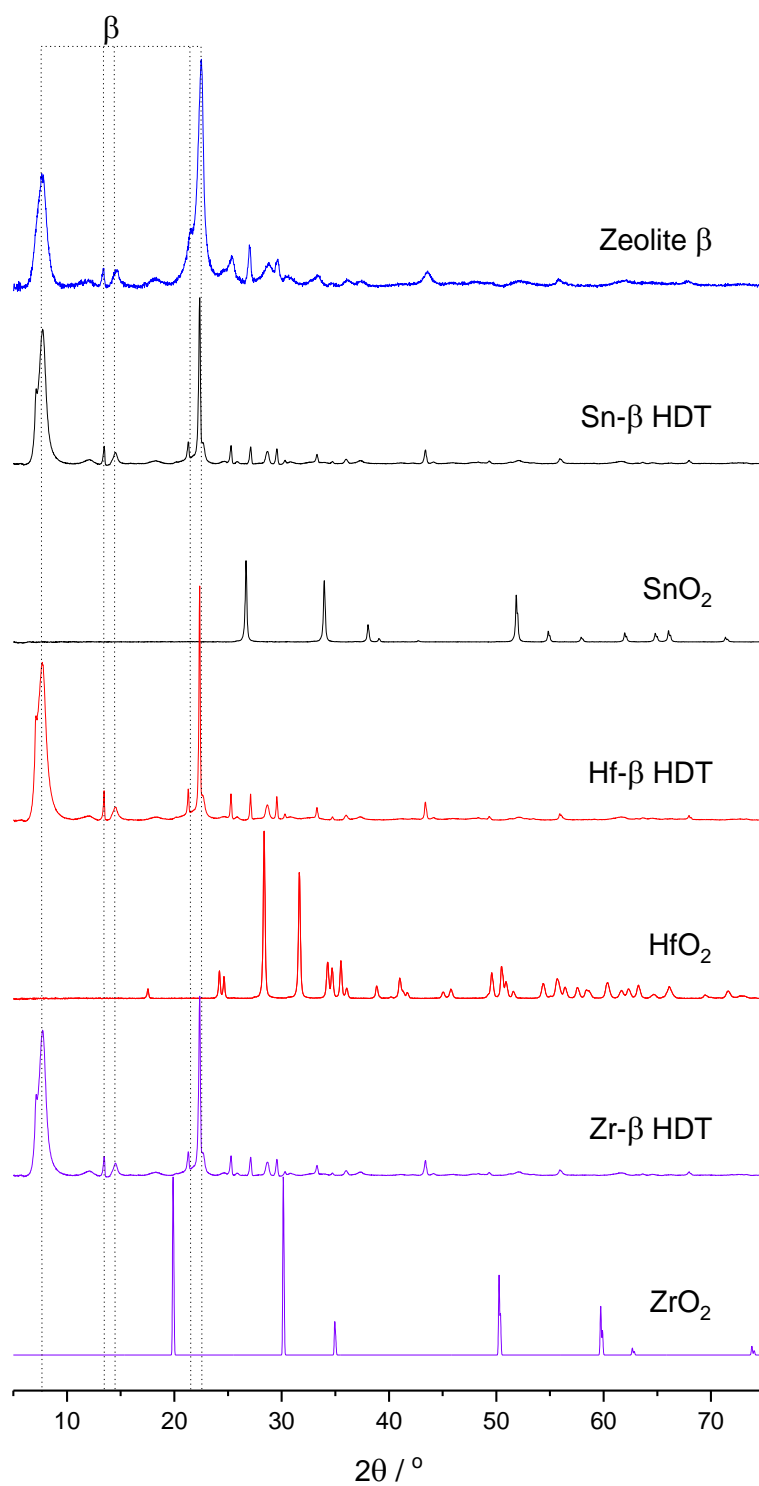


Figure 5.1: pXRD pattern of different β zeolites, prepared by HDT method compared to each respective oxide (SnO₂, HfO₂ and ZrO₂) pattern.

5.2.1.2. Catalytic activity

In order to find an appropriate catalyst for the desired Guerbet reaction (Scheme 5.1), the selected Lewis acidic β zeolites described in the previous section were tested for the Meerwein–Ponndorf–Verley (MPV) reduction of furfural with 2-butanol as solvent and hydrogen donor as described in Section 2.3.9.

The comparison of the activity of the different metal containing β zeolites prepared by HDT method is presented in Figure 5.2; Sn- β , Hf- β and Zr- β 1 wt.% HDT were tested for the MPV reaction of furfural, using a Plug Flow Reactor (PFR) at 100 °C. All the tested zeolites are active at 100 °C without further optimisation of conditions required. Zr- β shows poor activity for MPV reduction of furfural, presenting a maximum conversion of 21 % at short reaction time but losing activity after 20 h on stream. On the other hand, Sn- β and Hf- β exhibit higher levels of conversion of furfural. Both zeolites present similar initial activity, with 35 and 37 % of conversion respectively. Sn- β loses activity, with conversion decreasing to 24 % after 72 h on stream. However, Hf- β seems to gain activity over the reaction period, with an increase to a maximum conversion of 52 % after 80 h on stream.

To give further understanding, the initial activities of the selected catalysts are presented in Table 5.2 in terms of their initial turnover frequency (TOF_0 , mol furfural converted per mol of metal per h). The values obtained (between 1 to 8.2) are in the same order of magnitude than studies found in literature for this reaction.^{20,33} Accordingly, Hf- β is the most active of the three selected catalysts even without accounting for its increasing activity with time on stream.

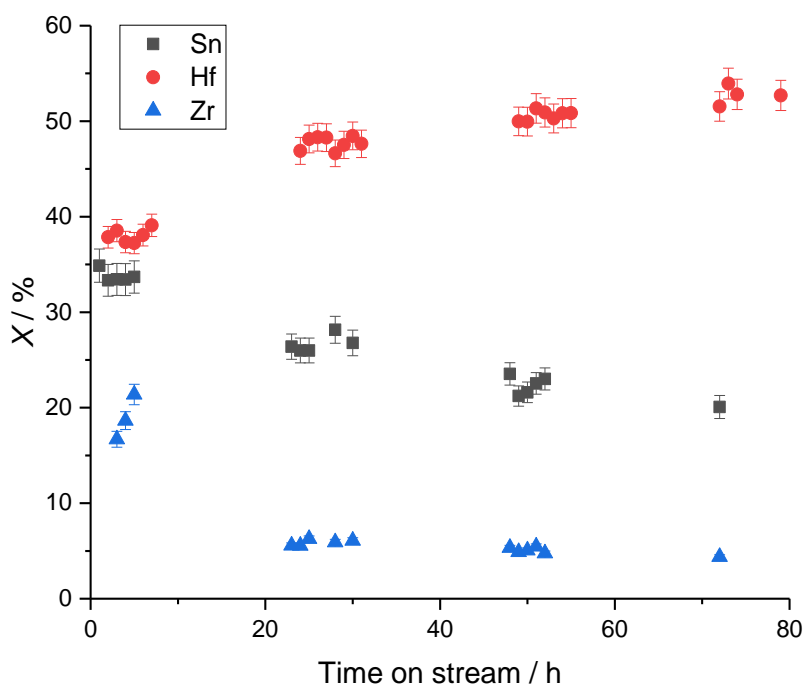


Figure 5.2: Conversion of furfural (X) over different metal (Sn, black squares; Hf, red circles; Zr, blue triangles) containing β zeolite 1 wt.% prepared by HDT method over time on stream. **Reaction conditions:** PFR, 100 °C, solution of furfural 0.1 M in 2-butanol, 10 bar.

Table 5.2: Initial turn over frequency for MPV reaction of furfural over β zeolites.

Catalyst	Sn- β	Hf- β	Zr- β
TOF ₀ ^[a]	6.9	8.2	1.0

[a] mols furfural reacted x mols metal⁻¹ x h⁻¹. **Reaction conditions:** PFR, 100 °C, solution of furfural 0.1 M in 2-butanol, 10 bar, 1h.

Although catalytic evolution with time is a very immediate way to determine stability, time is not always the best parameter against which the stability of a catalyst can be compared. More indicative is the number of substrate turnovers (ρ), which is the number of the catalytic cycles that the catalyst can perform without losing a certain extent of its initial activity.³⁴ For a better comparison of the stability of the presented catalysts, the relative performance (X/X_0 , chosen as a way to normalise the different levels of conversion presented for the different catalysts) of each of these β zeolites is compared at the same number of substrate turnover rather than time on stream (Figure 5.3).

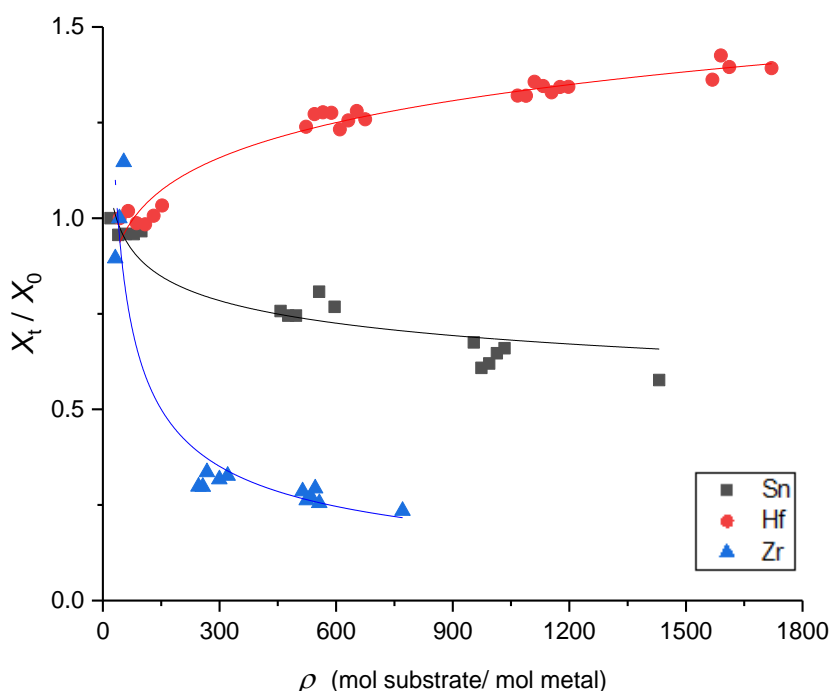


Figure 5.3: Relative catalytic activity (X_t/X_0) of Sn, Hf and Zr- β zeolites 1 wt.% over reactor turnover (ρ). **Reaction conditions:** PFR, 100 °C, solution of furfural 0.1 M in 2-butanol, 10 bar.

Figure 5.3 clearly shows the differences in stability of the used catalysts. Where Sn- β loses around 40 % of its initial activity over the reaction period, and Zr- β loses close to 80 %; on the contrary, the performance of Hf- β increases by approximately 40 %. Thus, it is concluded that Hf- β is the most stable of the tested catalysts.

For a better evaluation of the deactivation of the catalysts, a linearisation of the conversion versus time on stream plot (Figure 5.4) was made by applying the Levenspiel deactivation rate equation (Equation 5.1). In this case, the slope of the best fitting line provides a numerical value of a deactivation constant (k_d). The evaluation of k_d allow a more precise numerical comparison of the deactivation extent observed for different systems. Higher values of k_d correspond to higher deactivation rates.

$$\ln \left(\ln \left(\frac{[Fur]_0}{[Fur]_t} \right) \right) = \ln(k\tau) - k_d t \quad [Equation 5.1]$$

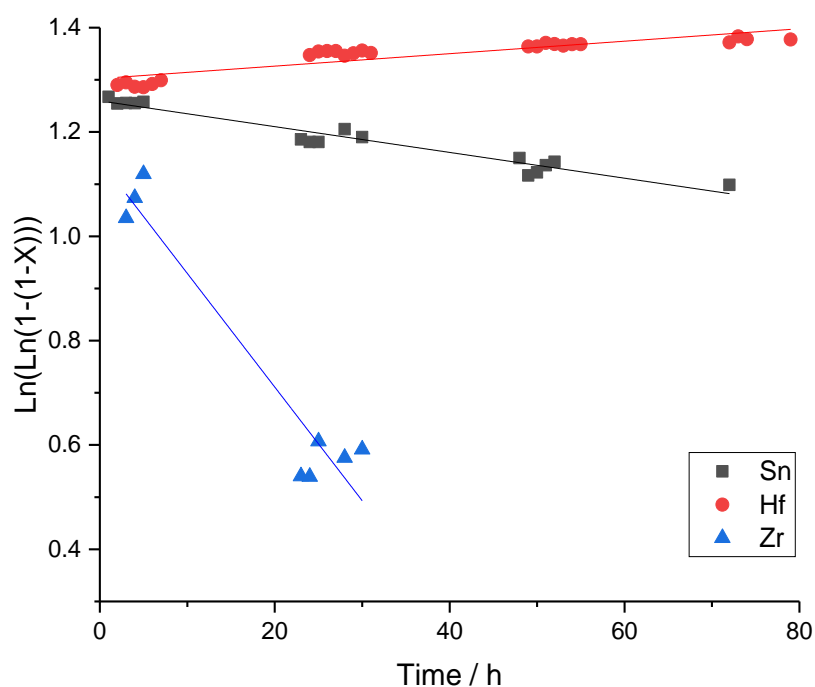


Figure 5.4: Levenspiel linearisation of conversion of furfural (X) over different metal (Sn, black squares; Hf, red circles; Zr, blue triangles) containing β zeolite 1 wt.% prepared by HDT method over time on stream. **Reaction conditions:** PFR, 100 °C, solution of furfural 0.1 M in 2-butanol, 10 bar.

Table 5.3: Initial turn over frequency for MPV reaction of furfural over β zeolites.

Catalyst	Sn-β	Hf-β	Zr-β
k_d (h^{-1}) [a]	0.002	-0.001	0.022

[a] Deactivation constant (k_d) Levenspiel linearisation slope, h^{-1} . **Reaction conditions:** PFR, 100 °C, solution of furfural 0.1 M in 2-butanol, 10 bar.

Based on the values of k_d , it can be seen that the deactivation of Zr- β is an order of magnitude higher than the other two catalysts. In light of this, Zr- β was then discarded due to its poor activity and stability.

In addition to the activity and stability, to satisfactorily perform the Guerbet reaction of ethanol to n-butanol it is necessary to find the most selective catalyst possible. It is imperative to remember that the Guerbet reaction is an extremely complicated system, with multitude of possible side reactions. Results obtained using Hf- β and Sn- β are compared by plotting the selectivity for furfuryl alcohol over conversion of furfural (Figure 5.5).

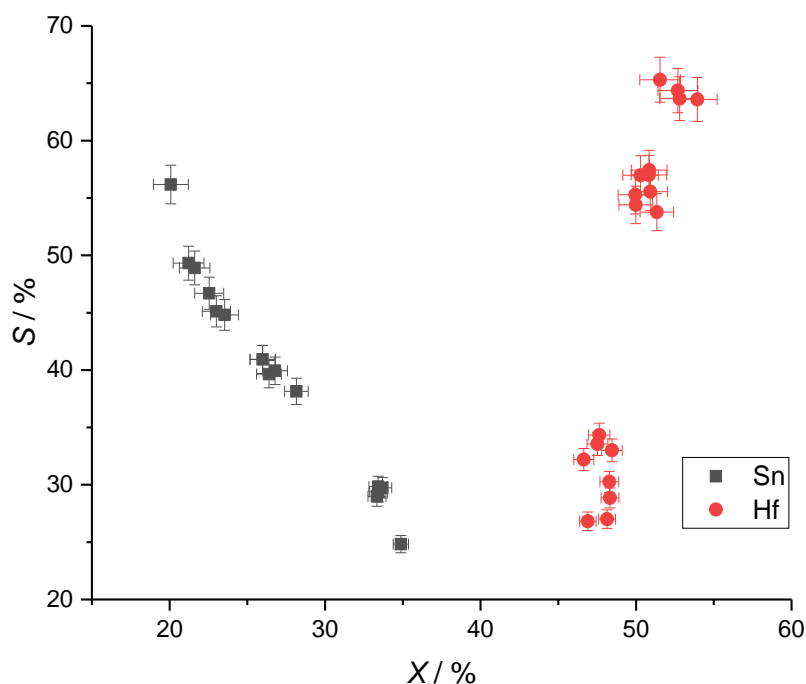
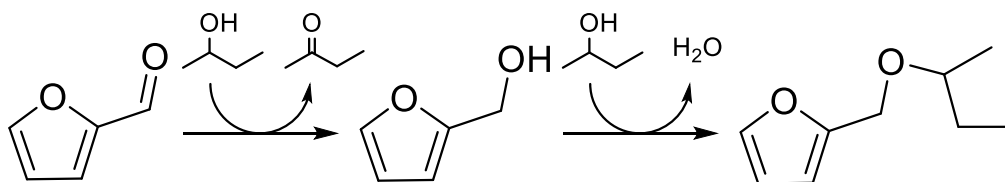


Figure 5.5: Selectivity for furfuryl alcohol (S) over conversion of furfural (X) using Sn- β (black squares) and Hf- β (red circles) prepared by HDT method. **Reaction conditions:** PFR, 100 °C, solution of furfural 0.1 M in 2-butanol, 10 bar.

As can be seen above, the two zeolites offer opposite trends. Sn- β shows deactivation over time and lower levels of furfural conversion. This effect is inversely proportional to selectivity for furfuryl alcohol *i.e.* as the catalyst deactivates, its conversion decreases and hence, selectivity increases. The appreciated change of selectivity with Sn- β corresponds to a consecutive etherification of furfuryl alcohol with 2-butanol to form 2-(butoxymethyl)furan, which can be detected by GC-FID, with the release of water (Scheme 5.6). Contrarily, Hf- β shows both an increase of activity and selectivity with time on stream. Reports of the consecutive etherification of furfuryl alcohol over Sn- β can be found in literature.^{18,27} At short reaction times, the furfuryl alcohol reacts with additional solvent molecules to produce the ether. Overall, both catalysts gain selectivity for furfuryl alcohol with time on stream, thus indicating that the catalysts simply lose the ability to mediate the second step of the reaction at a faster rate than they lose their ability to catalyse the initial MPV transfer hydrogenation reaction.



Scheme 5.6: General reaction scheme for MPV reduction of furfural to furfuryl alcohol with 2-butanol and etherification to 2-(butoxymethyl)furan.

With all the presented data it is concluded that Hf- β is the most active, selective and stable catalyst for the MPV reduction of furfural from the studied materials.

5.2.1.3. Characterisation of post synthetical β zeolites

The zeolites tested up to this point were obtained by the HDT synthesis method. However, as has been described in Section 5.1, such zeolites can be synthesised by post-synthetic methods such as SSI. As such, after discarding Zr- β for its poor performance, Sn- β and Hf- β zeolites 1 wt.% were prepared by SSI.

Before testing these new catalysts, it was necessary to confirm the correct structure of the desired zeolite. pXRD patterns of the β zeolites synthesised by SSI are presented in Figure 5.6, showing that the acid treatment applied to remove the Al from the zeolite framework does not change the crystalline structure (deAl- β); furthermore, only the signature peaks of β zeolite can be observed and none of the corresponding oxide peaks can be seen in the finished catalysts. Subsequently, porosimetry analysis on zeolites prepared by SSI was also performed; the data obtained is presented along with values for HDT synthesis for comparison (Table 5.4).

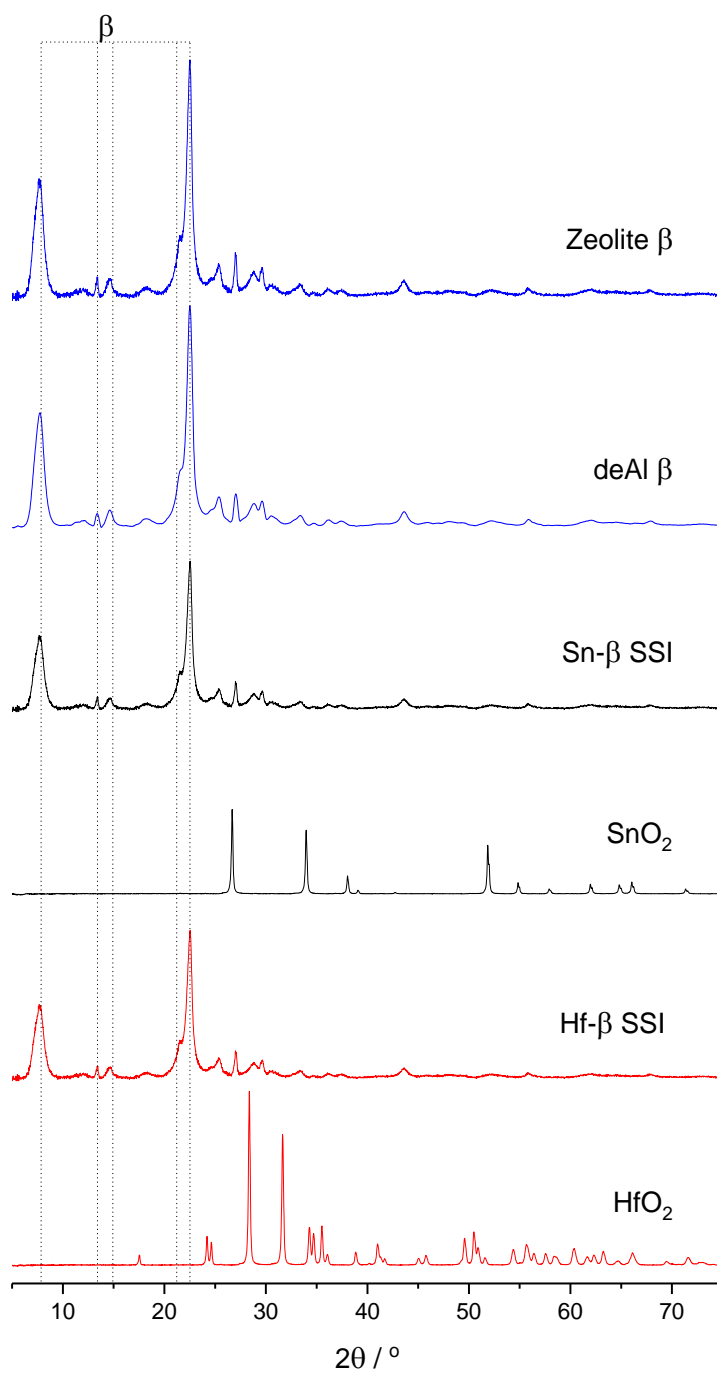


Figure 5.6: pXRD pattern of Sn- β and Hf- β prepared by SSI method compared to each respective oxide (SnO₂ and HfO₂) pattern.

Table 5.4: Porosimetry data for Sn- β and Hf- β prepared by SSI and HDT.

Catalyst	Specific surface area (m² g⁻¹) [a]	Micropore volume (cm³ g⁻¹) [a]	Metal loading (wt.%) [b]
Sn- β SSI	581	0.25	1.1
Sn- β HDT	391	0.19	1.0
Hf- β SSI	560	0.22	1.0
Hf- β HDT	433	0.22	1.1

[a] Specific surface areas were obtained by using BET equation and micropore volumes were obtained from t-plot method. **[b]** Metal loadings were obtained by ICP-AES analysis.

As can be seen, the zeolites prepared by SSI and HDT methods possess the same structure. However, materials show differences in specific surface area and micropore volume. Finally, the experimental metal loadings obtained were again checked to be 1 wt.% by the ICP-AES technique.

5.2.1.4. SSI versus HDT

In previous sections of this chapter, Sn- β , Hf- β and Zr- β prepared by the HDT method have been characterised and tested for the MPV reduction of furfural. Once Zr- β was discarded for its poor performance, Sn- β and Hf- β synthesised by SSI method have also been prepared and characterised. At this point the two sets of catalytic materials prepared by the two different synthetic methods were compared performing again the MPV reaction, as described in Section 2.3.9, starting with Sn- β (Figure 5.7). As shown below, Sn catalyst prepared by SSI presents higher catalytic activity at short reaction times, reaching a maximum conversion of furfural of 46 %. In the previous section, Table 5.4 evidenced how the two samples possess different levels of specific surface area, with Sn- β SSI showing close to 30 % higher surface area and bigger micropore volume. This higher surface area agrees with the greater activity exhibited by Sn- β SSI at low reaction times. Notwithstanding, after just 7 h of reaction, both zeolites display similar activity with more than 30 % conversion of furfural. Furthermore, both materials present deactivation during the reaction, although they are active for more than 70 h on stream, confirming long term reduction of furfural is feasible with catalysts prepared by these two different methods.

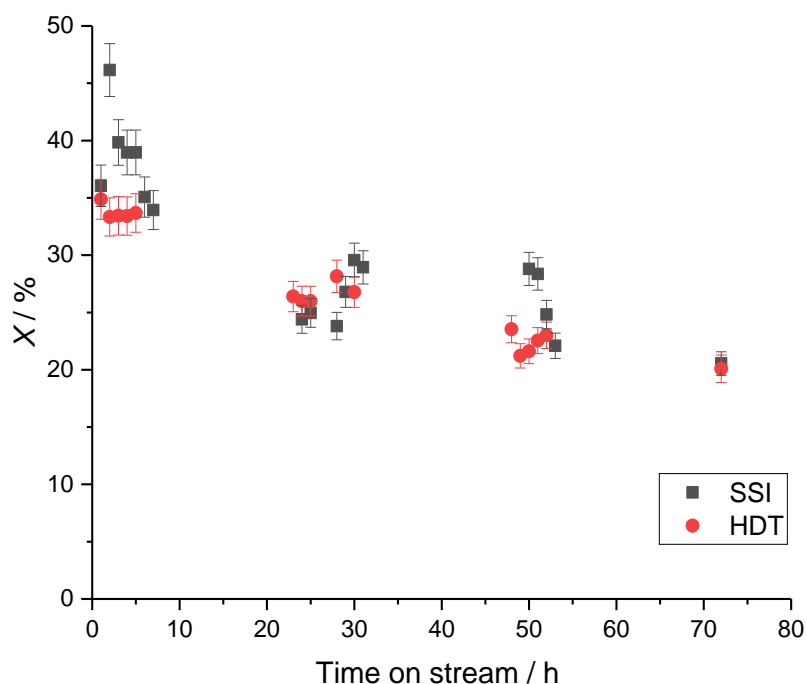


Figure 5.7: Conversion of furfural (X) over Sn- β zeolite 1 wt.% prepared by SSI (black squares) method and HDT (red circles) method over time on stream. **Reaction conditions:** PFR, 100 °C, solution of furfural 0.1 M in 2-butanol, 10 bar.

As has been described in Section 5.2.1.2, the tested β zeolites can also perform the etherification of furfuryl alcohol (Scheme 5.6) and gain selectivity for furfuryl alcohol with time on stream. The evaluation of selectivity for furfuryl alcohol manifests that this effect results more evident with Sn- β HDT, with higher selectivity than Sn- β SSI at all *iso*-conversion levels (Figure 5.8). Additionally, direct comparison of selectivity obtained at short and extended reaction periods, shown in Table 5.5, further highlights this effect. The Sn- β HDT catalyst reaches more than 50 % of selectivity for furfuryl alcohol after 72 h at these conditions; in contrast, Sn- β SSI is far less selective, reaching only 10.2 % of selectivity after the same time on stream. It is necessary to continue emphasising the need to find a catalyst as selective as possible to avoid the multiple side pathways presented for the Guerbet reaction; the difference in selectivity obtained with both materials points to Sn- β HDT as a more appropriate catalyst for the conversion of ethanol to butanol.

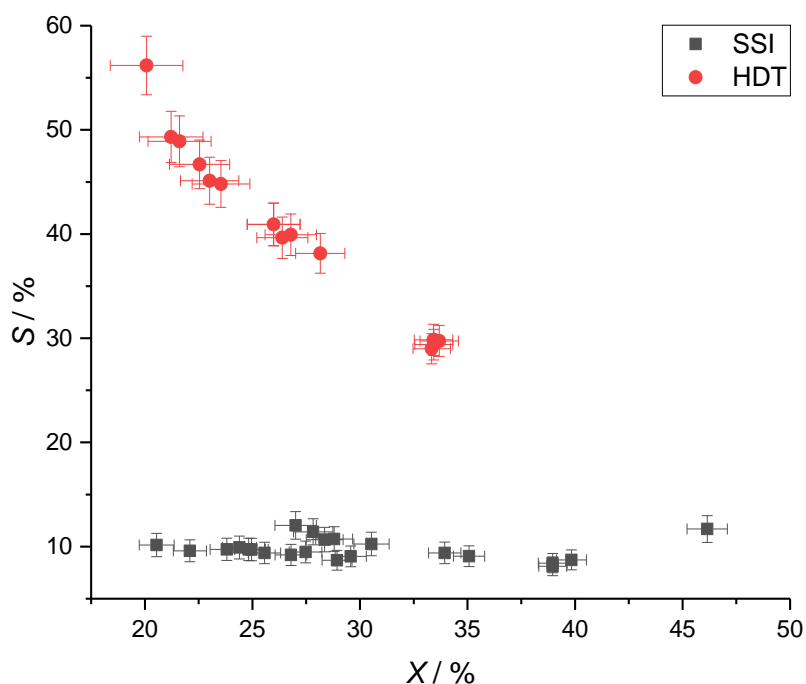


Figure 5.8: Selectivity for furfuryl alcohol (S) over conversion of furfural (X) using Sn- β (black squares) and Hf- β (Red circles) prepared by HDT method. **Reaction conditions:** PFR, 100 °C, solution of furfural 0.1 M in 2-butanol, 10 bar.

Table 5.5: Selectivity for furfuryl alcohol of Sn- β catalysts prepared by SSI and HDT methods at comparable conversion of furfural^[a]

<u>Time</u> h	<u>Method</u>	<u>X (%)</u> ^[b]	<u>S (%)</u> ^[c]
7	SSI	33.9	9.4
5	HDT	33.7	29.7
72	SSI	20.5	10.2
72	HDT	20.1	56.2

[a] Reaction conditions: PFR, 100 °C, solution of furfural 0.1 M in 2-butanol, 10 bar. **[b]** Conversion of furfural. **[c]** Selectivity for furfuryl alcohol.

Following the same line of investigation, Hf- β 1 wt.% catalysts prepared by SSI and HDT methods were also tested for the MPV reduction of furfural at the same reaction conditions

than previous experiments of this section (100 °C, solution of furfural 0.1 M in 2-butanol, 10 bar)

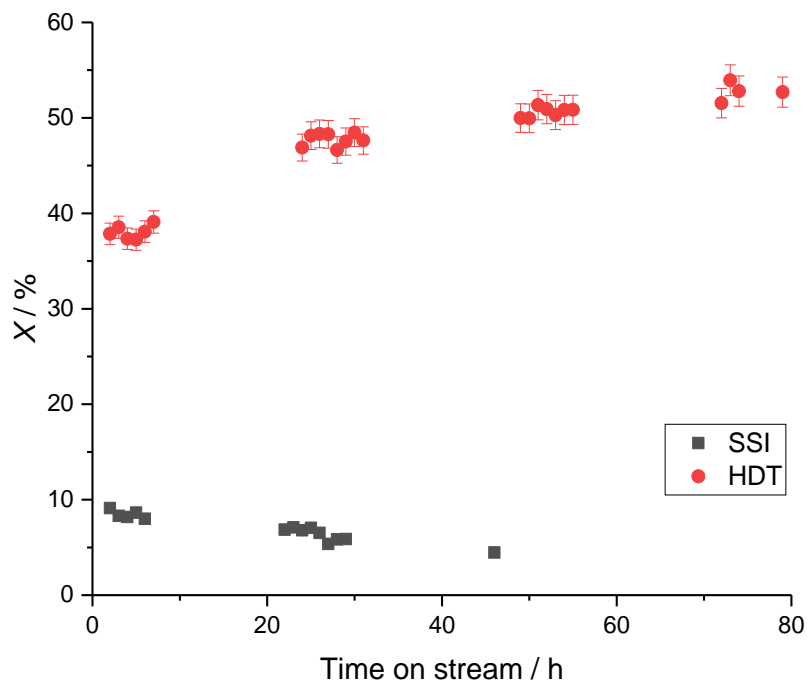


Figure 5.9: Conversion of furfural (X) over Hf- β zeolite 1 wt.% prepared by SSI (black squares) method and HDT (red circles) method over time on stream. **Reaction conditions:** PFR, 100 °C, solution of furfural 0.1 M in 2-butanol, 10 bar.

As can be seen in Figure 5.9, again the catalysts prepared by different methods present dissimilar activity. Unlike the case of Sn- β zeolites, which convert furfural in similar rate but show great differences in selectivity, Hf- β HDT shows close to four times more activity compared with its SSI analogue, with a conversion of furfural of 52 %. In addition, by plotting the selectivity to furfuryl alcohol against conversion for the two Hf- β catalyst (Figure 5.10), it is clear that difference in the selectivity of both catalysts can be appreciated: Hf- β HDT not only shows higher conversion, but also reaches a selectivity of 65 % towards furfuryl alcohol compared with the maximum of 29 % reached for Hf- β SSI.

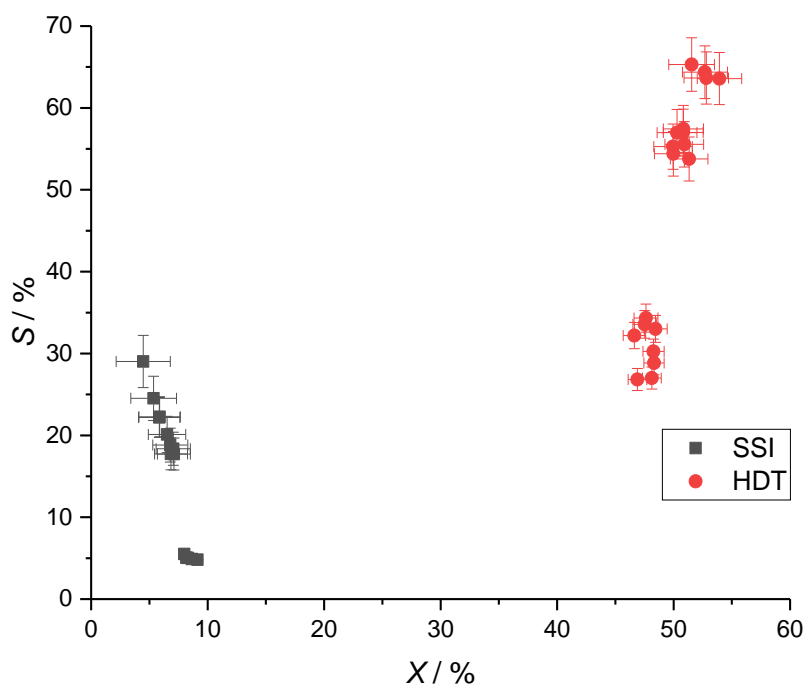


Figure 5.10: Selectivity for furfuryl alcohol (S) over conversion of furfural (X) using Sn- β (black squares) and Hf- β (Red circles) prepared by HDT method. **Reaction conditions:** PFR, 100 °C, solution of furfural 0.1 M in 2-butanol, 10 bar.

The differences in trends observed for the performance for the two β zeolites can be due to several factors, such as a poor degree of incorporation of Hf into the zeolite framework during the SSI synthesis. To confirm this hypothesis, further and deeper characterisation needs to be done in order to identify the active sites and its environment; however, the full characterisation and optimisation of the individual methods and materials is out of the scope of this study, which is to identify a catalyst that may be suitable for the upgrading of ethanol to n-butanol.

After testing the Sn and Hf separately, the two sets of data are compared to choose the best candidate to combine with a dehydrogenating agent to perform the Guerbet reaction; with this aim, the initial activities of the selected catalysts are presented by their initial turnover frequency (TOF_0 mols of furfural converted per mols of metal per time at initial activity) in Figure 5.11.

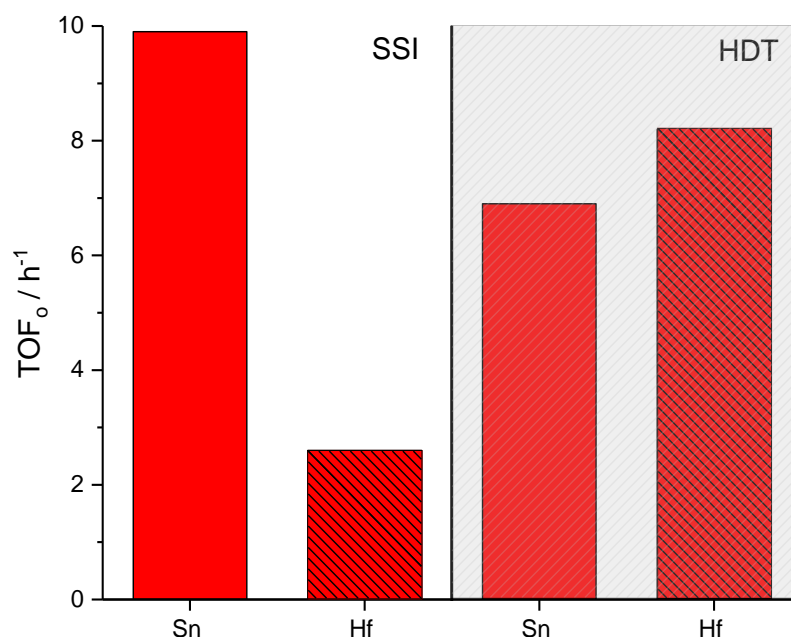


Figure 5.11: Initial TOF of Sn-β and Hf-β zeolites 1 wt.% prepared by SSI (clear) method and HDT (grey) method. **Reaction conditions:** PFR, 100 °C, solution of furfural 0.1 M in 2-butanol, 10 bar, 2 h on stream.

Sn-β prepared by the SSI method shows the highest levels of initial activity for the selected catalysts when considering TOF₀, though zeolites prepared by HDT method perform in a similar way; Hf-β SSI is the least active catalyst. To perform the upgrade of ethanol at industrial level it is necessary to identify a catalyst that is active and also selective and stable during the process, and the deactivation of these catalysts has already been presented.

A better evaluation of the deactivation of the catalysts can be achieved by linearisation of the conversion vs. time on stream curve, by applying the Levenspiel deactivation rate equation to obtain a deactivation rate, k_d (Figure 5.12). This plot allows to obtain a more accurate comparison for the stability of the different catalysts and highlights again the trend of Hf-β HDT, which improves its performance with time, translated in a negative value for k_d .

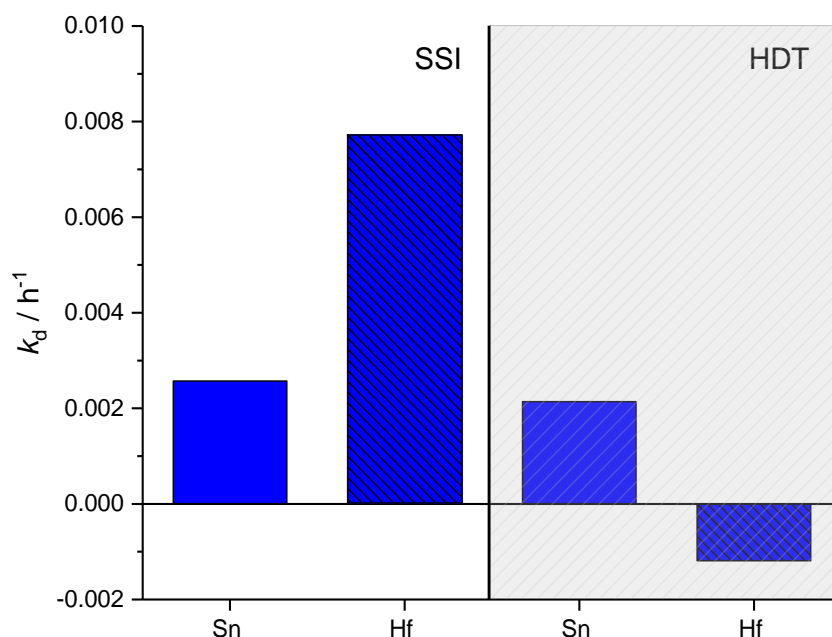


Figure 5.12: Deactivation constant (k_d) of Sn- β and Hf- β zeolites 1 wt.% prepared by SSI (clear) method and HDT (grey) method. **Reaction conditions:** PFR, 100 °C, solution of furfural 0.1 M in 2-butanol, 10 bar, 80 h on stream.

From all the presented data, it can be concluded the catalysts prepared by HDT method show an overall better performance that for the MPV reduction of furfural with 2-butanol. These results are in line with the work published for Hammond *et al.*³² where Sn- β prepared by HDT method is a more active and stable catalyst for glucose isomerisation. Here, the greater performance is attributed to differences in the active sites of Sn- β according to the different preparative methods used, and these differences may also explain the superior performance of HDT catalysts for the MPV reaction in this work. Hf- β HDT has shown the best overall performance, with high activity, highest selectivity and stability; consequently, this material is pointed as the most promising for the final goal, the Guerbet reaction of ethanol to n-butanol.

5.2.2. Aldol condensation

In the previous section, Hf, Zr and Sn containing β zeolites were tested for the MPV reduction of furfural. Following the same line of discussion, the studied zeolites were also tested for the Aldol condensation reaction and the condensation of benzaldehyde with acetone was chosen as a model reaction (Scheme 5.4). Sn- β has been previously reported to be a successful and

stable catalyst for this reaction.³⁵ Thus, the aim of this section is to test the mentioned β zeolites for the Aldol condensation of benzaldehyde to benzalacetone and identify the activity, and the stability of the catalyst, paying special attention to further condensation to dibenzylideneacetone.

From the previous data obtained by the continuous MPV reduction of furfural, β zeolites prepared by SSI showed low selectivity for the desired product in case of Sn- β , or low activity in case of Hf- β . Hence, as Hf- β 1 wt.% prepared by the HDT method has been shown to be the material with the best catalytic performance for the MPV reduction of furfural, this material was the first to be tested for the Aldol condensation of benzaldehyde, using a similar plug flow reactor to that employed for the MPV studies. The reaction was first tested at 100 °C, but due the low activity showed by this material, optimisation was required by increasing the temperature (Figure 5.13).

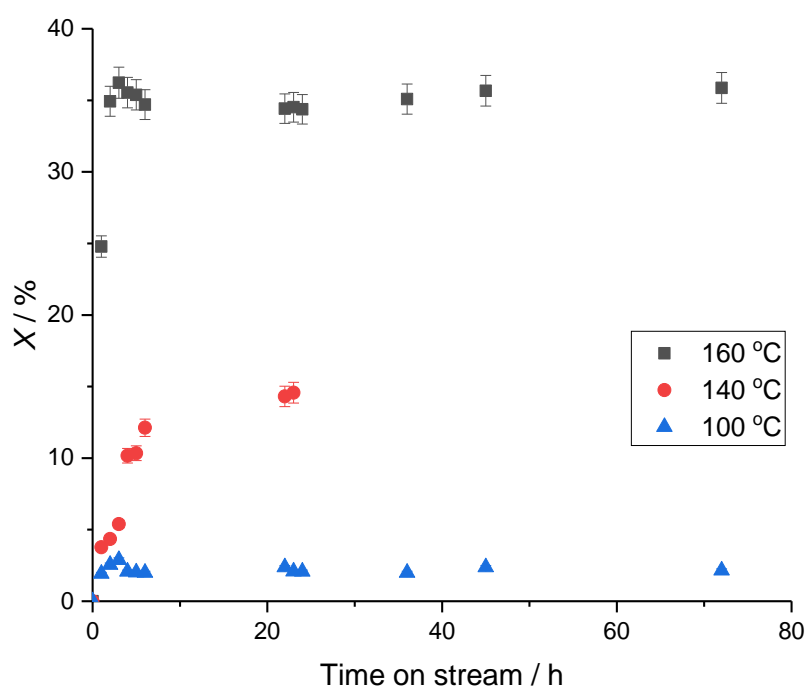


Figure 5.13: Conversion of benzaldehyde (X) over Hf- β zeolite 1 wt.% prepared by HDT method over time on stream at different temperatures between 100–160 °C. **Reaction conditions:** PFR, solution of benzaldehyde 0.1 M and acetone 0.3 M in toluene, 10 bar.

As can be seen, the conversion per unit time increases when higher temperatures are employed. For instance, the conversion reached at 100 °C is about 3 %. In contrast, 36 % conversion is obtained at 160 °C, without selectivity changes being observed (see below for further discussion). At 160 °C Hf- β HDT shows not just good activity, but also stability, maintaining these same levels of conversion during more than 70 h on stream and achieving selectivity for benzalacetone higher than 99 % in all the samples tested at these conditions without further condensation being observed.

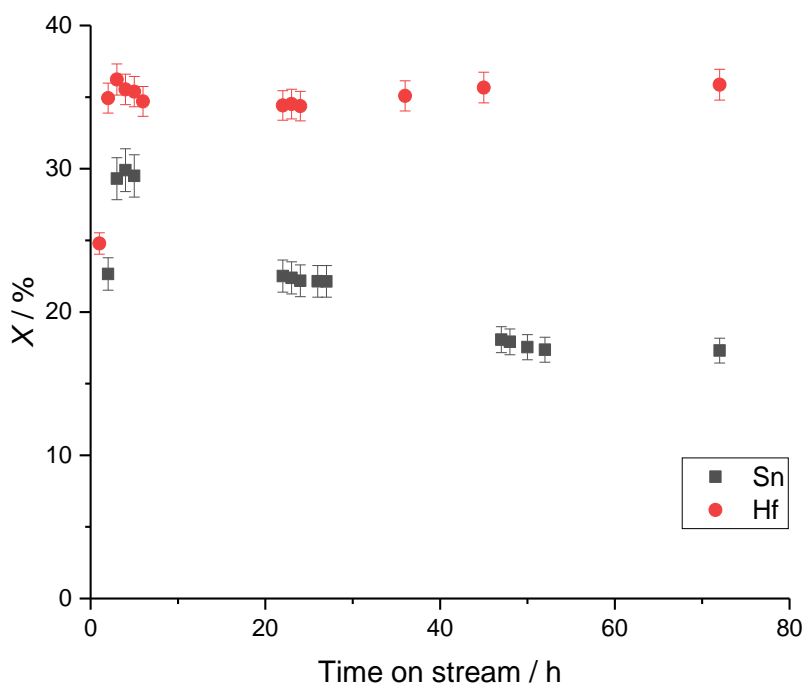


Figure 5.14: Conversion of benzaldehyde (X) over different metal (Sn, black squares; Hf, red circles) containing β zeolite 1 wt.% prepared by HDT method over time on stream. **Reaction conditions:** PFR, 160 °C, benzaldehyde 0.1 M and acetone 0.3 M in toluene, 10 bar.

Based on the MPV studies, Sn- β HDT was also tested at 160 °C (Figure 5.14) for this reaction and compared to Hf- β HDT. As can be seen, Hf- β HDT and Sn- β HDT react in a similar way to that observed for the MPV reduction of furfural. At 160 °C, Sn- β shows activity for the Aldol condensation of benzaldehyde with acetone, reaching 30 % conversion but at lower rates compared to Hf- β , which achieves more than 35 % of conversion. Interestingly, both β zeolites present excellent selectivity towards benzalacetone in all the samples tested for more than 70 h on stream. To better appreciate this, selectivity for benzalacetone is compared to the conversion of benzaldehyde for both Sn- β and Hf- β (Figure 5.15).

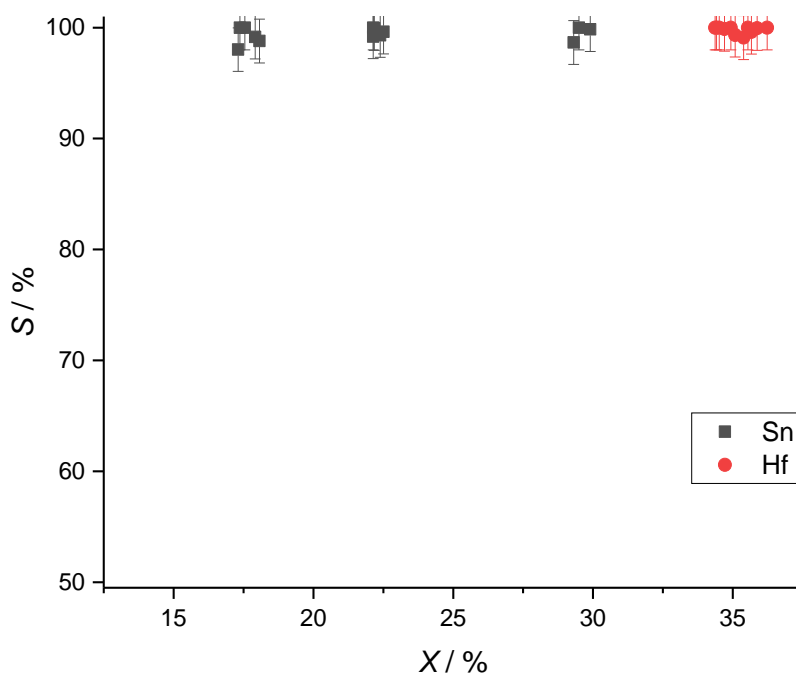


Figure 5.15: Selectivity for benzalacetone (S) over conversion of benzaldehyde (X) for Sn-β and Hf-β. **Reaction conditions:** PFR, 160 °C, benzaldehyde 0.1 M and acetone 0.3 M in toluene, 10 bar.

As can be observed in Figure 5.15, there are no significant changes in selectivity for either material, which is maintained above 98 % throughout all the reaction period. Importantly, no evidence of further condensation to dibenzalacetone was obtained. This may be because the morphology of the β zeolite prevents over condensation but would need further testing.

At this point Hf-β demonstrates higher activity and the same selectivity for benzalacetone as Sn-β, but there is a third point of discussion which is implicit in the last data presented: the stability of the catalyst. For a numerical comparison of the deactivation, k_d (Figure 5.16) was obtained applying the Levenspiel deactivation rate equation (Equation 5.2). From this analysis, it is again clear that Hf-β HDT is a very stable catalyst, exhibiting no deactivation over the reaction period, in contrast to Sn-β.

$$\ln\left(\ln\left(\frac{[Beal]_0}{[Beal]_t}\right)\right) = \ln(k\tau) - k_d t \quad [Equation 5.3]$$

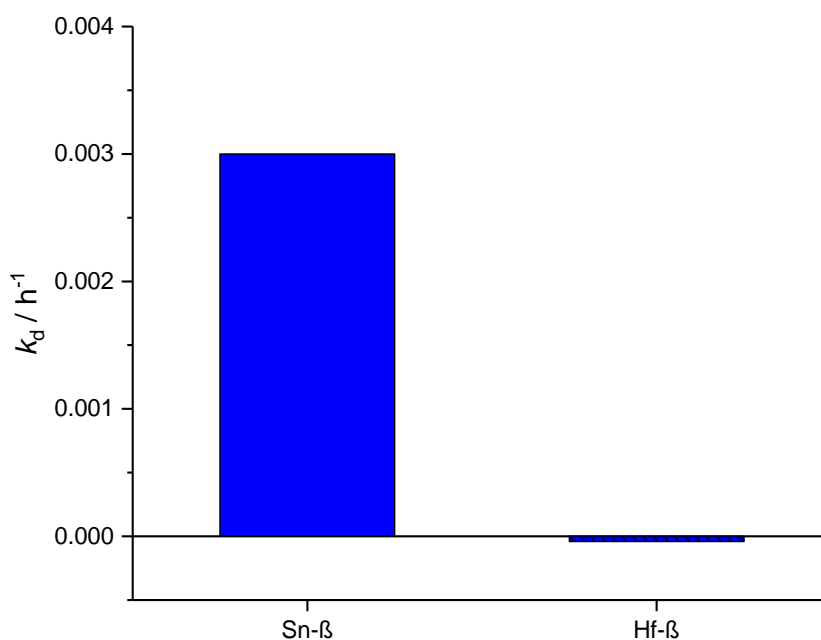


Figure 5.16: Deactivation constant (k_d) of Sn and Hf β zeolite 1 wt.% prepared by HDT method. **Reaction conditions:** PFR, 160 °C, benzaldehyde 0.1 M and acetone 0.3 M in toluene, 10 bar.

For all the data displayed in this section, it is easy to conclude that Hf- β HDT is the most active, selective and stable catalyst for the Aldol condensation.

5.3. Conclusions

The results presented in this chapter confirm that Lewis acidic β zeolites such as Hf- β and Sn- β 1 wt.% are suitable catalyst for both, the MPV reduction and Aldol condensation reactions and experiments in the continuous regime demonstrate the durability of these catalysts over 72 h on stream. The correct crystalline phase of the catalysts tested are confirmed by diffraction (XRD) analysis, and the correct loadings of metal were confirmed by emission spectroscopy (ICP-AES).

Two different methods of β zeolites synthesis have been presented: HDT and SSI methods and catalysts prepared by HDT method show a better performance for both reactions, Aldol condensation and MPV reduction.

Overall, Hf- β HDT is the best performing catalyst for both reactions, showing the highest levels of activity and selectivity, and exceptional durability.

These promising results reinforce the idea to evaluate the mixture of different solid catalysts for the full system of the Guerbet reaction. The high durability and selectivity showed by Hf- β , combined with the lack of further condensation to higher products points Hf- β as a promising catalyst for further application to the Guerbet reaction. Thus, in Chapter 6, the mixture of solid materials, Pd/C as a dehydrogenating/hydrogenating agent and Hf- β as Lewis acid for the condensation steps, are tested for the upgrading of ethanol.

References

- ¹ M. B. Smith, J. March, "Advanced Organic Chemistry", New York: Wiley Interscience, **2001**
- ² A. F. Carey, R. J. Sundberg, "Advanced Organic Chemistry Part B Reactions and Synthesis", 233 Spring Street, NY: Plenum. **1993**
- ³ V. Serra-Holm, T. Salmi, P. Mäki-Arvela, E. Paatero, L. P. Lindfors, *Org. Process Res. Dev.*, 2001, **5**, 4, 368–375
- ⁴ X. Sheng, N. Li, G. Li, W. Wang, A. Wang, Y. Cong, X. Wang, T. Zhang, *Green Chem.*, 2016, **18**, 13, 3707–3711
- ⁵ J. Yang, N. Li, S. Li, W. Wang, L. Li, A. Wang, X. Wang, Y. Cong, T. Zhang, *Green Chem.*, 2014, **16**, 12, 4879–4884
- ⁶ M. Li, X. Xu, Y. Gong, Z. Wei, Z. Hou, H. Li, Y. Wang, *Green Chem.*, 2014, **16**, 9, 4371–4377
- ⁷ I. Sádaba, M. Ojeda, R. Mariscal, J. L. G. Fierro, M. L. Granados, *Appl. Catal., B*, 2011, **101**, 3, 638–648
- ⁸ Jilei Xu, N. Li, X. Yang, G. Li, A. Wang, Y. Cong, X. Wang, T. Zhang, *ACS Catal.*, 2017, **7**, 5880–5886
- ⁹ A. Corma, L. Nemeth, M. Renz, S. Valencia, *Nature*, 2001, **412**, 423
- ¹⁰ R. Otomo, R. Kosugi, Y. Kamiya, T. Tatsumi, T. Yokoi, *Catal. Sci. Technol.*, 2016, **6**, 2787
- ¹¹ M. Moliner, Y. Roman-Leshkov, M. E. Davis, *Proc. Nat. Acad. Sci.*, 2010, **107**, 6164
- ¹² M. S. Holm, S. Saravanamurugan, E. Taarning, *Science*, 2010, **328**, 602
- ¹³ J. Jae, E. Mahmoud, R. F. Lobo, D. G. Vlachos, *ChemCatChem*, 2014, **6**, 508
- ¹⁴ A. Corma, M. Renz, *Angew. Chem. Int. Ed.*, 2007, **46**, 298
- ¹⁵ B. Tang, W. Dai, G. Wu, N. Guan, L. Li, M. Hunger, *ACS Catal.*, 2014, **4**, 2801
- ¹⁶ M. Boronat, A. Corma, M. Renz, *J. Phys. Chem. B*, 2006, **110**, 21168
- ¹⁷ A. Corma, M. E. Domine, S. Valencia, *Journal of Catalysis*, 2003, **215**, 294
- ¹⁸ C. Cundy, P. Cox, *Micropor. Mesopor. Mat.*, 2005, **82**, 1
- ¹⁹ S. Tolborg, A. Katerinopoulou, D. D. Falcone, I. Sadaba, C. M. Osmundsen, R. J. Davis, E. Taarning, P. Fristrup, M. S. Holm, *J. Mater. Chem. A*, 2014, **2**, 20252
- ²⁰ C. Hammond, D. Padovan, A. Al-Nayili, P. Wells, E. Gibson, N. Dimitratos, *Chem. Cat. Chem.* 2015, **7**, 322–331
- ²¹ P. Wolf, C. Hammond, S. Conrad, I. Hermans, *Dalton Trans.*, 2014, **43**, 4514
- ²² N. Deshpande, A. Parulkar, R. Joshi, B. Diep, A. Kulkarni, N. A. Brunelli, *J. Catal.*, 2019, **370**, 46–54
- ²³ M. M. Antunes, S. Lima, P. Neves, A. L. Magalhaes, E. Fazio, A. Fernandes, F. Neri, C. M. Silva, S. M. Rocha, M. F. Ribeiro, M. Pillinger, A. Urakawa, A. Valente, *J. Catal.*, 2015, **329**, 522–537
- ²⁴ B. Kamm, P. R. Gruber, M. Kamm, "Biorefineries—Industrial Processes and Products", Wiley-VCH, Weinheim, **2006**
- ²⁵ R. H. Kottke, Kirk-Othmer, "Encyclopedia of Chemical Technology", John Wiley and Sons, New York, vol. 12, **1998**

- ²⁶ H. E. Hoydonckx, W. M. Van Rhijn, W. Van Rhijn, D. E. De Vos, P. A. Jacobs, "Furfural and Derivatives", WileyVCH Verlag GmbH & Co. KGaA, Weinheim, **2012**
- ²⁷ K. Vanchinathan, G. Bhagavannarayana, K. Muthu, S.P. Meenakshisundaram, *Physica B.*, 2011, **406**, 4195–4199
- ²⁸ J.N. Chheda, J.A. Dumesic, *Catal. Today.*, 2007, **123**, 59–70
- ²⁹ S. Handayani, S. Matsjeh, C. Anwar, S. Atun, I. Fatimah, *J. Appl. Sci. Res.*, 2012, **8**, 5, 2457-2464
- ³⁰ J. Jae, G. A. Tompsett, A. J. Foster, K. D. Hammond, S. M. Auerbach, R. F. Lobo, G. W. Huber, *J. Catal.*, 2011, **279**, 257-268
- ³¹ M. Su, W. Li, T. Zhang, H. Xin, S. Li, W. Fan, L. Ma, *Catal. Sci. Technol.*, 2017, **7**, 3555-3561
- ³² L. Botti, R. Navar, S. Tolborg, J. S. Martinez-Espin, D. Padovan, E. Taarning, C. Hammond, *Top Catal.*, 2018, 1-14
- ³³ R. López-Asensio, C. Jiménez Gómez, C. García Sancho, R. Moreno-Tost, J. Cecilia, P. Maireles-Torres, *Int. J. Mol. Sci.*, 2019, **20**, 828
- ³⁴ C. Hammond, *Green Chem*, 2017, **19**, 2711-2728
- ³⁵ M. Su, W. Li, T. Zhang, H. Xin, S. Li, W. Fan, L. Ma, *Catal. Sci. Technol.*, 2017, **7**, 3555-3561

6. Multistep upgrade of ethanol by Guerbet reaction

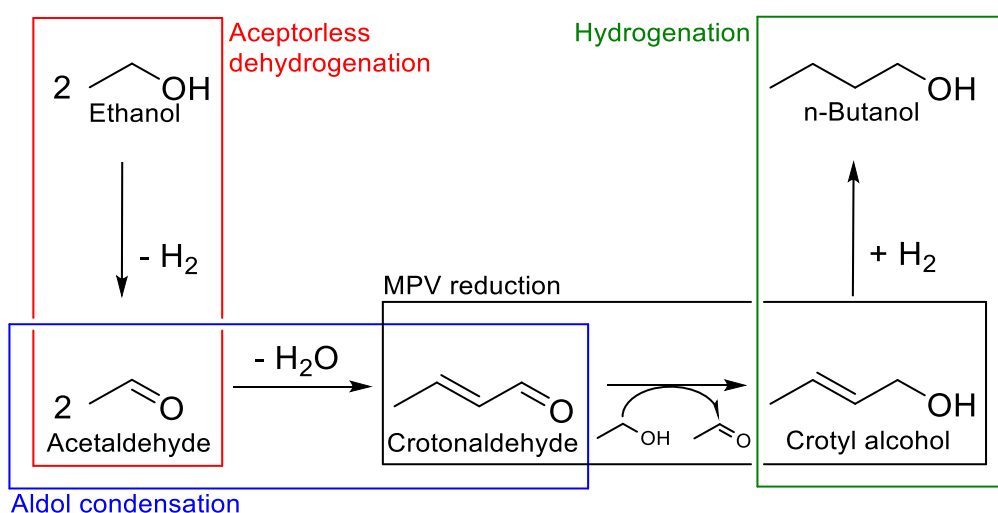
6.1. Introduction

Over the last decades, problems associated with the use of fossil fuels have become widely appreciated, leading to a growing urgency to find other energy sources that are more respectful to the environment. As has been presented in previous chapters, the family of bioalcohols, derived from biomass, are an interesting alternative for both energy production and for the C-based chemical industry. The most prominent bioalcohol is ethanol. However, this alcohol presents several disadvantages, particularly in its role as a biofuel (described in depth in Section 1.3.4.1), suggesting that higher alcohols like n-butanol can be more adequate as fuels. Having in mind that ethanol is a relatively abundant resource with a growing production, an economically attractive way to produce n-butanol is combining two molecules of ethanol through the Guerbet reaction.

In Chapter 3, a first approach to the Guerbet chemistry is described, using a Ru based homogeneous catalyst, chosen from the literature as being the state of the art catalyst for this reaction at the commencement of this study. However, after witnessing the complexity of the reaction through the experiments described in Chapter 3, it was decided to investigate the individual steps of the Guerbet process by use of model reactions. In Chapter 4 the first step of the Guerbet reaction, the acceptorless dehydrogenation, is studied, finding in Pd/C an excellent catalyst for the dehydrogenation of alcohols with release of H₂. In Chapter 5, β zeolites are presented as efficient catalysts for the next steps of the Guerbet reaction, those

being the Aldol condensation and MPV reduction. Therein, Hf- β 1 wt.% prepared by hydrothermal synthesis (HDT) exhibits the best performance, possessing higher activity and selectivity for the desired products when compared with other β zeolites.

After studying the different steps of the Guerbet reaction, the focus of this chapter will be combining the hydrogenation/dehydrogenation catalyst identified in Chapter 4 with the Lewis acidic catalyst identified in Chapter 5, to try to perform the Guerbet upgrade of ethanol to n-butanol in a more selective manner (Scheme 6.1).



Scheme 6.1: General scheme for the different steps of the Guerbet reaction of ethanol.

6.2. Results and Discussion

6.2.1. Dehydrogenation of ethanol

As described in Chapter 4, commercial Pd/C 5 wt.%, simply stated as Pd/C, is an excellent catalyst for the acceptorless dehydrogenation of alcohols like 1-phenylethanol, both in batch and in continuous flow. This good activity suggests Pd/C as a possible candidate to perform the first step of the coveted Guerbet reaction, that is, the acceptorless dehydrogenation of ethanol (Scheme 6.2).



Scheme 6.2: General reaction scheme for acceptorless dehydrogenation of ethanol.

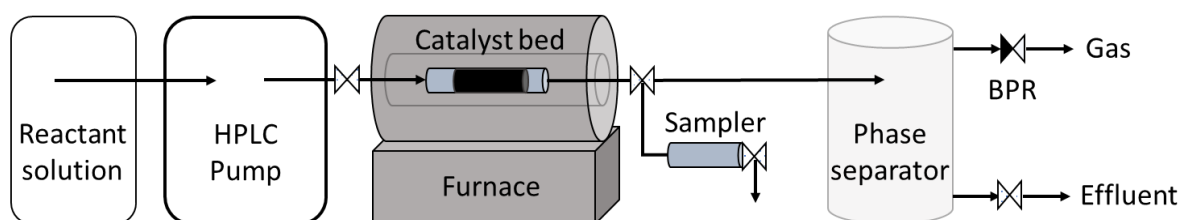
For instance, as detailed in Section 4.2.13, the use Pd/C with a solution of 1-phenylethanol in toluene leads to 17 % of conversion of this alcohol in continuous flow. Furthermore, experiments detailed in Section 4.2.13 in a Plug Flow Reactor (PFR), using a smaller secondary alcohol as substrate (2-butanol), showed that higher temperatures are required to perform the acceptorless dehydrogenation of less activated alcohols. As such, to achieve comparable activities at approximately similar contact times (using 0.1 g of Pd/C with a 0.5 M solution of 2-butanol in toluene), the reactor temperature needed to be increased from 130 to 200 °C to perform the dehydrogenation of 2-butanol. Following the same line of discussion, the necessity to increase the temperature again for ethanol can be expected. This fact can be better understood from the mechanistic studies detailed in Section 4.2.10, where the formation of a carbo-cationic intermediates during the acceptorless dehydrogenation is suggested. Accordingly, ethanol, as a primary alcohol in addition of being a smaller substrate, is less likely to react than a secondary alcohol like 2-butanol. A first approach testing the dehydrogenation of ethanol in continuous flow, at 200 °C with the same solution concentration as 2-butanol (0.5 M), resulted in poor levels of reactivity, with conversion values less than 1 % being observed; however, even at such low levels of conversion, the desired product, acetaldehyde, could be detected, suggesting the feasibility of the process. For this reason, to perform the continuous acceptorless dehydrogenation of ethanol, the temperature was gradually increased until obtaining comparable levels of conversion observed for the dehydrogenation of 1-phenylethanol and 2-butanol. Increasing the temperature to 290 °C, using the same amount of catalyst, the successful dehydrogenation of ethanol was observed over Pd/C. In fact, at these conditions, an ethanol conversion of 20 %, with an acetaldehyde selectivity of 73 %, was achieved. Working at such high temperatures could be argued that the reaction is thermodynamically controlled, however experiments carried out with ethanol at 290 °C without Pd/C catalyst show no conversion of ethanol, revealing the catalytic effect of Pd. The production of hydrogen could be confirmed by collecting the gas released from the back-pressure regulator, installed in the reactor, and analysing it by mass spectroscopy (MS). In Table 6.1 the different results for acceptorless dehydrogenation of alcohols are presented for a more visual comparison of the increase of temperature needed to perform the reaction with substrates of different reactivity.

Table 6.1: Conversion (X) of different alcohols at different temperatures (T) in PFR reactor, over Pd/C.

<u>Substrate</u>	<u>T</u> (°C)	<u>X</u> (%)
1-Phenylethanol	130	17.1
2-Butanol	130	0.0
2-Butanol	200	16.0
Ethanol	200	0.7
Ethanol	290	20.1

Reaction conditions: 0.1g Pd/C, substrate 0.5 M in toluene, different temperatures, 0.5 min contact time.

To perform the dehydrogenation of ethanol at 290 °C, some changes are needed to be made to the PFR. The increase of temperature above that of the boiling point of the solvent (toluene, 110 °C) requires an increase in the pressure of the system. To avoid changing the phase of the system to the gas phase, the pressure of the system was maintained by setting the back-pressure regulator at 33 bar, over that of the vapour pressure of toluene at the working temperature.¹ A new sampler was also designed to enable samples to be taken without disrupting the integrity of the reactor system. With a capacity of 1 mL, the sampler consists of a tube of stainless steel with two valves. Placed after the furnace, the sampler can be filled opening the first valve, keeping the system isolated from the atmosphere and avoiding big changes of pressure. Once filled, by closing the first valve of the sampler, the collected sample can be cooled down inserting the sampler in a bath of ice. The frozen sample can be then released and collected for analysis by opening the second valve of the sampler.

**Scheme 6.3:** Scheme of plug flow reactor for acceptorless dehydrogenation of 2-butanol and ethanol in continuous flow.

This new methodology was more suitable for working with ethanol and, particularly the product of its dehydrogenation, acetaldehyde, with boiling point of only 20°C. The collected samples

contain colour-less liquid and large quantities of gas. The gas can be attributed to the release of H_2 expected for the acceptorless dehydrogenation of ethanol (Scheme 6.2).

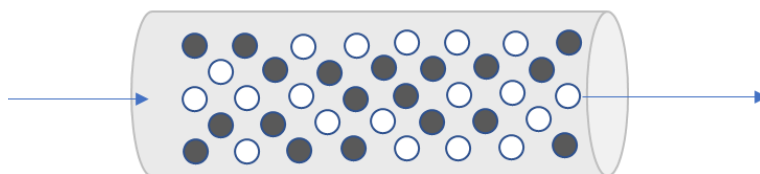


Scheme 6.4: General reaction scheme for dehydration of ethanol to diethyl ether.

For the acceptorless dehydrogenation of ethanol using Pd/C, diethyl ether was identified as the major by product (Scheme 6.4) with a 20 % of selectivity for this ether. The selective dehydration of ethanol to diethyl ether is an interesting because it is a renewable and promising oxygenated fuel for the use as an ignition additive for gasoline and diesel engines.² Diethyl ether can be produced from dehydration of ethanol when it is treated with strong acids like sulfuric acid but has also been reported its production with solid catalysts at high temperatures.^{3,4} The selective dehydration of ethanol to diethyl ether could be a valuable future line of investigation.

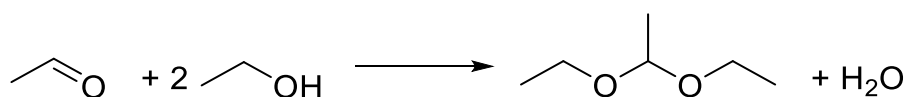
6.2.2. Condensation of ethanol

At this point, Pd/C and Hf- β HDT have been selected as active catalysts for the different steps of the Guerbet reaction. As such, both materials were combined in the same system in the attempt to achieve the desired upgrade of ethanol to n-butanol through the Guerbet reaction (Scheme 6.1). Thus, the two different catalysts were physically ground together to obtain a homogeneous solid mixture of the two materials (Scheme 6.5). Details can be found in Section 2.3.11.



Scheme 6.5: Representation of catalyst bed reactor for upgrade of ethanol using a physical mixture of Pd/C (black) and Hf- β HDT (white).

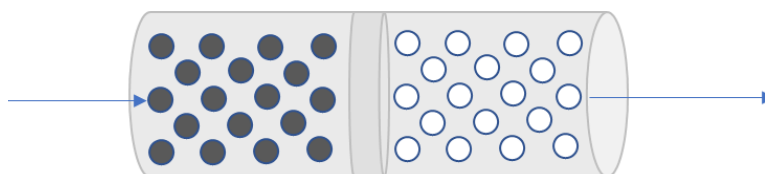
To test the catalytic activity of the described mixture of Pd/C and Hf- β HDT for the upgrade of ethanol, the PFR with the adapted sampler was used. A preliminary experiment was performed using a solution of ethanol in toluene (1 M), and 0.1 g of each catalyst (i.e. 0.2 g of catalyst, total) at 290 °C. Regrettably, this approach did not achieve Guerbet chemistry; the system showed 21 % conversion of ethanol but no acetaldehyde or Guerbet products were detected. Instead, the acetal 1,1-diethoxyethane was identified as main product (Scheme 6.6), produced at a selectivity of 67 %. Small quantities of diethyl ether as side product were also detected. 1,1-diethoxyethane, typically referred simply as acetal, is a reported product of acetalisation between acetaldehyde and ethanol.^{5,6} This confirms again the dehydrogenation of ethanol by Pd action but its combination with Hf- β HDT did not follow the desired pathway to form n-butanol.



Scheme 6.6: General reaction scheme for acetalisation of acetaldehyde with ethanol to 1,1-diethoxyethane.

The formation of acetal is yet another proof of the complexity of the Guerbet reaction. Any addition to the system may change completely the reactivity leading to unexpected products. To understand the role of various catalytic functionalities in the system, a number of control experiments were performed. Firstly, to understand the role of Hf- β HDT, a catalyst bed packed with 0.1 g of this zeolite was prepared and tested in continuous flow, at the same conditions used in the previous experiment (0.1g Hf- β HDT, ethanol 0.5 M in toluene, 290 °C , 0.5 min contact time); however, no conversion of ethanol was appreciated using Hf- β HDT alone for this reaction. It can be concluded that Hf- β HDT cannot perform the first step of the process, the acceptorless dehydrogenation. This result confirms the necessity of a dehydrogenating catalyst to perform the upgrade of ethanol.

With the aim to avoid the formation of acetal, a different strategy was adopted: Instead of mixing Pd/C and Hf- β HDT as a homogeneous physical mixture, these catalysts could be used in sequence (Scheme 6.7), physically separating both materials. Following this idea, a reactor bed was assembled similarly to Scheme 6.6, densely packing 0.1 g of Pd/C and 0.1 g of Hf- β HDT but separating the catalysts with glass wool.



Scheme 6.7: Representation of catalyst bed reactor for upgrade of ethanol using Pd/C (black) and Hf- β HDT (white) in sequence.

This new configuration in sequence achieved 22 % conversion of ethanol but again, no n-butanol was detected; instead crotyl alcohol was the major product, among acetaldehyde and diethyl ether, as happened with Pd/C. These results are in line with the proposed pathway of the Guerbet reaction (Scheme 6.4), suggesting the initial dehydrogenation of ethanol takes place in the first section of the catalyst bed, filled with Pd/C. Once the reaction mixture reaches the second section, packed with Hf-BEA HDT, the produced acetaldehyde undergoes Aldol condensation, to form crotonaldehyde, and MPV reduction, yielding crotyl alcohol. Unfortunately, crotonaldehyde could not be detected as the peak of this product overlaps with the peak of the solvent (toluene) in the chromatogram. However, this system lacks the last step of the Guerbet reaction, that is re-hydrogenation of crotyl alcohol to n-butanol. To perform this last step is necessary to add a hydrogenating agent, such as Pd/C, which is a reported active catalyst for hydrogenation of unsaturated compounds.^{7,8} This activity is also described in Section 4.2.7, where Pd/C is presented as an active catalyst for hydrogenation of styrene to ethylbenzene. At this stage it can be concluded that the production of n-butanol by Guerbet reaction of ethanol using the combination of Pd/C and Hf- β HDT is not achieved. However, the observation of Guerbet products such as crotyl alcohol clearly demonstrate that the Guerbet reaction of ethanol to n-butanol is feasible with the heterogeneous system. All presented results of this section are visually summarised in Figure 6.1.

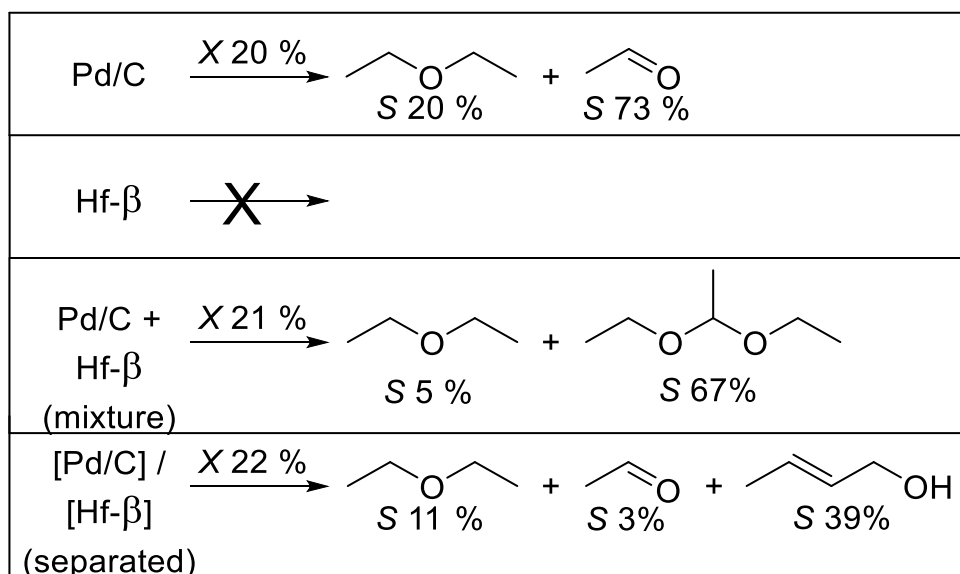


Figure 6.1: Different reactivities for ethanol using Pd/C and Hf-β catalysts with conversion (X) of ethanol and selectivity (S) for the different products. **Reaction conditions:** Continuous flow, 290 °C, ethanol in toluene, 4 h on stream.

6.2.3. Alternatives to Pd/C

As has been repeatedly displayed in this work, the upgrade of ethanol is an extremely complex process. The high reactivity of acetaldehyde combined with the vast amount of possible side reactions result in an arduous task to find an appropriated catalyst for this goal.

The results presented in the previous section indicate the promising potential of combining a dehydrogenating catalyst with a Lewis acidic silicate catalyst. However, the most active catalyst tested for dehydrogenation of alcohols, that is Pd/C, combined with an excellent catalyst for Aldol condensation of carbonyl compounds, Hf-β HDT, leads to the formation of acetal, without showing the desired Guerbet products. The physical separation of these two catalysts leads to the incomplete Guerbet reaction of ethanol, with the formation of crotyl alcohol. To begin to understand whether it is the Pd, or the support, that results in excessive acetal formation, a search for a substitute for Pd/C was carried out using again the dehydrogenation of 1-phenylethanol as model reaction. From a list of different catalysts tested at optimised reaction conditions, commercial Pd/Al₂O₃ 5 wt.%, simply denoted Pd/Al₂O₃, resulted the most promising option as substitute for Pd/C (Figure 6.2). Although Pd/Al₂O₃ showed an inferior performance to its analogue supported on C, the activity of this material was far superior to the rest of tested catalysts.

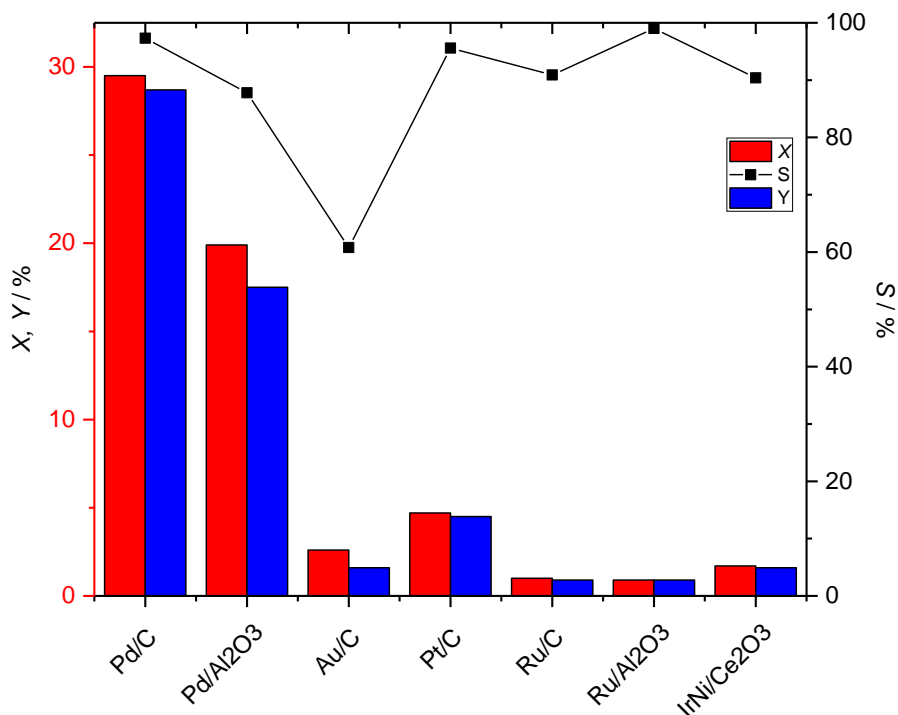


Figure 6.2: Conversion (X) of 1-phenylethanol (red), yield (Y) of acetophenone (blue) and selectivity (S) for acetophenone (black squares) for different catalysts. **Reaction conditions:** stainless steel reactor body with 100 mL pressurised round bottom flask. 20 mL of a solution 0.2 M of 1-phenylethanol in *p*-xylene, 0.08 mol.% of Pd/substrate molar ratio, 130 °C, static N₂ atmosphere, 0.16 h.

As can be seen in Figure 6.2, amongst a variety of oxide and C-supported catalysts, Pd/Al₂O₃ is second in activity only to Pd/C. Although both its activity and selectivity are somewhat lower than those displayed by Pd/C, Al₂O₃ is known to possess very different properties to C, in terms of acidity, basicity and functionality.^{9,10} Having identified Pd/Al₂O₃ to be a suitable candidate for dehydrogenation, and hence the first step of the Guerbet reaction, it was tested as a catalyst for the dehydrogenation of ethanol. In line with the data presented above, its activity was evaluated in the PFR at 290 °C and the system pressurised at 33 bar with a back-pressure regulator. Considering the lower activity showed by Pd/Al₂O₃ for dehydrogenation of 1-phenylethanol compared to Pd/C, the amount of catalyst was doubled to 0.2 g, and the concentration of ethanol eluent increased to 1 M using toluene as solvent. This second measure was adopted to facilitate the detection of products like acetaldehyde. At the described conditions, conversion of ethanol of more than 50 % was detected. The major pathway observed involved the dehydrogenation of ethanol to acetaldehyde, although a second pathway due to the dehydration of ethanol to diethyl ether was also observed as a side reaction. As is the case for C, dehydration of ethanol to diethyl ether over Al₂O₃ catalyst is a well-reported reaction at high temperatures.^{11,12} Unexpectedly, the formation of n-butanol was also detected in this experiment by GC but can be easily explained. Reports of Al₂O₃ acting

as Lewis acidic catalysts for Aldol condensation can be found in literature.^{13,14} As has been repeatedly described in this study, Pd is an active material for acceptorless dehydrogenation of alcohols and can also act as a hydrogenating agent for olefins. Once acetaldehyde is formed, the Al₂O₃ support can act as catalyst for the Aldol condensation of acetaldehyde and, in combination with Pd yield n-butanol. Thus, the intention of combine a dehydrogenating agent with a Lewis acid catalyst is shown successful. Although feasible for this approach, the capability of Pd/Al₂O₃ alone for the entire Guerbet reaction is relatively modest, as its selectivity to n-butanol did not reach values higher than 5 % (Table 6.2). To increase the selectivity towards n-butanol, the use of a better catalyst for the Aldol condensation and MPV reduction seems necessary.

Table 6.2: Conversion (*X*) of ethanol and selectivity (*S*) for major products for reaction of ethanol over Pd/Al₂O₃.

<i>X</i> (%)	<i>S</i> (%)		
	Acetaldehyde	Diethyl ether	n-Butanol
56.3	11.52	11.23	5.7

Reaction conditions: 290 °C, PFR, 1.1 min contact time for Pd, 33 bar, ethanol 1 M in toluene.

6.2.4. Guerbet reaction over Pd/Al₂O₃ and effect of Hf-β HDT

As has been described in previous chapters, the final aim of this study is to combine a dehydrogenating catalyst and a Lewis acid catalyst to perform the upgrade of ethanol. In Section 6.2.2, combining a dehydrogenation catalyst (Pd/C) with a Lewis acid catalyst capable of Aldol condensation (Hf-β HDT) resulted in acetalisation of acetaldehyde with the resulting formation of acetal. On the other hand, an alternative to Pd/C, Pd/Al₂O₃, was tested with the unexpected production of n-butanol. To demonstrate the hypothesis presented in Section 6.2.2vthat the acetal formation is due the effect of the C support and to analyse the effect of Hf-β HDT, the Hf containing β zeolite was homogeneously mixed with Pd/Al₂O₃ in a relation 1 to 1. The mixture was then tested at the same reaction conditions described for Pd/Al₂O₃. The results obtained are presented in Table 6.3.

Table 6.3: Conversion (X) of ethanol and selectivity (S) for major products for reaction of ethanol over Pd/Al₂O₃ and Hf- β HDT.

<u>Catalyst</u>	<u>X (%)</u>	<u>S (%)</u>		
		Acetaldehyde	Diethyl ether	n-Butanol
Pd/Al ₂ O ₃	56.3	11.52	11.23	5.7
Pd/Al ₂ O ₃ + Hf- β HDT	47.2	6.82	9.12	15.3

Reaction conditions: 290 °C, PFR, 1.1 min contact time for Pd, 33 bar, ethanol 1 M in toluene.

As can be seen in Table 6.3, the addition of Hf- β HDT triplicates the selectivity towards n-butanol showed by pure Pd/Al₂O₃, reaching 15.3 % against the previous 5.7 %. This is despite the overall conversion decreasing by approximately 16 %, and the fact that n-butanol is clearly a consecutive product of the reaction; it also reduces the selectivity for acetaldehyde and diethyl ether. The Hf- β clearly has a beneficial role in the formation of n-butanol. A secondary effect is the decrease in activity with a 9 % less conversion of ethanol when Hf- β HDT is combined with Pd/Al₂O₃.

Having identified that mixtures of Pd and Hf catalysts are active for the Guerbet reaction the system must be optimised to improve the selectivity towards n-butanol. Thus, various quantities (and hence, ratios) of Hf- β HDT were mixed with Pd/Al₂O₃. The amount of Pd/Al₂O₃ remained constant in all mixtures (0.2 g). In this way, the Pd catalyst was mixed with increasing amounts of Hf- β HDT to achieve mass ratios from 1-0 to 1-5. For simplicity, the different mixtures were labelled with their Pd-Hf mass ratios: Pd-Hf 1-0 indicates a catalyst bed only consisting of 0.2 g Pd/Al₂O₃, whereas Pd-Hf 1-5 indicates that 5 times more Hf- β HDT was mixed with the Pd catalyst (hence, 0.2 g Pd/Al₂O₃ and 1.0 g Hf- β HDT). The mixtures were densely packed in catalyst beds and tested in continuous flow for the upgrade of ethanol, at 290 °C, using 1 M solutions of ethanol in toluene. The results are presented in Table 6.4.

Table 6.4: Conversion (X) of ethanol and selectivity (S) for n-butanol over mixtures of Pd/Al₂O₃ and Hf- β HDT.

Catalyst ratio ^[a]	X (%)	S (%)
Pd-Hf 1-0	56.3	5.7
Pd-Hf 1-1	47.2	15.3
Pd-Hf 1-2	41.8	18.6
Pd-Hf 1-5	68.7	5.6

[a] Catalyst ratio expressed as relative mass of catalyst. **Reaction conditions:** 290 °C, PFR, 1.1 min contact time for Pd, 33 bar, ethanol 1 M in toluene.

As can be seen in Table 6.4, increasing the amount of Hf from the mixture Pd-Hf 1-1 to 1-2 improves the selectivity for n-butanol until 18.6 % and again reduces the conversion from 47 % to 41.8 %, showing a clear trend in reactivity by the increasing amount of Hf. However, when higher levels of zeolite are present (mixture 1-5), the trend changes, leading again to an increase of conversion (which reaches 68.7 %) but at the cost of losing selectivity for n-butanol. At this point is necessary to understand if the β zeolite framework causes any interference in the reaction. To do so, a siliceous *i.e.* Hf free, sample of a β zeolite was combined with Pd/Al₂O₃ in a new catalyst bed with a ratio of 1 to 5 (labelled as Pd- β 1-5). The results are presented in Table 6.5 and compared with Pd-Hf 1-0 and Pd-Hf 1-5.

Table 6.5: Conversion (X) of ethanol and selectivity (S) for major products for reaction of ethanol over Pd/Al₂O₃ and Hf- β HDT.

Catalyst ratio ^[a]	X (%)	S (%)		
		Acetaldehyde	Diethyl ether	n-Butanol
Pd-Hf 1-0	56.3	11.5	11.2	5.7
Pd-Hf 1-5	68.7	3.0	10.6	5.4
Pd- β 1-5	56.5	11.2	11.3	5.6

[a] Catalyst ratio expressed as relative mass of catalyst. **Reaction conditions:** 290 °C, PFR, 1.1 min contact time for Pd, 33 bar, ethanol 1 M in toluene.

In Table 6.5 the mixture of Pd/Al₂O₃ and H-β zeolites shows a similar performance to the experiments with pure Pd/Al₂O₃. This reactivity confirms that the different activities observed for different Pd-Hf ratios can be attributed mainly to Hf and the undoped zeolite framework itself produces barely any effect in the reaction.

With a more general idea of the role of each element in the system, a deeper analysis of the presented data was performed. From the described experiments, amongst the already mentioned products acetaldehyde, diethyl ether and the desired n-butanol, other identified products included 2-butanol and small quantities of n-hexanol. Reports of the formation of the isomer 2-butanol for the Guerbet reaction can be found in literature¹⁵ due to the tautomerization of the aldol intermediate and, as is described in Chapter 3, n-hexanol formation is a product of the over condensation of acetaldehyde with C₄ products. It is necessary to highlight the absence of higher products such as n-octanol or 2-ethyl-1-butanol; the fact that no higher alcohols are detected suggests that the repeatedly mentioned “cascade of reactions” could be controlled by using Lewis acids. This effect could be attributed to the product shape selectivity presented by zeolites like β.^{16,17} The three-dimensional channels of the zeolites may not allow the formation of larger molecules like n-octanol, controlling the over condensation of Guerbet products. To better understand the behaviour of each used mixture of catalysts, selectivity for the different main products was plotted over conversion of ethanol (Figure 6.3 and Figure 6.4).

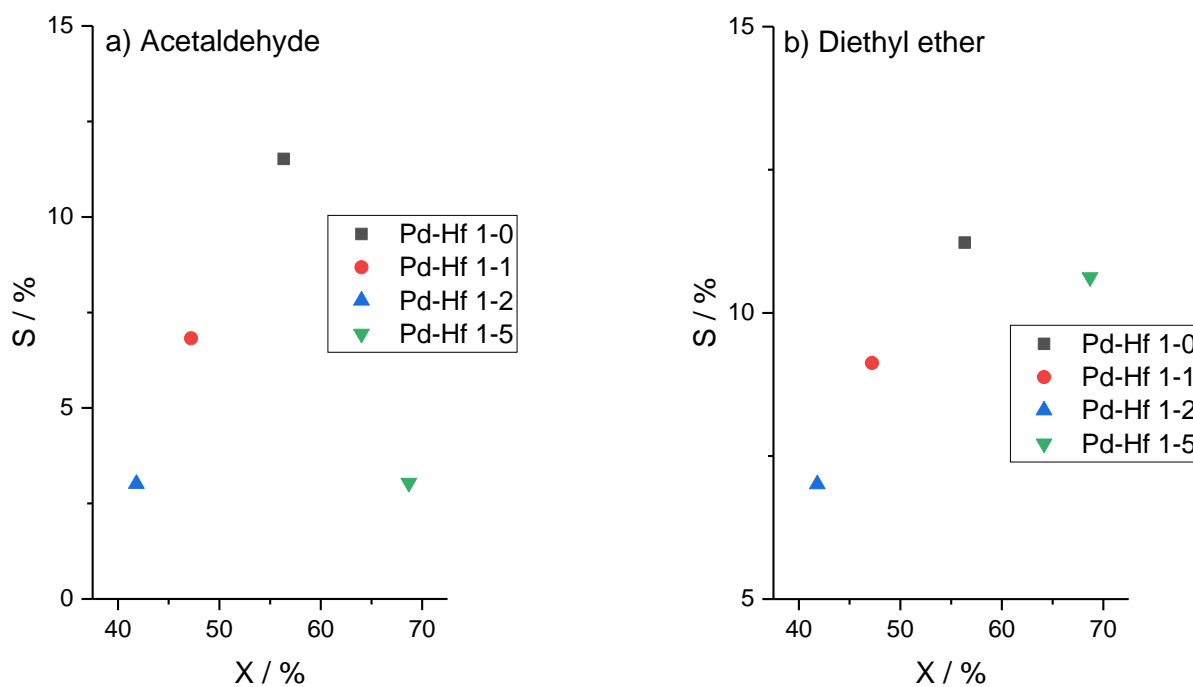


Figure 6.3: Selectivity (S) for **a)** acetaldehyde and **b)** diethyl ether over conversion (X) of ethanol for different mixtures of Pd/Al₂O₃ and Hf- β HDT. **Reaction conditions:** 290 °C, PFR, 1.1 min contact time for Pd, 33 bar.

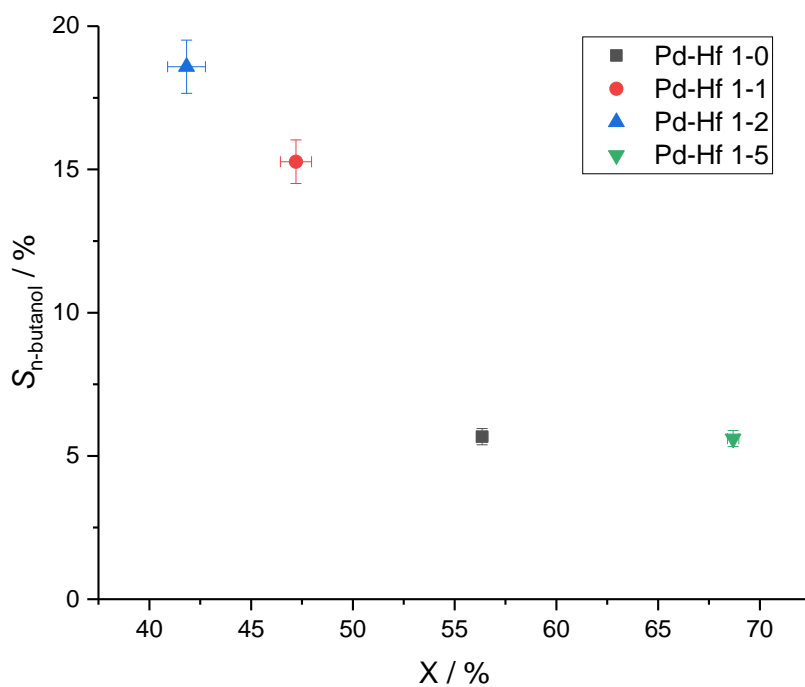


Figure 6.4: Selectivity (S) for n-butanol over conversion (X) of ethanol for different mixtures of Pd/Al₂O₃ and Hf- β HDT. **Reaction conditions:** 290 °C, PFR, 1.1 min contact time for Pd, 33 bar.

Figure 6.3 presents the selectivity for acetaldehyde and diethyl ether as a function of ethanol conversion for every mixture of Pd/Al₂O₃ and Hf-β HDT. As can be seen, a clear trend in activity can be appreciated; the mixture Pd-Hf 1-0, for which pure commercial Pd/Al₂O₃ was used as catalyst, shows the highest levels of selectivity for acetaldehyde and diethyl ether at higher conversions; adding Hf-β HDT to the mixture, as in mixture Pd-Hf 1-1, where same amounts of both catalysts were used, decreases the selectivity for these products. The effect is more evident in mixture Pd-Hf 1-2, where double amount of Hf-β HDT was used towards Pd/Al₂O₃. It has been proved how Al₂O₃ can perform the second and third steps of the Guerbet reaction (Scheme 6.4), Aldol condensation and MPV reduction, and is active for n-butanol synthesis; however, the addition of Hf-β HDT favours the Aldol condensation, and leaves less unreacted acetaldehyde, increases n-butanol production.

For Figure 6.4, the selectivity of n-butanol over conversion of ethanol is presented for every mixture used. The results presented in this figure are in line with the previous discussed idea, the beneficial effect of Hf for the condensation steps. The Mixture Pd-Hf 1-2 shows the higher selectivity for n-butanol and descends in mixtures with less or no Hf presence. It can be concluded that the increasing amount of Hf favours the production of n-butanol, which reinforces the idea of Hf-β HDT promoting the upgrade of ethanol through Guerbet reaction whilst the use of pure Pd/Al₂O₃ leads to more unreacted acetaldehyde and dehydration to yield diethyl ether.

Until this point, no attention has been paid to mixture Pd-Hf 1-5. This mixture shows a different behaviour from the rest, breaking the trend established for Pd-Hf 1-0,1,2. This change in the pattern suggests that there is an optimal ratio between the two metals, Pd and Hf, to correctly perform the upgrade of ethanol to n-butanol by Guerbet reaction. A product distribution is presented in Figure 6.5 to better summarise all the results for these ratios; as each mixture present different levels of activity and selectivity, the yield of all individual products was chosen as a better means of comparison.

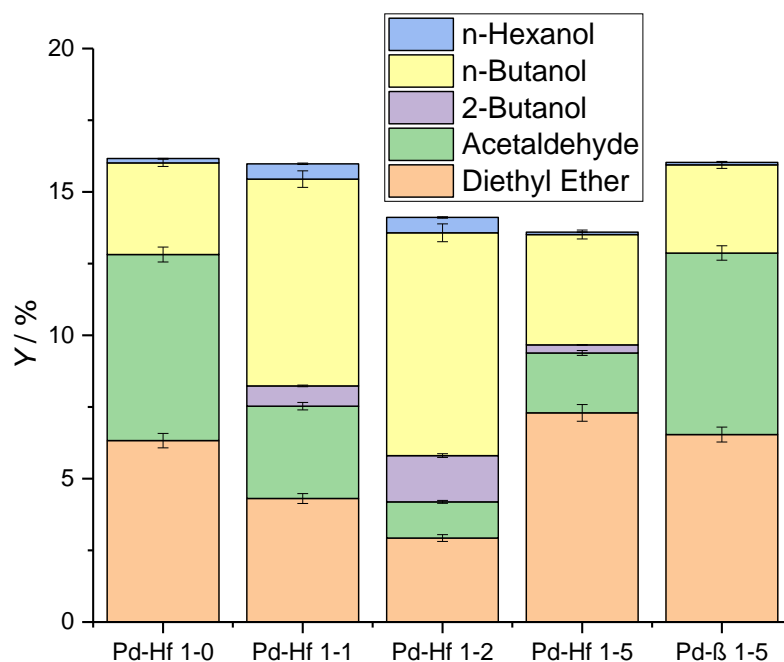


Figure 6.5: Product distribution expressed as yields (Y) for different mixtures of Pd/Al₂O₃ with Hf-β HDT and β zeolite. **Reaction conditions:** 290 °C, PFR, 1.1 min contact time for Pd, 33 bar, ethanol 1 M in toluene.

In Figure 6.5, the accumulated yields of the different products detected during the reaction are presented for every mixture, to give a better picture of the general reactivity. As can be seen, Pd-Hf 1-0 produces low quantities of n-butanol and has a strong preference for the formation of diethyl ether. Increasing amounts of Hf improve the production of n-butanol, decreasing the preference diethyl ether and leaving less unreacted acetaldehyde. Additionally, the distinctive behaviour of Pd-Hf 1-5 can be also observed, not following the previously labelled trend, where higher amounts of Hf-β benefit the formation of n-butanol.

Finally, the importance of Hf is appreciated with mixture Pd-β 1-5, where Pd/Al₂O₃ was mixed with a Hf free zeolite, H-β. This mixture shows similar performance to pure Pd/Al₂O₃, with the same product distribution, which confirms that the β zeolite framework itself does not affect the reaction. The different activities observed can therefore be attributed to the role of Hf.

For all the presented data, it is concluded that n-butanol can be obtained through the Guerbet reaction using solid mixtures of commercial Pd/Al₂O₃ 5 wt.% with Hf-β HDT. The optimal way to proceed is with low mass ratios of Pd-Hf 1-1. Nevertheless, the Guerbet chemistry of ethanol is extremely complex and the system remains in early stages with room for further optimisation.

6.2.5. Gaseous products

The upgrade of ethanol to n-butanol by the Guerbet reaction is the main objective of this work. In the previous sections of this chapter, the successful production of n-butanol has been detailed using solid mixtures of Pd/Al₂O₃ and Hf-β HDT. At this point it must be highlighted the low carbon balance (C.B.) observed during the analysis of the collected mixtures for the experiments above (Table 6.6).

Table 6.6: Carbon balance (C.B.) for Guerbet reactions of ethanol over mixtures of Pd/Al₂O₃ and Hf-β.

Mixture	Pd-Hf 1-0	Pd-Hf 1-1	Pd-Hf 1-2	Pd-Hf 1-5
C.B. (%)	55.0	62.7	65.9	40.6

Reaction conditions: 290 °C, PFR, 1.1 min contact time for Pd, 33 bar, ethanol 1 M in toluene, ethanol 1 M in toluene.

In Table 6.6, the C.B. obtained from the analyses of the Guerbet reaction using the different catalyst mixtures are presented showing levels between 65 and 40 %. Then, in Figure 6.6, C.B. is represented over conversion of ethanol. In this figure, it can be noticed that higher levels of activity result in lower C.B. The low levels of C.B. combined with the observed trend suggest other products are present in the mixture. As described above, no larger products or oligomers thereof could be detected by GC-FID and MS. However, some peaks were detected at short retention times in the chromatograms. This may indicate the presence of low boiling point products. Cooling the sampling system in ice, prior to analyses, resulted in the detection of two additional products, those being butane and 1,3-butadiene, identified by GC-MS. In previous chapters, it was detailed how 1,3-butadiene can be obtained from ethanol through the Lebedev process (Scheme 6.9) at high temperatures (>250 °C), and how important this product is with regards to the production of polymers and synthetic rubber. Several studies have been published covering the formation of 1,3-butadiene over Lewis acidic β zeolites.¹⁸⁻²⁰ The selective production of this alkene from ethanol at relatively low temperatures (<300 °C) would be a very economical interesting process and a valuable future line of investigation.

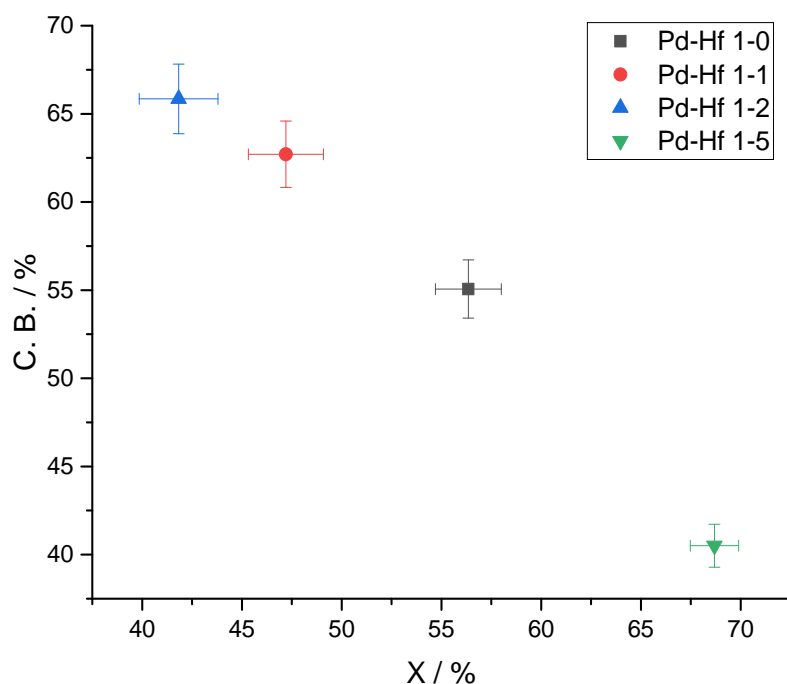
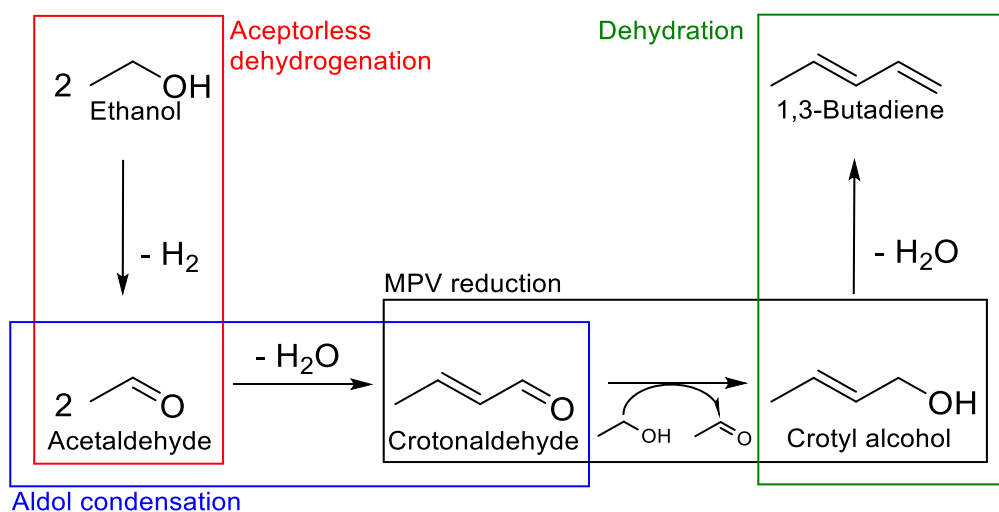
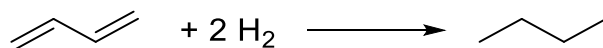


Figure 6.6: Carbon balance (C.B.) over ethanol conversion (X) for different mixtures of Pd/Al₂O₃ with Hf-β HDT and β zeolite. **Reaction conditions:** 290 °C, PFR, 1.1 min contact time for Pd, 33 bar, ethanol 1 M in toluene.



Scheme 6.9: General scheme for the different steps of the Lebedev reaction of ethanol.

In the other hand, the hydrogenation of 1,3-butadiene in the working conditions can be expected. The purification of butane by hydrogenating 1,3-butadiene (Scheme 6.10) has been broadly used and can be found in literature using Pd-based catalysts.²¹⁻²³



Scheme 6.10: General scheme for the hydrogenation of 1,3-butadiene to butane.

Although 1,3-butadiene and butane could be identified by GC-MS, their complex solubility parameters as a function of solvent and temperature, in addition to their highly volatile nature, resulted in difficulties with gaining accurate quantification values. Nevertheless, employing estimated response factors (CF) that were derived from accurate calibrations of n-butanol and comparable compounds (1-phenylethanol, styrene and ethylbenzene), allowed approximate values of yield to be calculated.

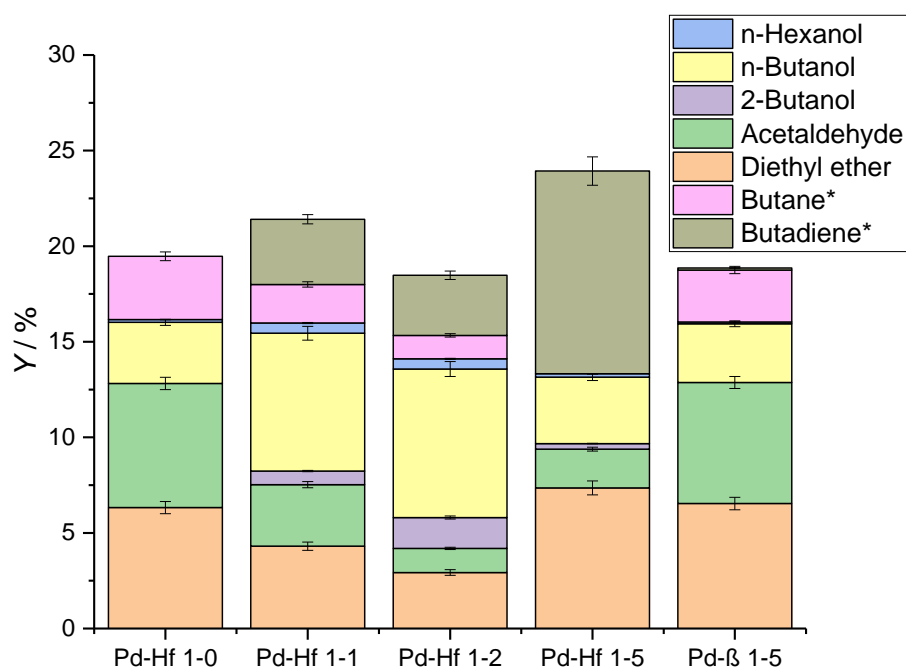


Figure 6.7: Product distribution expressed as yields (Y) for different mixtures of Pd/Al₂O₃ with Hf-β HDT and β zeolite. **Reaction conditions:** 290 °C, PFR, 1.1 min contact time for Pd, 33 bar, ethanol 1 M in toluene.

Figure 6.7 shows the product distribution with the yields obtained by GC-FID with the adapted CF. The values presented for of butane and 1,3-butadiene help to understand the trend for their selectivity, even if they present large values of experimental error. The preference for butane decreases with higher contents of Hf. While butane in mixture Pd-Hf 1-0 reaches a yield close to 6 %, no butane is detected for Pd-Hf 1-5. In the complete opposite, the largest quantities of 1,3-butadiene are detected with the use of Pd-Hf 1-5, with a yield of 14 %, and whereas it cannot be detected using Pd-Hf 1-0. The superior selectivity of Pd-Hf 1-5 for 1,3-

butadiene may indicate that higher amounts of Hf lead preferentially to the dehydration of crotyl alcohol to form 1,3-butadiene instead of re-hydrogenation to n-butanol. This observation supports the idea that concrete ratio of Pd and Hf are necessary to correctly perform the Guerbet reaction and yield the final n-butanol.

The detection and quantification of butane and 1,3-butadiene may seem unorthodox; however, the results showed high accuracy and repeatability. To prove it, different catalyst beds were packed with the same amounts of Pd/Al₂O₃ and Hf-β HDT in ratios 1 to 5 and tested at the same conditions and all the experiments showed the same results, with 1,3-butadiene as the major product (Figure 6.8).

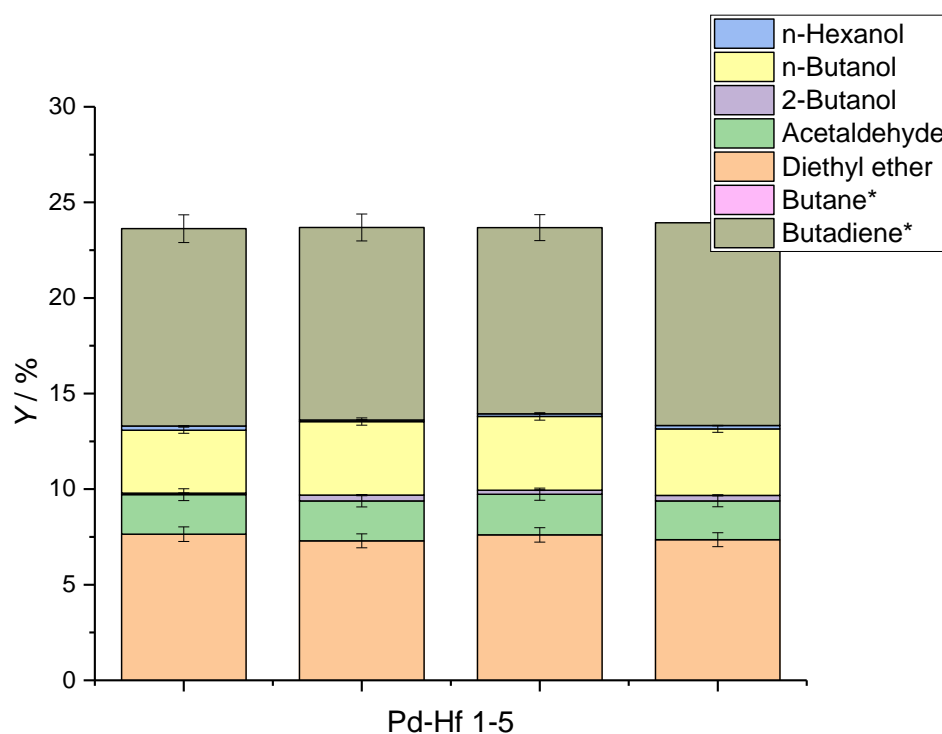


Figure 6.8: Product distribution expressed as yields (Y) for different products for different mixtures of Pd/Al₂O₃ with Hf-β HDT in a ratio of 1 to 5. **Reaction conditions:** 290 °C, PFR, 1.1 min contact time for Pd, 33 bar, ethanol 1 M in toluene.

6.2.6. Adaptability of the system and optimisation to n-butanol

During this chapter, the upgrade of ethanol to n-butanol using mixtures of Pd based catalyst with Hf based catalyst has been presented. The feasibility of this reaction has been demonstrated along the effect of different amounts of Hf-β HDT causes to the reaction. Finally, a list of the major products for each experiment has been displayed with figures of product distribution for each Guerbet reaction using the labelled solid mixtures of Pd and Hf. With all

the presented data an interesting idea comes up, that the system is flexible and tuneable. The combination of a Pd catalyst and different amounts of Hf- β HDT presents different reactivities, leading to different product distributions, which would allow the synthesis of different species with the same catalyst, resulting very attractive for energy production and industrial purposes alike. Being able to produce different valuable products as are acetaldehyde, diethyl ether, n-butanol and 1,3-butadiene just by changing the ratios between Pd and Hf is appealing; however, further optimisation of the system is required to achieve this goal.

Nevertheless, even if the same system allows the production of different chemicals, each particular component should be optimised before this strategy can be adopted for industrial purposes. For the main goal of producing n-butanol, some optimisation was carried out with the described reactor: mixtures Pd-Hf 1-1 and 1-5 were selected as the most representatives, Pd-Hf 1-1 being the most efficient for n-butanol production (Guerbet reaction) and Pd-Hf 1-5 for 1,3-butadiene (Lebedev process). In view of the high conversions presented at 290 °C, these two catalysts were tested in continuous flow at lower temperatures, at 250 and 200 °C respectively. A 1.0 M solution of ethanol in toluene was again used and the system pressurised to 33 bar with the back pressure regulator. The product distributions obtained are presented in Figure 6.9.

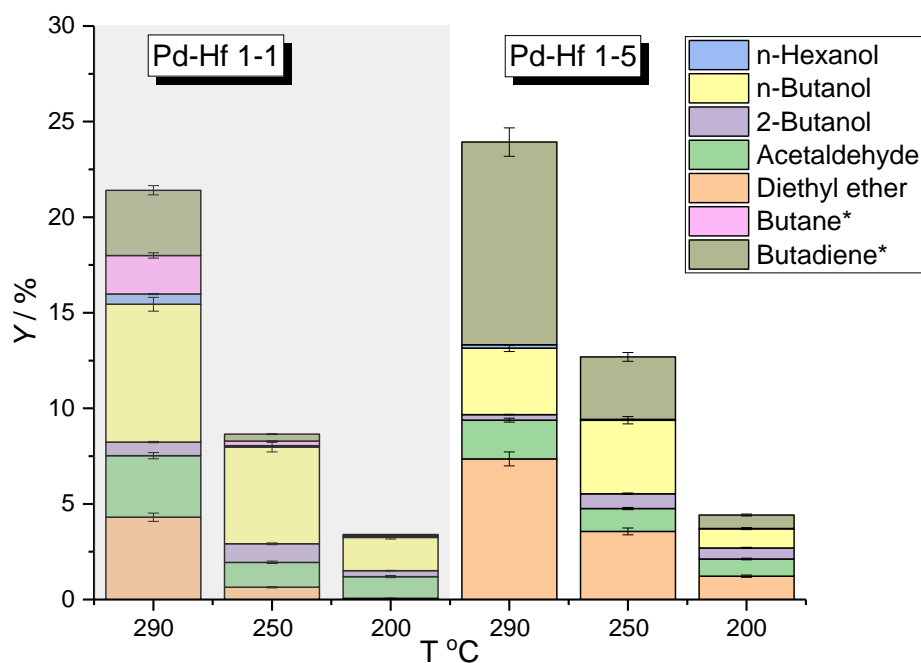


Figure 6.9: Product distribution expressed as yields (Y) for different products at different temperatures for different mixtures of Pd/Al₂O₃ with Hf- β HDT in a ratio of 1 to 1 and 1 to 5. **Reaction conditions:** PFR, 1.1 min contact time for Pd, 33 bar, ethanol 1 M in toluene.

As can be seen in Figure 6.9, decreasing the temperature highly benefits the Guerbet reaction and harms the Lebedev chemistry. Naturally, in both cases the catalytic activity falls upon lowering the temperature. In the specific case of Pd-Hf 1-1, decreasing the temperature from 290 to 250 °C does not reduce dramatically the yield of n-butanol, with a loss of only 2 %. However, 1,3-butadiene and diethyl ether practically disappear. With Pd-Hf 1-5, the same change in temperature halves the yield for diethyl ether and reduces 1,3-butadiene by two thirds; meanwhile, the yield of n-butanol remains with the same value. For all this, it can be concluded that higher temperatures favour the Lebedev dehydration to 1,3-butadiene and more moderate temperatures improve the selectivity towards the desired n-butanol.

6.3. Conclusions

The upgrading of ethanol to more valuable products is a promising route for the generation of sustainable energy. In this context, the Guerbet reaction seems to be an efficient way to obtain a desirable product such as n-butanol from ethanol. The most important conclusion achieved in this chapter is that it is possible to perform the upgrade of ethanol to n-butanol with the Guerbet reaction, combining a dehydrogenating agent as Pd with a Lewis acid as Hf- β . The presented data allows to conclude that the optimal way to perform the upgrade of ethanol to n-butanol by Guerbet reaction is using a homogeneous mixture of Pd/Al₂O₃ with Hf- β HDT in ratio Pd-HF 1-1 at 250 °C.

The initially selected catalyst for dehydrogenation, Pd/C showed an undesired pathway to acetal without producing n-butanol. For that reason, this dehydrogenating catalyst was substituted by its analogue, Pd/Al₂O₃. Surprisingly, the Al₂O₃ support of the catalyst also demonstrated low levels of ability to catalyse the Aldol condensation itself, albeit at poor levels of performance, showing poor selectivity for n-butanol and large quantities of unreacted acetaldehyde. Physically mixing Pd/Al₂O₃ with Hf- β HDT increases the selectivity for n-butanol. However, the system is in very early stages and more optimisation could be done for the reactor and for analytics.

The last conclusion achieved in this work is the flexibility of this system. Different amounts of Hf- β HDT changes the reactivity of the catalyst, tailoring the production of different valuable chemicals like diethyl ether, acetaldehyde, 1,3-butadiene and the coveted n-butanol. The optimisation to the individual products is possible: for example, higher temperatures favour the Lebedev process to 1,3-butadiene, and more moderate temperatures lead to n-butanol with the Guerbet reaction. This can open new and exciting lines of investigation.

References

- ¹ N. W. Krase, J. B. Goodman, *Ind. Eng. Chem.*, 1930, **22**, 113
- ² B. Bailey, J. Eberhardt, S. Goguen, J. Erwin, *SAE Transactions*, 1997, **106**, 1578-1584
- ³ T. Kamsuwan, P. Prasertthdam, B. Jongsomjit, *J. Oleo Sci.*, 2017, **66**, 2, 199–207
- ⁴ D. Jingfa, Z. Guirong, D. Shuzhong, P. A. N. Haishui, W. Huaiming, *Appl. Catal.*, 1988, **41**, 13–22
- ⁵ H. Zhang, Y. Wu, L. Li, Z. Zhu, *ChemSusChem*, 2015, **8**, 1226
- ⁶ M. R. Capeletti, L. Balzano, G. Puente, M. Laborde, U. Sedran, *Appl Catal A-Gen.* 2000, **198**, 1-4
- ⁷ D. Teschner, J. Borsodi, A. Wootsch, Z. Révay, M. Hävecker, A. Knop-Gericke, S. D. Jackson, R. Schlögl, *Science*, 2008, **320**, 86-89
- ⁸ M. García-Mota, B. Bridier, J. Pérez-Ramírez, N. López, *J. Catal.* 2010, **273**, 92-102
- ⁹ V. H de Beer, F. J. Derbyshire, C. K. Groot, R. Prins, A. W. Scaroni, J. M. Solar, *Fuel*, 1984, **63**, 8, 1095-1100
- ¹⁰ P. Boorman, *J. Catal.*, 1991, **128**, 2, 537-550
- ¹¹ J. F. DeWilde, J. Czopinski, A. Bhan, *ACS Catal.*, 2014, **4**, 12, 4425-4433
- ¹² H. Knözinger, H. Bühl, E. Röss, *J. Catal.*, 1968, **12**, 121–128
- ¹³ A. A. Esmaeili, M. S. Tabas, M. A. Nasser, F. Kazemi, *Monatsh. Chem.*, 2005, **136**, 571–576
- ¹⁴ D. Pore, R. Allj, A. S.C. Prabhakar, R. R. Alavala, U. Kulandaivelu, S. Boyapati, *Lett. Org. Chem.*, 2012, **9**, 447-450
- ¹⁵ A.S. Ndou, N. Plint, N.J. Coville, *Appl Catal A-Gen.*, 2003, **251**, 337–345
- ¹⁶ G. Kostrab, M. Lovič, I. Janotka, M. Bajus, D. Mravec, *Appl. Catal.*, 2007, **323**, 210-218
- ¹⁷ N. Ghani, A. Jalil, S. Triwahyono, M. Aziz, A. Rahman, M. Hamid, S. Izan, M. Nawawi, *Chem. Eng. Sci.*, 2019, **193**, 217-229
- ¹⁸ P. Müller, S. P. Burt, A. M. Love, W. P. McDermott, P. Wolf, I. Hermans, *ACS Catal.*, 2016, **6**, **10**, 6823-6832
- ¹⁹ O. V. Shvets, K. M. Konyshva, M. M. Kurmach, *Theor. Exp. Chem.*, 2018, **54**, 2, 138-145
- ²⁰ P. I. Kyriienko, O. V. Larina, S. O. Soloviev, S. M. Orlyk, C. Calers, S. Dzwigaj, *ACS Sustain. Chem. Eng.*, 2017, **5**, 3, 2075-2083
- ²¹ Q. Yang, R. Hou, K. Sun, *J. Catal.*, 2019, **374**, 12–23
- ²² T. Odoom-Wubah, Q. Li, M. Chen, H. Fang, B. Bediako, I. Adilov, J. Huang, Q. Li, *ACS Omega*, 2019, **4**, 1, 300-1310
- ²³ Y. Feng, L. Zhou, Q. Wan, S. Lin, H. Guo, *Chem. Sci.*, 2018, **27**, 5890-5896

7. Conclusions and pertaining challenges

7.1. Final conclusions

Considering the globally increasing concerns on fossil fuel feedstocks, and particularly their negative environmental impact and their prompt depletion, investigation of renewable alternative energy sources has become of high importance. Within all the kinds of renewable alternatives, bioethanol has gained great relevance in the last decades. Although ethanol is currently used as biofuel, as a result of its growing production, this alcohol also presents great potential as a platform molecule to satisfy the necessities for chemical production, built upon C-containing materials; however, ethanol still presents several drawbacks as biofuel, such as low energy density and absorption of H₂O, amongst others, resulting in problems in storage and transportation. For these reason, higher alcohols like n-butanol would be better options to replace the conventional fossil fuels. The main reason why butanol has not been considered as an alternative fuel is that its production has never been cost effective at large scale when renewables are used as feedstock. In that concern, the condensation of two molecules of bioethanol through Guerbet chemistry would result in an economically attractive way to produce a renewable and efficient fuel.

The main bottlenecks during the Guerbet upgrade of ethanol is the selectivity for n-butanol. The Guerbet reaction has been studied for more than 100 years and despite its success for the industrial production of higher alcohols, the process is extremely difficult for the ethanol upgrade to n-butanol. After a detailed analysis of the existing literature about the pathway of the Guerbet reaction and its multiple side reactions (Chapter 1), this can be attributed to the

high reactivity of acetaldehyde and mainly to the “cascade of reactions”, where the products of Guerbet reaction turn into substrate of a new Guerbet cycle, producing bigger products. Accounting a lack of a catalyst able to perform every step of the Guerbet reaction, some advances have been made in the last decade using homogeneous catalysts combined with bases like EtOH or NaOH. Therefore, the first part of this thesis (Chapter 3) focused in the use of a combination of $[\text{RuCl}_2(\eta^6\text{-}p\text{-cymene})]_2$ with the homogenous ligand 2-(diphenylphosphino)ethylamine and EtONa for the Guerbet reaction of ethanol. The role of the ligand 2-(diphenylphosphino)ethylamine has been studied, revealing its importance in terms of maximising the selectivity towards n-butanol; however, despite the good results found in literature,¹ the system studied in Chapter 3 presents low conversion of ethanol (29 %) at the reported conditions. In addition, despite the beneficial effect of 2-(diphenylphosphino)ethylamine, this methodology does not stop the “cascade of reactions”, leading to the formation of higher alcohol, amongst other larger products.

The results presented in Chapter 3 using homogeneous catalysts set the basis to the new strategy of studying the individual steps of the Guerbet reaction, performing model reactions with more adequate catalysts for every step, with the ultimate aim of combining the optimised catalysts into one system of improved performance. To do so, Chapter 4 focused on the acceptorless dehydrogenation of alcohols, a relatively new process, making a strict and detailed analysis necessary. In this chapter, commercial Pd/C 5 wt.% is identified as a suitable heterogeneous catalyst for the dehydrogenation of 1-phenylethanol in inert atmosphere (N_2), with release of H_2 . The development of a novel batch reactor is presented, which allows the collection of the H_2 produced, confirming the acceptorless nature of the reaction. This new reactor also allows full kinetic analysis of all the reaction products and kinetic parameters, including the gaseous products. Accurate kinetic studies are presented, with the obtention of the activation energy (92 kJ/mol) from an Arrhenius plot. Furthermore, a negative Hammett correlation alongside a Kinetic Isotope Effect > 1 are obtained by the use of benzyl alcohol and para-substituted and deuterated benzyl alcohols. These results revealed mechanistic similarities between acceptorless dehydrogenation to aerobic oxidation mechanisms. The hydrogenation capability of the Pd is also evidenced through the reversibility of the dehydrogenation and the side reactions. The characterisation (XPS, XRD, TEM and BET) presented in this chapter, alongside kinetic studies, revealed structure-activity relationships of the Pd species. Finally, in order to perform an accurate investigation of the durability of the materials, and hence understanding its industrial feasibility, the continuous flow conditions are introduced in this chapter. The catalytic performance of Pd/C is studied using a Plug Flow Reactor (PFR), evidencing the durability of the catalyst over 50 h on stream. It is concluded that PFR results are especially appropriate for the study of the Guerbet reaction and its

superior performance in regard to the batch reactors is illustrated with higher Space-Time Yields (STY).

In Chapter 5, the viability of Lewis acidic zeolites as catalysts for the subsequent steps of the Guerbet reaction, the Aldol condensation and the Meerwein–Ponndorf–Verley (MPV) reduction, is explored. These inorganic silicates with three dimensional networks appear to be attractive candidates to catalyse the mentioned reactions due to their interesting properties. In particular, Sn-, Zr- and Hf containing β zeolites were chosen as candidates to be combined with a dehydrogenating and hydrogenating agent (Pd) to perform the upgrading of ethanol, as several reports can be found in regards its activity for the Aldol condensation² and MVP reaction.^{3,4} Two different methodologies to synthesise these materials are presented, those being the hydrothermal method (HDT) and Solid State Incorporation (SSI) method. In this chapter, the presented characterisation confirms the correct crystalline phase of the materials tested by diffraction (XRD) analysis, and the correct loadings of metal were confirmed by Atomic Emission Spectroscopy (ICP-AES). All the zeolites tested possess comparable pXRD pattern and metal content. However, catalysts prepared by HDT method showed consistent textural properties such as specific surface area, catalysts prepared by SSI showed higher specific surface area, leading to different performances. Overall, Hf- β HDT is chosen as the best performing catalyst for both reactions, showing the highest levels of activity and selectivity, and exceptional durability with experiments in the continuous regime over 72 h on stream.

In the final part of this work (Chapter 6), the mixture of solid materials, Pd/C as a dehydrogenating/hydrogenating agent, and Hf- β HDT as Lewis acid for the condensation step, are tested for the upgrading of ethanol. The first challenge faced in this chapter is the necessity of higher temperatures (>250 °C) to perform the dehydrogenation of ethanol with Pd catalyst. The increase of temperature leads to a redesign of the PFR and an increase of the system pressure needed, which allows to perform the reaction in a satisfactory and safe way; however, combining the selected catalyst for dehydrogenation, Pd/C, with Hf- β HDT results in an undesired formation of acetal, without producing n-butanol. Whether it is the Pd, or the support, that results in the acetal formation, it is concluded that an alternative to Pd/C results necessary to perform the Guerbet reaction of ethanol to n-butanol. The presented substitute, Pd/Al₂O₃, not just results as an active catalyst for the acceptorless dehydrogenation of ethanol, but also shows an unexpected activity for the full pathway of the Guerbet reaction, yielding low levels of n-butanol. The combination of Pd/Al₂O₃ with Hf- β HDT improves the selectivity to n-butanol, showing the beneficial effect of the Hf for the Guerbet reaction. Moreover, the mixture of the selected catalysts, using different ratios of Pd and Hf, result in dramatic changes to the product distribution. This fact reveals the most important achievement in this work: The

system is not just active for one reaction, but is a flexible system that can be directed for the production of different chemicals of interest, opening new and exciting lines of investigation.

Finally, the heterogeneous mixture of Pd/Al₂O₃ with Hf-β HDT, presented in Chapter 6, despite staying in early stages with room for further optimisation, is concluded to be an attractive alternative to the homogeneous strategy presented in Chapter 3. Even though higher temperatures are needed, the new system show several advantages. The first and most important improvement is that no higher alcohols or products of further condensation could be detected (aside of small quantities of n-hexanol), even at higher levels of conversion. This observation may suggest that the use of Lewis acidic zeolites can contain the “cascade of reactions”. This system also does not need the use of bases like EtONa, improving the durability of the reactor. Another advantage of the presented system is the higher productivity of the PFR, presenting STY between 30 and 40 times higher than the Ru based homogeneous option (Table 7.1).

Table 7.1: Relative performance of different catalysts for the Guerbet reaction of ethanol to n-butanol at different temperatures, with conversion (X) of ethanol, yield (Y) of n-butanol and Space-Time Yields (STY)

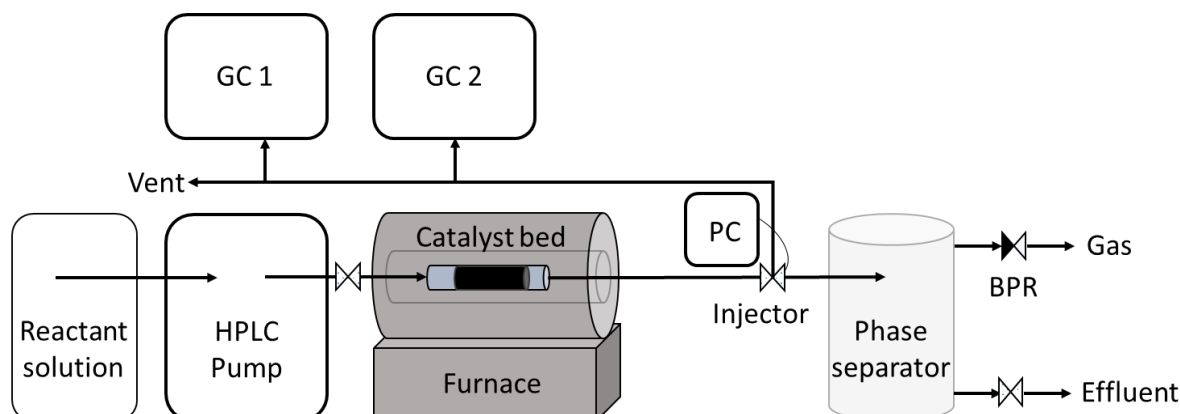
Catalyst	T °C	X (%)	Y (%)	STY (g_(product) mL⁻¹ h⁻¹) [a]
Pd/Al ₂ O ₃ + Hf-β HDT (Pd-Hf 1-1)	290	47.2	7.8	0.83
Pd/Al ₂ O ₃ + Hf-β HDT (Pd-Hf 1-1)	250	19.4	5.1	0.63
[RuCl ₂ (η ⁶ -p-cymene)] ₂ + 2-(diphenylphosphino)ethylamine	150	29.6	7.8	0.02

[a] STYs calculated at maximum conversion as grams of reactant converted per mL (reactor volume), per h. Volume of catalyst bed used as the reactor volume. Only the liquid volume was used as the reactor volume.

7.2. Pertaining challenges and final remarks

The results presented in this work confirm the feasibility of the Guerbet reaction towards ethanol conversion to n-butanol catalysed by a combination of a dehydrogenating/hydrogenating agent (Pd) with a Lewis acidic silicate (Hf-β HDT), resulting in an effective and safe way to perform this reaction. However, the system remains in an early state, with room for optimisation.

7.2.1. Optimisation of analytical methods



Scheme 7.1: Scheme of plug flow reactor for Guerbet reaction with on-line GC acceptorless dehydrogenation of 2-butanol and ethanol in continuous flow.

In Chapter 6, the optimisation of the system mixing Pd/Al₂O₃ with different amounts of Hf-β HDT leads to mixtures of liquid and gaseous products. Obtaining samples for analysis in this case is problematic, as the collection of gases is difficult and several of the liquid components are highly volatile, leading to a complicated sampling process. This could be solved with an online GC system (Scheme 7.1).⁵ In the modified system, the products leaving the reactor could be directed towards the online GC system through a selecting valve that is used to inject samples at specified intervals. Operation of the sampling valves would be controlled by a PC, with software directing the system to acquire samples at pre-set times. The samples could be led to two different GC, equipped with different setups. One could be calibrated for liquid products like ethanol, acetaldehyde or n-butanol, and a second GC to detect gaseous products such as 1,3-butadiene. The fact that all the system is isolated from the atmosphere would prevent any losses and the stability of the catalyst used could be studied without constant supervision; however, an accurate design of the reactor is needed, and many considerations must be taken. For instance, the full system including reactor, GCs and PC controller would be substantially bigger than the current setup, needing a large space. The proper design would be very complex and will need time for optimisation, and the total cost of the system would need to be also considered.

7.2.2. Improving n-butanol selectivity and other products

Despite the fact that many challenges have been tackled and solved during this work, many new questions and future research lines have also been generated. The most important achievement of this thesis is the development of a flexible system, which can be tailored to produce different interesting products (such as n-butanol, diethyl ether, acetaldehyde and 1,3-butadiene), simply by changing the relative amounts of Pd-Hf. For that reason, the study of different parameters is necessary. In Chapter 6, the effect of the temperature of the system is observed, where the Lebedev product (1,3-butadiene) benefits from high Hf/Pd ratios and higher temperatures (Pd-Hf 1-5, 290 °C), meanwhile n-butanol production is favoured by lower ratios and temperature (Pd-Hf 1-1, 250 °C). In this concern, other parameters like concentration of ethanol or levels of H₂O present in the system could be studied with the appropriate equipment. Another parameter worth of study is the system pressure, as high pressures go against the thermodynamics of the Guerbet reaction, in concrete the first step (dehydrogenation of alcohols with release of H₂). Working at lower pressures will require a different solvent which remains in liquid phase at the working temperatures (>200 °C), however an appropriate substitute to toluene has not been found at the time of this work.

In this work, Lewis acidic zeolites like Hf- β HDT have been presented as an interesting option to catalyse the Guerbet reaction when combined with dehydrogenating agents (Pd); however, one of the weak points during the development of this catalyst is its difficult synthesis. The classical hydrothermal synthesis requires long times, highly hazardous reactants (HF) and can only proceed at low metal contents (<2 wt.% of Sn), discouraging its production at larger scales.⁶ For this reason, different approaches can be explored, like the post-synthetic synthesis method of SSI, employed for the preparation of catalysts used in Chapter 5. SSI method been shown to be fast and scalable.⁷ The catalysts presented in this thesis prepared by SSI method result in lower activity and selectivity to the desired n-butanol. Lower efficiency of metal incorporation has been reported as the metal loading increases (> 5 wt.%), leading to the formation of inactive oxide species like SnO₂.⁸ Therefore, further studies are needed in regards of the process of incorporating the metal in the framework, including mechanistic studies, the use of different solid metal precursors and the use of different post-synthetic procedures.

Other parameter that could be explored in order to improve the selectivity to n-butanol is the type of zeolite structure. Some examples exist in literature where Sn has been incorporated inside a zeolite with a different structure to β ,⁹ and by extension, may open the possibility to incorporate other metals like Hf; however, their stability under hydrothermal conditions is unknown. Many parameters would need to be considered, such as the efficiency of metal

incorporation and the acidity of the zeolite. In order to improve the diffusive properties of the zeolite, and to mitigate possible pore blocking, hierarchical zeolite could represent a solution, as they already shown to be beneficial during the continuous flow performance of organic reactions.¹⁰ A deeper characterisation of these materials would also be necessary. It seems that the acid-base surface sites play a fundamental role in the Guerbet reaction, for that reason the study of Lewis and Bronsted acid sites by spectroscopy techniques using probe molecules will be of a great importance.

Finally, the use of the same zeolite framework as support for Pd is an option worthy of study. As has been repeatedly established, the Guerbet reaction is a really complex system. The different supports for Pd presented in this work (activated C and Al₂O₃) have shown different chemistry, attributed to the acidity of the material. For that reason, the deposition of Pd over Hf-β HDT could be a potential way to avoid side reactions as dehydration to diethyl ether. A preliminary attempt was carried out using Wet Impregnation Method (IMP). In this method, the required amount of metal precursor solution to prepare 1 g of catalyst was added into a 50 mL round bottom flask with a magnetic stirrer (700 rpm) at 25 °C. Deionised H₂O was added to adjust the total volume to 16 mL, before the flask was immersed in an oil bath and the temperature was increased to 60 °C. Once the temperature was reached, the zeolite support was gradually added, and the resultant slurry was stirred for 15 min. The oil bath temperature was then increased to 95 °C and stirred until full evaporation of the H₂O, leaving a dry solid. The catalysts were heat treated in a tubular combustion furnace (Carbolite MTF12/38/400) at 200 °C for 3 h in 5 % H₂/Ar (10 °C min⁻¹ ramp rate, flow rate of 100 mL min⁻¹). The catalyst prepared were named as Pd 1-5 % in regard its Pd loading, and a preliminary test was carried out for the Guerbet upgrade of ethanol, at 290 °C). The results obtained are compared with the previous reported mixtures (Figure 7.1).

In Figure 7.1, despite low yields for n-butanol, all the prepared catalysts present activity for the production of n-butanol through the Guerbet reaction. Interesting new product distributions are obtained, with lower presence of dehydration products like diethyl ether and 1,3-butadiene. The large amounts of acetaldehyde observed could be explained by pore blockage, hindering the diffusion of this to the active centres of the zeolite, or the removal of the properties of the support hindering the condensation step. Herein, these preliminary results open interesting lines of research based on the deposition of Pd over Lewis acidic zeolites. Different methods of incorporation and the optimal metal loadings are aspects that may also be studied.

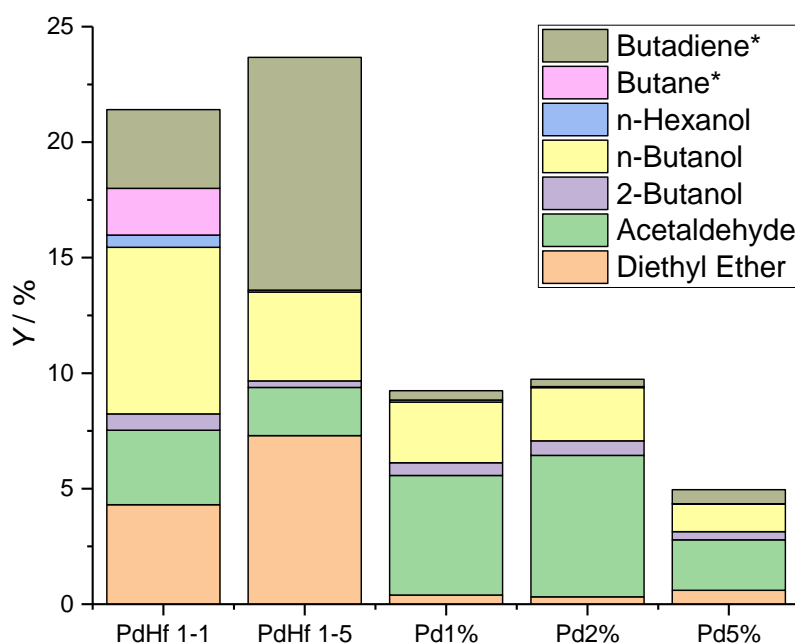


Figure 7.1: Product distribution expressed as yields (Y) for different mixtures of Pd/Al₂O₃ with Hf-β HDT and Pd doped Hf-β zeolites. **Reaction conditions:** 290 °C, PFR, 1.1 min contact time for Pd, 33 bar, ethanol 1M in toluene.

References

- ¹ R. L. Wingad, P. J. Gates, S. T. G. Street, D. F. Wass, *ACS Catal.*, 2015, **5**, 5822–5826
- ² O. Kikhtyanina, R. Bulanekb, K. Frolichb, J. Cejkac, D. Kubicka, *J Mol. Catal. A-Chem.*, 2016, **424**, 358-368
- ³ M. Boronat, A. Corma, M. Renz, *J. Phys. Chem. B*, 2006, **110**, 21168
- ⁴ A. Corma, M. E. Domine, S. Valencia, *J. Catal.*, 2003, **215**, 294
- ⁵ N. O. Elbashir, C. B. Roberts, *Ind. Eng. Chem. Res.*, 2005, **44**, 3, 505-521
- ⁶ R. van Grieken, C. Martos, M. Sánchez-Sánchez, D. P. Serrano, J. A. Melero, J. Iglesias, A. G. Cubero, *Micr. Mesop. Matter.*, 2009, **119**, 176-185
- ⁷ C. Hammond, S. Conrad, I. Hermans, *Angew. Chem. Int. Ed.*, 2012, **51**, 11736-11739
- ⁸ C. Hammond, D. Padovan, A. Al-Nayili, P. P. Wells, E. K. Gibson, N. Dimitratos, *ChemCatChem*, 2015, **7**, 3322–3331
- ⁹ W. N. P. van der Graaf, C. H. L. Tempelman, E. A. Pidko, E. J. M. Hensen, *Catal. Sci. Technol.*, 2017, **7**, 3151
- ¹⁰ A. Al-Nayili, K. Yakabi, C. Hammond, *J. Mater. Chem. A*, 2016, **4**, 1373

Acknowledgements

In first place, I would like to thank Ceri for giving me the opportunity to do my PhD in his group. Without his advice and constant guidance, the quality of my work would have not been the same. But most of all, I thank him for the enjoyable time and for the positive atmosphere that he created within the group.

A special thanks also to Nikos, whose support and scientific (and not) advice have been useful and valuable during this period.

Also, a special thanks to Davide for his help with the XPS analysis, Luca and Ricardo for the help with zeolite synthesis, and to the rest of the people in the group for the nice atmosphere, both inside and outside the lab.

Finally, big thanks to Keiko, who has been with me, side by side every day, for her unconditional support and all her kind words.